DEVELOPMENT OF A DNA VACCINE AGAINST SARS-COV

NEGATIVE REGULATION OF THE IFN-α SIGNALING BY THE INFLUENZA MATRIX PROTEIN (M1)

Dissertation

zur

Erlangung der naturwissenschaftlichen Doktorwürde
(Dr. sc. nat.)
vorgelegt der

Mathematisch-naturwissenschaftlichen Fakultät

der

Universität Zürich

von

Bettina Thea Oberle
von Full-Reuenthal, AG

Promotionskomitee
Prof. Dr. Karin Mölling (Vorsitz)
Prof. Dr. Urs Greber
PD Dr. Jovan Pavlovic (Leitung der Dissertation)

Zürich, 2006

Table of Contents

ABBREVIATIONS

A549	human lung carcinoma cell line
ACE2	angiotensin converting enzyme 2
BCV	bovine coronavirus
CoV	Coronavirus
CMV	cytomegalovirus
CpG	non-methylated dinucleotide, C-Gs, linked by a phosphodiester bond
cRNA	cellular RNA
DIG	detergent-insoluble glycosphingolipids
E	Envelope protein; SARS-CoV
ELISA	enzyme linked immunoabsorbent assay
ER	endoplasmic reticulum
FCS	fetal calf serum
GPI	glucosyl phosphatidyl inositol
HASF	Spike with HA-leader sequence and Flag-epitope
HASFG	Spike with HA-leader sequence, Flag-epitope and GPI-anchor sequence
HCV	human coronavirus
HE	hemagglutinin esterase
HEK 293	human embryonal kidney cells
HR	heptad repeat
HSV	herpes simplex virus
IBV	avian infectious bronchitis virus
i.d.	intradermally
i.m.	intramuscular
i.n.	intranasally
IFN	interferon
IFNAR	interferon α receptor
IgG	Immunoglobulin G
IgM	Immunoglobulin M
IRF	Interferon regulatory factor
ISRE	interferon-stimulated response element
ISG	interferon-stimulated gene
ISGF	interferon-stimulated gene factor
Jak	janus kinase
M	Matrix protein of SARS-CoV
M1	Matrix protein of Influenza A
M2	Ion channel (H^+) of Influenza A
MDCK	Madin-Darby canine kidney
MHV	mouse hepatitis virus
MLV	mouse leukemia virus
mRNA	messenger RNA
MxA	myxovirus resistance protein A
N	Nuclear protein of SARS-CoV
NA	Neuraminidase
NC	ribonucleoprotein core
NP	Nucleoprotein
NS1	non-structural protein 1
NS2	non-structural protein 2
PA	protein acidic
PB1	protein basic 1
PB2	protein basic 2
PBS	phosphate buffered saline
PCR	polymerase chain reaction
PKR	protein kinase R
PKC	protein kinase C
RACK1	receptor of activated kinase C 1
RBD	receptor binding domain
RNP	ribonucleoprotein
S	Spike protein; SARS-CoV
SF	Spike with Flag-epitope
SFG	Spike with Flag-epitope and GPI-anchor sequence
SARS	severe acute respiratory syndrome
STAT	signal transducer and activator of transcription
SV5	simian virus 5
SV40	simian virus 40
TGEV	transmissible gastroenteritis virus of swine
Tyk	tyrosine kinase
Vero E6	African green monkey kidney cells
WHO	World Health Organisation
WSN	
vRNA	viral RNA

Summary: Part I

Classical vaccine strategies include the development of attenuated organisms, whole killed organisms, and protein subunits. These traditional vaccination methods have remained ineffective to several important emerging viruses like HIV, herpes, dengue fever, hepatitis C and influenza. Consequently, new technologies are required. Plasmid DNA expressing an antigen of interest is a new approach for immunization. Injection of DNA vaccines results in antigen expression in transfected host cells, and priming of both humoral and cellular immune responses. DNA vaccines induce potent immune responses in various animal models, but only modest immune responses in clinical trials. Different strategies have been used to increase the potency of DNA vaccines. Plasmids have been altered, by sequence optimization of the antigen, or insertion of bacterial CpG motifs to improve the immune response. Furthermore, DNA vaccines are co-administered with chemokines, cytokines and other molecules to enhance their efficiency, or applied in prime-boost regimens, together with a viral vector or a recombinant protein.

The aim of this study was to improve the immunogenicity of plasmid DNA by genetic modifications of the antigen of interest. As a target antigen we chose the severe acute respiratory syndrome coronavirus (SARS-CoV) S-protein. The SARS-CoV epidemic in 2003 identified a new etiologic agent providing a new challenge to find a potent vaccination. The S-protein is the major viral glycoprotein protruding from the viral shell and identified as the main antigen of the virus. The S-protein is known to be a weak antigen (Yang et al., 2004) and optimization of the antigen presentation at the cell surface was suggested to improve antigenicity.

The genetic modifications include two different strategies: (1) Exchange of the leader sequence of the S-protein (SF; S-protein with a Flag-epitope) with the influenza A haemagglutinin (HA) leader sequence (HASF), which should result in enhanced expression of the antigen and increased trafficking to the cell surface (Xiao et al., 2003). (2) Replacement of the transmembrane (TM) and the cytoplasmic (CP) region of the S-protein by the sequence for glycosyl-

phosphatidyl-inositol (GPI)-anchor attachment for SF and HASF, resulting in SFG and HASFG, respectively. GPI-anchors redirect proteins to lipid rafts, special microdomains of the plasma membrane (Brown & Waneck, 1992, Brown, 1992, Laude & Prior, 2004, Simons & Ikonen, 1997), which should increase and optimize the presentation on the cell surface.

The results of this study showed enhanced expression for HASF compared to the S-protein (SF). Furthermore, SFG and HASFG were co-localized with detergent-insoluble membranes (lipid rafts). HASFG, the S-protein displaying both genetic modifications showed increased expression as well as co-localization with lipid rafts. The immune response in mice was measured for the different S-protein constructs. Mice transfected with a plasmid coding for HASF or SFG showed a two-fold increase in their antibody titer compared to SF. Transfection with p-HASFG enhanced the antibody titer three-fold compared to SF. The HA leader sequence as well as the GPI-anchor sequence were identified to improve the presentation at the cell surface and therefore to enhance the immune response in mice. In conclusion, this study revealed three genetically modified immunogens against the SARS-CoV inducing an improved antibody response in mice. The genetic modifications may provide a technology platform for enhancement of the immune response.

Summary: Part II

Complex organisms have evolved sophisticated mechanisms to prevent and control infection by various pathogens or viruses. Among these mechanisms the interferon (IFN) system, which is part of the innate immune system, represents the first step of defense against viral infection in vertebrates. Secretion of IFNs prepares uninfected cells for combating oncoming virus. Products of IFN-stimulating genes (ISGs) mediate an antiviral action (reviewed in (Sarkar & Sen, 2004)). Once an antiviral state has been established in an infected cell, protein synthesis is inhibited and apoptosis may be initiated. The invading virus will be impaired in infection and replication, which provides time for an adaptive immune response (Stark et al., 1998). Therefore, viruses must overcome the antiviral response provided by the cell in order to establish infection (Alcami, 2003, Samuel, 2001). They found intriguing ways in multiple pathways to evade the IFN system of the host organism.

The influenza A virus is counteracting the IFN system by inhibiting the type I IFN production through the non-structural viral protein 1 (NS1). Paradoxically delNS1, the NS1 deletion mutant of influenza virus, could still propagate in the host cell (Garcia-Sastre et al., 1998b). This observation suggested a second mechanism by which the virus was able to circumvent the cellular defense mechanisms. However, no conclusive results have been obtained.

This study demonstrates an antagonistic activity of the M1-protein of influenza A in the IFN-α signaling pathway. An IFN-stimulated response element (ISRE)-promoter-driven reporter system was used to detect the negative regulation of the IFN signaling cascade by the M1-protein. This effect was independently confirmed by direct measurement of MxA transcript levels in influenza A infected cells. These data identified the IFN-α signaling cascade as target of the virus. The M1-protein did not exert an effect on IFN transcription, suggesting that in contrast to the influenza NS1 protein, it interfered with the action rather than the production of IFN-α. M1 was shown to inhibit the phosphorylation of several IFN-α signaling proteins and to interact with Janus kinase 1 (Jak1), tyrosine kinase 2 (Tyk2) and receptor activated kinase C 1 (RACK1). In conclusion, this study

elicited an alternative mechanism of influenza A to counteract the innate immune response.

PART I

1 INTRODUCTION

1.1 SEVERE ACUTE RESPIRATORY SYNDROME-CORONAVIRUS (SARS-COV)

In late 2002, cases of a life-threatening respiratory disease with no identifiable cause were reported from Guangdong Province, China. By the time of March 2003, there has been a worldwide outbreak of the severe acute respiratory syndrome (SARS), transmitted through a novel coronavirus strain (SARS-CoV). SARS is a serious respiratory illness that leads to significant morbidity and mortality in elderly populations (Table 1). Aggressive quarantine measures successfully terminated the disease. The SARS epidemic was officially controlled by July 2003 (Ashraf, 2003, Fleck, 2003). Currently, there are no SARS cases recorded and most likely the virus does not circulate anymore.

No. of infections	8096
No. of deaths	774
Antibodies	IgM and IgG
Viraemia	60% of patients
Incubation period	2-10 days
Infectious period	around day 10 of illness
Pathogenesis	Infection of ciliated respiratory tract epithelial cell
	2 disease mechanisms: 1) Direct lytic effect of the viral host cell; coronavirus replication has several effects: cellular necrosis, lysis, apoptosis or cell fusion to form syncytia. 2) Host immune response; acute inflammatory response; acute hepatitis, may be result of immune-mediated, rather than direct viral damage.

Table 1: General information and statistics obtained upon the SARS-CoV outbreak.

The natural reservoir of SARS-CoV is currently unknown. SARS-CoV is likely transmitted from animal hosts to humans. The virus rapidly adapted to the new

host and not only became transmissible between humans but also more pathogenic. There is a possibility that SARS-CoV gets transmitted again from its natural host to humans. Therefore it is important to develop a vaccine, providing protective immunity.

SARS-CoV belongs to the family of *Coronaviridae* (Table 2). Coronaviruses are found in a wide range of animal species. Animal and human coronaviruses have been classified into three different serological groups based on their antigenicity. SARS-CoV is not closely related to any subgroup of known CoVs, although it is suggested to resemble most the group II CoVs (Snijder et al., 2003).

Order	**Nidovirales**	
Family	**Coronaviridae**	**Arteriviridae**
Subfamily	Coronaviruses Toroviruses	Equine arteritisvirus Lactatehydrogen-induced virus (mouse) Simian haemorrhagic fever virus

Table 2: The order of the nidovirales and their subfamily.

Coronaviruses are enveloped, round shaped viruses of approximately 80-120 nm in diameter, with a positive-stranded large genomic RNA. The genome of SARS-CoV is 29'727 nucleotides in length. The full length genome sequence of SARS-CoV has been elucidated within few weeks after the identification of this novel pathogen (Rota et al., 2003). Coronavirions contain several structural proteins: the Spike glycoprotein (S), which forms the 20-nm glycosylated peplomers characteristic for coronaviruses, protruding from the virion envelope. The membrane protein (M) is spanning the membrane three times and the envelope protein (E) are two more glycoprotein,. The nucleocapsid protein (N), associated with the genomic RNA, and the hemagglutinin esterase glycoprotein (HE), which is protruding the shell and exists in some of the group II Coronaviruses (see Figure 1). SARS-CoV does not include the structural protein HE.

The genomic organization of the SARS-CoV RNA is typical for coronaviruses, having the characteristic gene order 5'-replicase (rep), spike (S), envelope (E), membrane (M), and nucleocapsid (N)-3' and short untranslated regions at both termini. In addition to the conserved genes, the SARS-CoV genome contains

eight novel ORFs at the 3' end (Snijder et al., 2003). To date, the functions of these genes remain unknown, although their absence from other genomes suggests unique functions that might be advantageous to SARS-CoV replication, assembly or virulence (Ziebuhr, 2004).

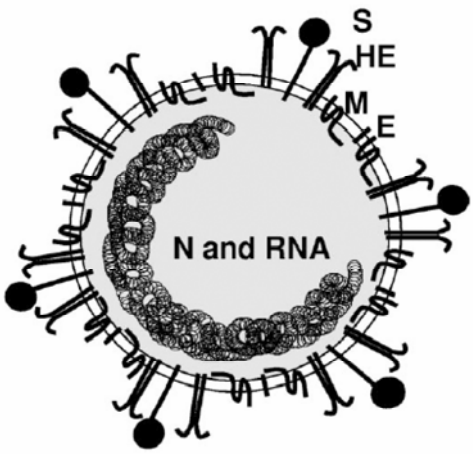

Figure 1: Model of a coronavirus particle. The virus particle consists of an internal helical RNA-protein nucleocapsid surrounded by an envelope. N is complexed with genomic RNA to form the nucleocapsid. S forms the large glycosylated peplomers. M is hydrophobic. E is a minor component of the membrane. The hemagglutinin-esterase (HE), another glycoprotein present only in some coronaviruses, forms smaller spikes on the virion (adapted from Weiss and Navas-Martin, 2005).

1.1.1 VIRAL MULTIPLICATION CYCLE

The first step in viral infection is the binding of viral proteins to a cellular receptor. Coronaviruses bind to specific cellular receptors via the S-protein (Fig. 2). It has been shown that a cellular metallopeptidase, angiotensin-converting enzyme 2 (ACE2), binds a 193 AA fragment of the SARS-CoV S-protein (Li et al., 2004).

SARS-CoV has the potential to enter cells via two different pathways, depending on the presence of proteases in the environment. One possibility is the binding of SARS-CoV S-protein to its cellular receptor ACE2, which promotes internalization into endosomes (Simmons et al., 2004). Proton influx into the endosome can trigger the membrane fusion by acidification. If proteases like trypsin or thermolysin are present in the environment, SARS-CoV is adsorbed onto the cell surface, proteases cleave the S-protein, which leads to a conformational change

of the S-protein and mediates fusion between the viral and cellular membranes. This results in the release of the nucleocapsid into the cell. Protease-mediated entry resulted in over a 100-fold more efficient infection than entry through endosomes (Matsuyama et al., 2005).

The genomic RNA of coronaviruses is capped and polyadenylated and serves as an mRNA for synthesis of the RNA-dependent RNA polymerase (Fig. 2). Upon entry into the cell, the 5' end of the genomic RNA, ORFs 1a and 1b, are translated into pp1a and pp1ab; pp1ab is translated via a ribosomal frameshift mechanism (Bredenbeek et al., 1990). Proteolytic processing of pp1a and pp1ab leads to the production of the mature polymerases, that form the replicase complex. Using the genomic RNA as template, the polymerase generates a full length, minus-strand that contains a 5' poly-U sequence. New plus strand genomic RNAs and a 3'co-terminal nested set of subgenomic mRNAs are generated from the minus-strand template. A leader RNA (60 - 90 bases) is found in the genome only once at the 5' end, and is also found at the 5'end of each mRNA.

Subgenomic mRNAs of Coronaviruses consist of a 'leader' and a 'body' fragment that are non-contiguous in the genome sequence: they are transcribed from sequences in the 3'end and the 5'-terminal part of the genomic (-) strand RNA, respectively. The connection between the two segments of the subgenomic mRNA is formed by a conserved junction site sequence that is found both at the 3'end of the common leader sequence and at the 5'end of the mRNA body. Proteins are translated from the first AUG after the leader sequence at the 5'end of each mRNA.

The membrane protein (M) plays a key role in assembly of coronaviruses. It has the ability to form a complex with the S and HE glycoproteins (Nguyen & Hogue, 1997), or the S-protein alone for the viruses that do not contain the HE protein (Opstelten et al., 1995b). The S-protein is prevented from being transported to the plasma membrane (PM), but instead the M protein retains it intracellularly. Thus, specific M-S interactions determine the intracellular transport of the S

protein and direct its packaging into virus particles. The nuclear protein (N) binds the genomic RNA via the leader sequence. It recognizes a stretch of RNA that serves as a packaging signal and leads to the formation of the helical ribonucleoprotein (RNP) complex during assembly (Lai & Cavanagh, 1997). The RNP presumably needs to interact with the envelope proteins to ensure its uptake into virions.

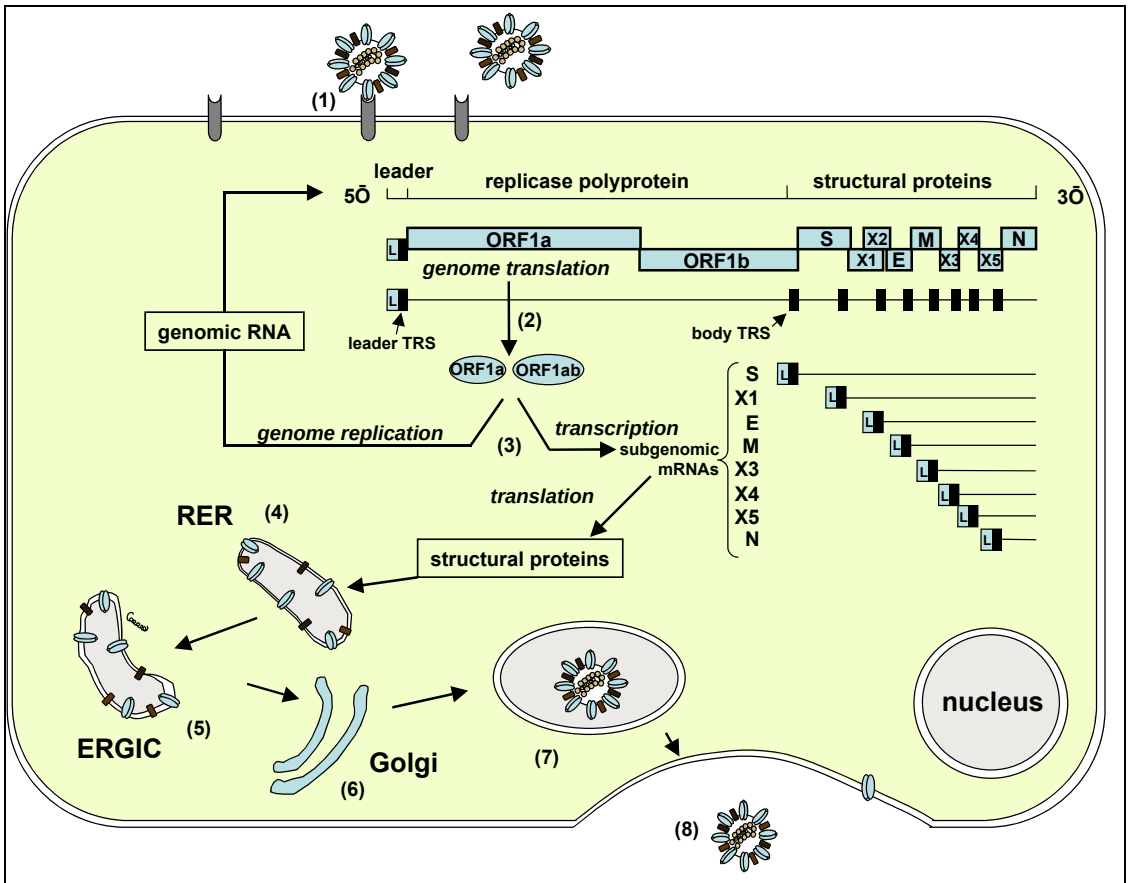

Figure 2: Model of Coronavirus replication. (1) virus binds to cellular receptor and enters host cell. (2) ORF1a and ORF 1ab are tranlated from the genomic RNA to produce the viral RNA polymerase. (3) Genomic RNA is transcribed into (-) stranded RNA and subsequently into genomic RNA for progeny virus particles and subgenomic RNA for the synthesis of structural proteins. (4) Structural proteins are produced in the rough ER (RER). (5) Structural proteins undergo interaction with each other in the intermediate compartment (ERGIC). (6) Structural proteins are processed in the golgi compartment and viral particles assembled in (7) endosomes, which travel to the cell surface and release the progeny virus (8).

Virus budding occurs intracellularly at membranes of the intermediate compartment, between the endoplasmic reticulum (ER) and the Golgi complex (ERGIC). Virus particles bud into the lumen of these intracellular compartments.

As shown in Figure 3, newly assembled virions are transported by vesicular transport to the cell surface, where they are released via exocytosis (Garoff et al., 1998).

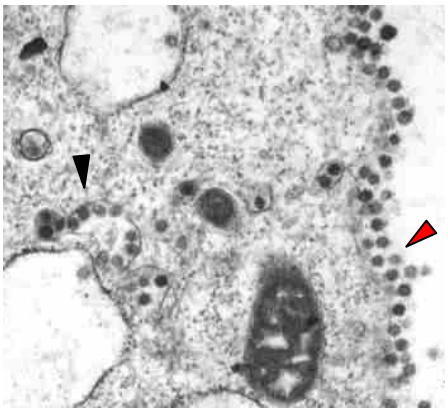

Figure 3: Visualization of coronavirus budding and release through electron microscopy (picture from www.un.com). Black arrow indicates virus particles in vesicles; red arrow indicates virus particles at the cell surface.

1.2 S PROTEIN

1.2.1 CHARACTERIZATION OF CORONAVIRUS S PROTEIN

The S-protein is a type I membrane protein that is synthesized as a precursor in the rough ER of the host cell and co-translationally N-glycosylated. The SARS-CoV S-protein is subdivided into an N-terminal part (S1) and a C-terminal part (S2). S1 is responsible for binding to cellular receptors and thus determines the host range and tissue tropism. Whereas S2 contains an internal fusion peptide and is responsible for virus and host cell membrane fusion for cell entry (Gallagher & Buchmeier, 2001). The mature protein is assembled in homo-oligomers. Homotrimers of S are extremely stable, such that S oligomers are partially resistant to SDS denaturation and reduction (Delmas & Laude, 1990).

The SARS-CoV S-protein consists of 1255 amino acids (aa), where aa 1-1195 represent the extracellular part, aa 1196-1218 the transmembrane and 1219-1255 the intracellular part (Fig. 10). A leucine zipper motif terminates 10 amino

acid residues close to the transmembrane domain. The leucine zipper motif of the S-protein contains 5 heptad repeats. By analogy to the role of the leucine zipper domain in several transcription factors, it has been suggested that the motif may be responsible for the oligomerization of the S-protein.

The S-protein contains 23 putative N-linked glycosylation sites, among which 12 have already been verified (Krokhin et al., 2003, Ying et al., 2004). S-trimers are formed in the ER of the host cell and move towards the Golgi to acquire complex N-glycans (Nal et al., 2005, Niemann et al., 1982).

Mature S-proteins of most coronaviruses are cleaved by host cell proteases located in the Golgi apparatus to yield S1 and S2 (Frana et al., 1985). The SARS-CoV S-protein lacks this basic amino acid cleavage site found in group II and group III coronaviruses (Rota *et al.*, 2003), and shortly after the discovery of SARS-CoV, the S-protein was predicted not to be proteolytically cleaved (Supekar et al., 2004). Nevertheless, as demonstrated lately by Simmons and co-workers, the S-protein seems to be proteolytically cleaved by cathepsin L (Simmons et al., 2005). Thus, it is reasonable to assume that the S-protein has a different cleavage site.

1.2.2 LOCALIZATION OF THE S-PROTEIN

When S-proteins from different coronaviruses are exogenously expressed, a large portion remains intracellular (Vennema et al., 1993) The infectious bronchitis virus glycoprotein was reported to be intracellularly retained because of a dilysine motif, resulting in retention in the ER (Lontok et al., 2004), whereas the porcine coronavirus (transmissible gastroenteritis virus; TGEV) exhibits a novel sorting signal for intracellular localization (Schwegmann-Wessels et al., 2004). Co-expression of the glycoproteins M and E affects the intracellular transport of the S-protein of MHV: instead of being transported to the cell surface, the S-protein is retained intracellularly by its association with the M-protein (Opstelten et al., 1995a).

Retention and transport of the SARS-CoV S-protein is still a matter of controversial discussion. The transport of SARS-CoV S-protein to the cell surface

was currently shown and compared to the control TGEV S-protein in an immunofluorescence study. The TGEV S-protein contains a tetrapeptide (YEPI) for intracellular retention. A SARS-CoV S-protein double mutant was predominantly retained intracellularly (Schwegmann-Wessels et al., 2004). Another research group (Lontok et al., 2004) discovered a dibasic signal (KXHXX) at the C-terminal 11 amino acids of the TGEV S-protein as well as the SARS-CoV S-protein. This signal is similar to the dilysine signal in the IBV S-protein (KKXX). Mutagenesis of the dibasic motif (KXHXX) resulted in loss of intracellular localization. The KXHXX signal is likely to contribute to the localization of the S-protein in the ERGIC.

1.3 VACCINES

1.3.1 CONVENTIONAL VACCINES

The English physician Edward Jenner first employed the principle of vaccination in the 18th century. He used cowpox virus to combat smallpox infections (Jenner E., Reprinted by Cassell, 1986, London). Since the introduction of vaccination in the 1950s and 1960s there have been a steady stream of new vaccines becoming available. Numerous viral diseases are successfully treated by vaccination, as depicted in Table 3.

The production of conventional vaccines utilizes two different strategies: (1) attenuation of virulent organisms, or (2) killing of virulent organisms. Live attenuated vaccines are developed by growing viruses for generations under sub-optimal conditions (e.g. in tissue culture at 25°C). These viruses can still replicate in humans, but do not cause a disease. The oral polio vaccine has, as well as vaccines for mumps, measles and rubella have been developed by this method. Dead vaccines are produced from whole organisms that have been killed (e.g. by formaldehyde treatment). Inactivated pathogens do not replicate and cause no disease in the host. Dead vaccines in use today include those against polio and influenza virus.

Disease	Vaccine type
Adenovirus	Live attenuated
Chicken pox (VZV)	Live attenuated
Hepatitis A	Inactivated
Hepatitis B	Subunit (genetically engineered)
Influenza	Subunit
Japanese encephalitis	Inactivated
Measles	Live attenuated
Mumps	Live attenuated
Poliomyelitis	Live attenuated (Sabin); Inactivated (Salk)
Rabies	Live attenuated
Rotavirus	Live attenuated
Rubella	Live attenuated
Smallpox	Live attenuated
Tick-borne encephalitis	Inactivated
Yellow fever	Live attenuated

Table 3: Human viral vaccines, currently available commercially.

1.3.2 DNA VACCINES

DNA vaccines are plasmids encoding viral antigens, which are expressed in the immunized host. The most commonly used plasmids utilize a minimal backbone containing a selectable marker, an origin of replication active in *Escherichia coli* (*E.coli*), a strong viral promoter active in eukaryotic cells, such as the immediate early CMVintA promoter, and a transcriptional chain terminator or polyadenylation signal sequence. The potential of a DNA vaccine plasmid to induce an effective immune response is directly related to the level of expression of the encoded protein in eukaryotic cells (Montgomery et al., 1994). DNA plasmids have been widely used to develop vaccines against various pathogens as well as for cancer, autoimmune disease and allergy.

DNA vaccination involves the introduction of nucleic acid into tissues for expression in host cells. Unlike gene therapy, genetic integration is not intended. Indeed, the construction of a DNA vaccine is designed to permit localized, short-term expression of the target antigen (Donnelly et al., 2003). However, DNA vaccines can be randomly integrated into host cell DNA by recombination. The probability of such an event lies between 10^{-6} and 10^{-7} per transfected cell. Since myocytes, the main targets of the injected DNA (Liu, 2003), are non-dividing cells, the frequency of integration of foreign DNA into these cells should be even

lower. Avoiding the insertion of sequence repeats can minimize the risk of recombination events. These repeats could create transposon-like elements, enabling the integration. The integration of plasmid DNA however, may cause no effect on the expression of endogenous genes (Rajcani et al., 2005).

If the corresponding DNA vector is delivered into muscle tissue or to skin epidermis, the expressed protein elicits a specific cytotoxic T cell (CTL) response as well as antibody production (Rajcani et al., 2005).

DNA vaccines have several advantages compared to recombinant protein subunit vaccines produced in bacteria or yeast. The plasmid-encoded protein is produced endogenously and therefore folded and glycosylated identical as through infection. Thus conformational epitopes might be presented correctly to the host immune system. Furthermore, it is of great importance to design products that are easy to manufacture on an industrial scale and in non-industrialized countries, which is the case for naked DNA vaccines (Moelling, 1998).

It has been more than a decade ago, since the first publications reported that immune responses could be induced by the injection of bacterial plasmids into vertebrates. This approach has generated substantial interest because of its speed, simplicity and ability to elicit both, humoral and cellular immune responses (Cox et al., 1993, Donnelly et al., 1997, Fynan et al., 1993, Robinson, 1997, Robinson & Torres, 1997, Wang et al., 1998). DNA-encoding HIV antigens were the first DNA vaccines against infectious diseases to be tested in humans (MacGregor et al., 1998). Clinical trials for several other DNA vaccines are currently in process, including HIV, malaria, Hepatitis B, influenza (Epstein et al., 2005, Smith et al., 2005, Wang et al., 2005). In 2005, two DNA vaccines were licensed for use in animals (Lorenzen & LaPatra, 2005, Powell, 2004).

However, researchers have to deal with technical problems concerning DNA vaccine potency. The reasons for the failure of many DNA vaccines to induce potent immune responses in humans have not been elucidated. However, it is assumed, that low levels of antigen production, inefficient cellular delivery of DNA

plasmids and insufficient stimulation of the innate immune system affect the potency of a DNA vaccine.

Several strategies have been developed to increase the potency of DNA vaccines, as illustrated in Table 4. Investigations on different delivery systems, like electroporation and microparticle formulation showed an enhanced immune response compared to ordinary DNA transfection (Hermanson et al., 2004, Megede et al., 2006, Otten et al., 2005). DNA vaccines were applied together with adjuvants (CpG motifs, cytokines, chemokines) or in combination with a viral vector or a recombinant protein in a prime-boost regimen, showing increased immune response, compared to a simple DNA immunization. Priming with DNA was followed by boosting with recombinant adenovirus serotype 5 (rAd5) vectors (Casimiro et al., 2003, Shiver et al., 2002), recombinant modified vaccinia Ankara (rMVA) vectors (Amara et al., 2001), and recombinant vesicular stomatitis virus (rVSV) vectors (Egan et al., 2005).

Virus	DNA vaccination strategy	Reference
HIV	**DNA-prime + MVA vector-boost** (Int.AIDS Vacc.Initiative & Oxf.Univ.; phaseI & II)	Smith J.M. et al, AIDS Res.Hum.Retroviruses, 2005
	DNA encoding env/rev & gag/pol genes in combination with HAART	Hejdeman B. et al, AIDS Res.Hum.Retroviruses, 2004
	DNA-prime encoding genes and boost with Ad5 (Merck & VRC; phaseI)	Mascola J. et al, J. of Virology, 2004
Hepatitis B	**Plasmid DNA by particle-mediated epidermal delivery** (i.e.; phase I)	Rottinghaus S. et al, Vaccine, 2004
Influenza	**Plasmid DNA** (clinical trial)	Ulmer J. et al, Science, 1993
	pDNA-HA or -NP, coadministration of a Schiffbase forming drug	Charo J. et al, J. of Virology, 2004

Table 4: DNA vaccination strategies of viral diseases that are currently in clinical or preclinical trials.

1.3.3 SARS-CoV as Model: Antiviral Agents and Vaccines

During the SARS outbreak in 2002-2003, the spread of the disease was primarily controlled by strict quarantine protocols and patient isolation. In parallel multiple antiviral strategies have been proposed immediately. Several laboratories are involved in developing a SARS vaccine utilizing different types of SARS-CoV-derived immunogens.

1.3.3.1 NAKED DNA

The wild-type full-length S gene was used as a candidate DNA vaccine. The S-protein under the regulation of a CMV promoter could induce the production of specific IgG antibodies against SARS-CoV in mice with a seroconversion ratio of 75% after 3 times of immunization (Zhang et al., 2004).

A DNA vaccine based on the codon-optimized S sequence has been shown to induce T cell and neutralizing antibody responses, as well as protective immunity, in a mouse model. Sequence optimization was required and a deletion of 13 nucleotides in the cytoplasmic domain of the S protein yielded an improved immune response compared to the full-length protein. Protection was mediated by the humoral immune response (Yang et al., 2004).

A plasmid encoding the full-length nucleocapsid protein (N) of SARS-CoV was used, because the N-protein is more conserved than the other structural proteins. The immune responses induced by i.m. immunization were evaluated in a murine model. The study showed that the N-protein of SARS-CoV not only is an important B cell immunogen, but also can elicit cellular immune responses (Zhao et al., 2005). These results indicate that the N-protein may also be of potential value in vaccine development against SARS-CoV.

1.3.3.2 VIRAL VECTORS

An adenoviral-based vaccine has been shown to induce strong SARS-CoV-specific immune responses in rhesus macaques. A codon-optimized fragment of the S-protein (S1), the M-protein, and the N-protein were combined in an adenoviral delivery system to induce virus-specific immunity. Rhesus macaques were immunized i.m. with a combination of the three Ad5-SARS-CoV vectors and a booster vaccination after 4 weeks. The vaccinated animals all displayed antibodies against the S1-fragment and T-cell responses against the N-protein. All vaccinated animals showed strong neutralizing antibody responses to SARS-CoV infection *in vitro* (Gao et al., 2003).

In another study, a recombinant attenuated modified vaccinia virus, Ankara (MVA) expressing the S-protein of SARS-CoV was used. BALB/c mice were

infected i.n. or i.m. with MVA/S. Serum antibodies of the immunized mice showed neutralization of SARS-CoV *in vitro*. Passive transfer of serum from mice immunized with MVA/S to naive mice also reduced the replication of SARS-CoV in the respiratory tract after challenge, demonstrating a role for antibodies in protection (Bisht et al., 2004).

An attenuated recombinant Vesicular Stomatitis virus (VSV-S) expressing the SARS-CoV S-protein was developed as well. Mice vaccinated with VSV-S developed SARS-neutralizing antibodies and were able to control a challenge with SARS-CoV performed one month or four months after a single vaccination (Kapadia et al., 2005).

Furthermore the preparation of convalescent plasma, donated by patients who have recovered from SARS has been performed (Soo et al., 2004).

In summary, none of these diverse strategies was efficient enough for full protection. Therefore it is important to find other strategies improving the humoral immune response.

1.3.4 IMMUNE RESPONSES INDUCED BY DNA VACCINE

DNA vaccines elicit efficient antigen specific antibodies and cytotoxic T cells in mice. Induction of a primary antibody response depends on the antigen and the number of immunizations. An immunization protocol with intervals helps to prolonge the presence of antigen and supports thereby both the primary and the secondary phases of antibody response. Application of DNA vaccines also induces a cytolytic T cell response. Upon injection of the naked DNA into the muscle (i.m.), the plasmid is taken up by myocytes and the antigen is synthesized. Only antigen-presenting cells can prime cytolytic T cells. Thus, if a non-antigen presenting cell takes up the DNA vaccine and produces the protein antigen, it must deliver the antigen to a professional antigen-presenting cell by a process called cross-priming, to induce cytolytic T cells (Srivastava & Liu, 2003).

In general, i.m. injections predominantly rise a Th1 response with high titers of IFN-γ secreting T-cells providing help to cytotoxic T cells, and production of IgG2α antibodies. Plasmids encoding soluble antigens mostly induce Th2 type

responses, independent of the method or route of inoculation. The mechanisms by which DNA plasmids rise different types of T cell help is not well understood. A general overview of the immune response elicited by naked DNA is depicted in Fig. 4.

Several studies with larger animals report that multiple doses of DNA in nonhuman primates (Amara et al., 2001) induce an immune response that is weak and short lasting. DNA priming and protein boosting have been shown to generally increase immune responses (Kong et al., 2005).

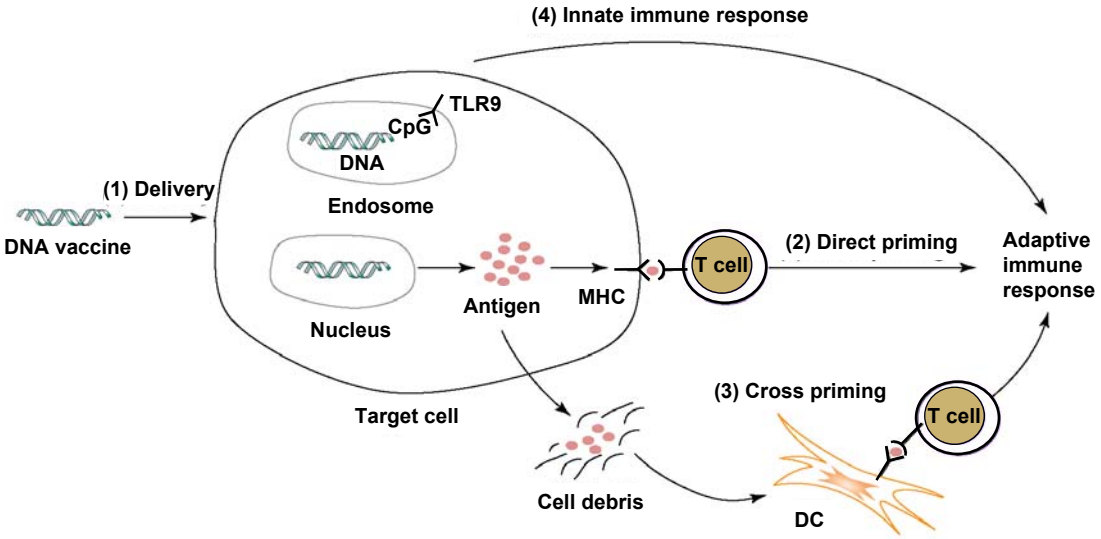

Figure 4: Mechanism of action of plasmid DNAuptake. DNA uptake can be facile or facilitated. When expressed by APCs, the antigens can be processed and presented by major histocompatibility complex (MHC) molecules directly to naive T cells (direct priming). Alternatively, the antigens that are released from transfected cells (e.g. by apoptosis) can be internalized by surrounding cells like DCs for presentation by MHC molecules (cross priming). Certain CpG motifs can interact with TLR9 that is present on the membrane of endosomes of DCs and some other immune cells, thereby eliciting innate immune responses. The innate immune response can promote adaptive immune responses against the antigen produced by or transferred to DCs (adapted from Ulmer J. et al, Trends in Mol Med, 2006).

1.3.5 ANIMAL MODEL

Current animal models of SARS infection that faithfully mimic the human disease do not exist. It is presently not possible to evaluate relative vaccine efficacy; however, a variety of novel approaches, including adaptation of virus to different

species, the development of transgenic animals expressing the human ACE-2 receptor, and the use of aged animals in challenge models, may contribute to this effort in the future (Kong et al., 2005).

1.4 DIG'S AND GPI-ANCHORED PROTEINS

The plasma membrane of eukaryotic cells is composed of hundreds of different lipid species. A spatial organization of these lipid enriched areas into discrete microdomains known as membrane rafts is thought to be important in the generation of distinct signal outputs (Parton & Hancock, 2004). These "islets" are also called lipid rafts, glycosphingolipid-enriched microdomains (GEMs) or detergent-insoluble, glycolipid-enriched complexes (DIGs). In contrast to the bulk membrane, these complexes are relatively resistant to solubilization with commonly used detergents such as Triton-X 100, NP-40 or CHAPS. DIGs are held together mainly by hydrophobic interactions between saturated fatty acid residues (Baumgartner et al., 2003, Horejsi, 2003). Most of the available data are based on analysis of the preparations obtained by density gradient ultracentrifugation of low-temperature detergent lysates. Because of their high lipid content, DIGs float to a low density during gradient centrifugation, which enables any associated proteins to be identified and distinguishes DIGs from detergent-soluble complexes (Simons & Ikonen, 1997).

Recently a variety of new techniques (FRET, laser trap, single particle trap) have been used to study the cell surface, with the aim to resolve the size, distribution and dynamics of the DIGs without caveolaer characteristics (Laude & Prior, 2004). Until now there was no substitute to see lipid rafts in the microscope convincing us of their existence and providing models for their organization and function. This is in contrast to other microdomains, like caveolae and clathrin-coated vesicles, also localized in DIGs upon density gradient centrifugation and visible in the electron microscope, composed of 50-150nm invaginations.

Characteristic protein components of DIGs include GPI-anchored proteins (Schroeder et al., 1994), many acylated proteins including Src family kinases

(Song et al., 1997), growth factor receptors, integrins (Baron et al., 2003) and cholesterol binding proteins including caveolin (Sargiacomo et al., 1993).

1.4.1 GLYCOSYL PHOSPHATIDYL INOSITOL (GPI)-ANCHORED PROTEINS

GPI-anchored proteins form a diverse family of molecules that include membrane-associated enzymes, adhesion molecules and receptors. Although it remains obscure why so many proteins are endowed with a GPI anchor, the presence of a GPI anchor does confer some functional characteristics to proteins: (1) it is a strong apical targeting signal in polarized epithelial cells (Brown D, cell, 1992); (2) GPI-anchored proteins can activate T cells of the immune system (Brown, 1993); (3) proteomic analysis revealed a 10-fold enrichment of signaling proteins in rafts versus total membrane (Foster et al., 2003) and (4) they allow proteins an increased lateral mobility (Varki, A et al., Essentials of Glycobiology, 1999).

It is possible to artificially target various proteins to membrane rafts by fusion of the required sequence for any modification by the GPI moiety (Cebecauer et al., 1998, Premkumar et al., 2001). GPI-anchored proteins are translocated across the membrane of the endoplasmic reticulum (ER) and are initially anchored by a hydrophobic amino acid sequence. Immediately after synthesis, the hydrophobic sequence is cleaved on the luminal side of the ER (Boothroyd et al., 1981) and replaced by the GPI-anchor (Fig. 5). The efficiency of GPI-anchor addition is sequence-dependent (Moran & Caras, 1994). Once the signal is recognized the protein is cleaved and the new C-terminus is covalently linked to the preformed GPI portion (Menon et al., 1988). The topology of this process results in the localization of GPI-anchored proteins on the extracytoplasmic face of the membrane (Brown & Rose, 1992).

In 2003, the Plasmodium falciparum antigen Pfs230 was conjugated to an amino acid sequence responsible for the GPI-anchor attachment, resulting in an improved immunogenicity in mice compared to the Pfs230 alone (Fanning et al., 2003).

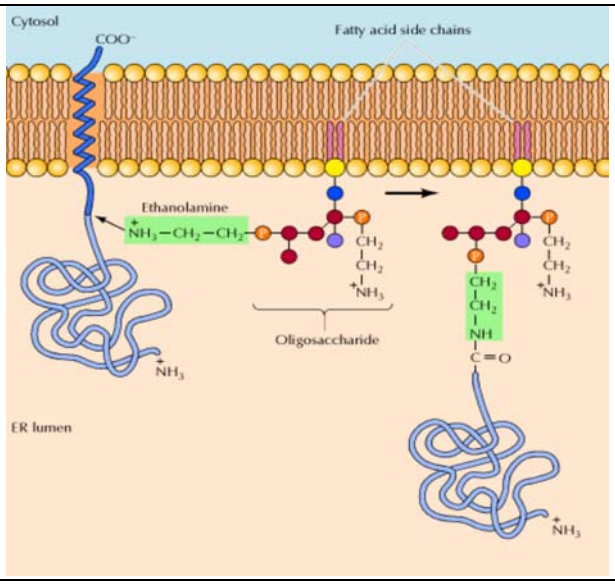

Figure 5: Attachment process of a GPI-anchor to the C-terminus of a protein. GPI-anchors are assembled in the ER and added to polypeptides anchored in the membrane by a C-terminal membrane-spanning region. The latter is cleaved, and the new CT is joined to the NH_2-group of ethanolamine after translation is completed, leaving the protein attached to the membrane by the GPI-anchor (Varki, A et al., Essentials of Glycobiology, 1999).

1.5 AIMS OF THIS PROJECT

Classical vaccination methods have been shown to induce insufficient immune responses for certain viruses. Vaccination with naked DNA showed protection in mice experiments in a variety of studies. However, most vaccines remained inefficient in larger mammals. The ability of naked DNA to induce protective immunity needs to be improved. Until now, DNA plasmids have been modified by sequence optimization, expression enhancement and stimulation by adjuvants. Furthermore, administration of plasmid DNA in combination with other immunogens (prime-boost), generally resulted in an enhanced immune response. However, the protection for many approaches was still not satisfactory.

In this study we investigated the improvement of DNA vaccination by two genetic modifications of the target antigen. (1) The exchange of the S-leader sequence by the influenza A HA-leader sequence (HASF). The HA-leader is known to enhance expression and glycosylation efficiency and translocation to the cell surface (Gething & Sambrook, 1982). (2) The TM and CP region of the S-protein

were replaced by the GPI-anchor attachment sequence. GPI-anchored proteins display an increased lateral mobility and appear in high density on lipid rafts.
These modifications should allow an improved immune response through increased and optimized presentation of the target antigen on the cell surface. The SARS-CoV S-protein was used as antigen of interest. However, these two genetic modifications could be transferable to antigens of various other viruses, providing a new technology of DNA vaccination.

2 MATERIALS AND METHODS

2.1 PLASMID CONSTRUCTION

The S glycoprotein encoding cDNA was amplified by RT-PCR as three fragments using viral RNA as template (kindly provided by Prof. Doerr, Institute of Medical Virology, Frankfurt).

The resulting three cDNAs were subcloned separately into the pVR1012. The gene fragments 1 and 2 were then inserted into pBluescript and excised as a single fragment using Not*/* and Sal*/* restriction enzymes, fragment 3 was digested using Sal*/* and BamH*/*. These cDNAs were then inserted into the Not*/*/BamH*/* sites of the pVR1012 plasmid to generate full-length S. Sequence analysis of the construct proved sequence identity with the Frankfurt1 (Fra1) isolate.

All S constructs were cloned by PCR to encode a Flag-epitope at the C terminus for expression and localization analyses. The STOP codon was replaced by a Flag epitope encoding sequence followed by a STOP codon using primers (reverse primer: TGCGTAGGATCCTTATTTATCGTCATCGTCTTTGTAGTCACC TGTGTAATGTAATTTGACACCCTTGAGA).

Forward primers amplified the haemagglutinin signal sequence of the influenza virus A/PR/8/34 (1: GTCGATGCGGCCGCCACCATGAAGGCAAACCTACTGGT CCTGTTATGGCACTTGCAGCTGCAGATGCAGACCGGTGCACCACTTTTGAT GAT; 2: TCGATGCGGCCGCCACCAT), covering the sequence coding 16 amino acids and a reverse primer at the beginning of the S gene (CAATCAACAGCATC TGTGATTGTACC). The corresponding PCR product was inserted into the Not*/* and Pst*/* sites of pBS(-)KS.SF. The sequence of HASF was subsequently cut with Not*/* and BamH*/* and ligated into pVR1012. As the GPI-anchor itself provides the characteristic sequence for membrane binding, we amplified the truncated, soluble S (sSF) as template for th PCR reactions. In a first step we amplified the 3'-end of sS (forw: GGCCGTGATGTTTCTGATTTCACTG; rev: CAACGTGAAAC ACGTGTGCCCAGATAGAAGACGGGTAGTACCTGAACCTTTATCGTCATCGT CTTTGTAGTCACC) coding for a portion of the GPI-anchor recognition

sequence. In a second step we completed the 3'-end to the whole coding region of this GPI-anchor sequence with TGCGTAGGATCCCTAAGTCAGCAAGCCCATGGTTACTAGCGTCCCAAGCAAACCTGTCAACGTGAAACACGTGTGCCCA as reverse primer. The product was digested with Bgl*II* and BamH*I* and ligated into pBS(-)KS.SF and pBS(-)KS.HASF.

2.2 CELL CULTURE

Human embryonal kidney cells (HEK293T) were cultured at 37°C and 5% CO_2 in Dulbecco's Modified Eagle Medium (DMEM, Gibco) containing 10% fetal calf serum (FCS). The cells were split every second day before reaching confluency.

2.3 TRANSFECTION

2.3.1 CALCIUM-PHOSPHATE TRANSFECTION

HEK293 T cells were transfected with different plasmids using the Calcium-Phosphate transfection method (Ref). Cells were seeded one day before transfection and the culture medium was changed 1h before transfection. 10cm plates at about 80% confluency were transfected with 10μg plasmid DNA diluted in 450μl dH_2O and 50μl 2.5M $CaCl_2$. 500μl 1xBBS (50mM BES, 280mM NaCl and 1.5mM Na_2HPO_4 adjusted to a pH of 6.94) is added drop wise while vortexing the tube. DNA precipitates were incubated at room temperature for 20min and added drop wise to the cells. Cells were incubated at 37°C and 5% CO_2 for 18h and fresh medium was added. Analyses were performed 48h after medium change.

2.3.2 LIPOFECTAMINE TRANSFECTION

1h prior to Lipofectamine-transfection the medium of the cells was changed and fetal calf serum (FCS)-free medium (D-MEM, Gibco) was added. DNA was diluted in OptiMEM® (Gibco). Lipofectamine™ 2000 (Invitrogen) was diluted in

OptiMEM® and incubated for 5min at room temperature. The diluted DNA and Lipofectamine™ 2000 were combined, incubated for 20min at room temperature and added to the cells. Medium was changed 4h after transfection and D-MEM + 10% FCS (Brunschwig) was added.

For a 10cm plate the following amounts were used: 10μg DNA in 1.5ml Opti-MEM® and 30μl Lipofectamine™2000 in 1.5ml Opti-MEM®.

2.4 PROTEIN ASSAY'S

2.4.1 PLASMA MEMBRANE EXTRACTION

One 10cm plate of HEK 293T cells were used per condition to isolate plasma membrane fractions using a protocol published by Bogan et al. (Bogan J, mol cell biol, 2001). Cells were rinsed twice with ice-cold phosphate-buffered saline (PBS, Gibco) and cells were lysed in TSD buffer (20mM Tris-HCl, 250mM sucrose, protease inhibitors). A preclearing spin was performed two times at 800g for 5min, the supernatant was collected and centrifuged at 16'000g for 20min. The pellet was resuspended in 1ml 1xTSD and pelleted once more. The pellet was then resuspended in 1ml of 1xTSD and layered on 2ml of a 1.12 M sucrose cushion, followed by centrifugation at 95'000g for 65min, the interface was taken and the samples were resuspended in TD buffer (20mM Tris-HCl, protease inhibitors). The resuspended fractions were again centrifuged at 60'000g for 10min and the pellet resuspended in NETN-buffer (20mM Tris-HCl pH7.5, 100mM NaCl, 1mM EDTA, 0.5% NP-40 and protease inhibitors). Protein concentration was measured and aliquots of the lysates were stored at –20°C.

2.4.2 LIPID RAFT EXTRACTION

Lipid rafts were prepared by detergent extraction on ice and flotation on sucrose gradients using a protocol previously described (Baumgartner et al, blood, 2003). About $2x10^7$ HEK293 T cells were rinsed with PBS, and lysed in 300ml of metabisulfite-Triton-X 100 (MBS-T) buffer (25mM MES, 150mM NaCl with pH6.5,

0.5% Triton X-100, protease inhibitors) for 30min on ice. The lysates were scraped from the dish with a rubber policeman and a sucrose gradient was produced. Therefore an equal volume of 85% sucrose solution in MBS (MBS-T without Triton X-100) was gently mixed with the cellular lysates to generate a 42.5% solution at the bottom of a SW55ti ultracentrifugation tube. The lysate/sucrose mixture was subsequently overlaid on ice with 2ml of a 35% sucrose solution (diluted in MBS) and 1ml of 5% sucrose solution (diluted in MBS) containing protease inhibitors. Ultracentrifugation was performed in a Beckman SW55Ti rotor at 47000rpm (200'000g) for 18h at 4°C. A visible band at the interface 5/35% of the sucrose gradient represented the DIGs. Fractions were taken out at this interface and at the bottom of the tube, where soluble proteins fractionate. Protein concentration was measured and aliquots of the lysates were stored at –20°C and the composition of the DIGs was analyzed by Western blot.

2.4.3 IMMUNOFLUORESCENCE

HEK293T cell monolayer was rinsed twice with cold PBS before fixing them with 3% Paraformaldehyde for 15min at room temperature. After three more washing steps with PBS cells are permeabilized in 0.25% Triton X-100 for 5min at RT. Permeabilized cells are washed 3x 5min with PBS and transferred on a plastic box covered with a hydrophobic surface. The primary AB was added in a small volume (35µl for one cover slip) of an appropriate antiserum dilution (anti-FLAG M2, mouse; 1:500) and incubated for 60min at RT. The cover slips are washed three more times with PBS and 35µl of the secondary antibody is applied (dilution 1:100) and incubated for 30min. at RT. The cover slips are finally rinsed 3 times with PBS and mounted with cell side down onto microscope slide. As mounting solution either use Mowiol (Hoechst). In order to allow slides to dry, they are stored o/n before viewing under the microscope. Longer storage of the cover slips in the dark at 4°C.

2.5 ANTIBODIES AND WESTERN BLOTTING

For Western blotting, transfected cells were diluted in SDS Laemmli buffer and boiled at 95°C for 5min-10min. Samples were electrophoresed in SDS-7.5% polyacrylamid gels (SDS-PAGE), and the proteins were transferred onto nitrocellulose membranes (Hybond^{TM}-ECL^{TM}). Membranes were blocked with 5% skim milk TBS/Tween buffer (20mM Tris-HCl pH=7.5, 0.5 M NaCl, 0.05% Tween 20) and mouse anti-Flag (Sigma), rabbit anti-caveolin-1 (Santa Cruz Biotechnology, Inc.) or mouse anti-human transferrin receptor (Zymed Laboratories Inc.) antibodies were diluted 1:500 in 5% skim milk TBS/Tween buffer and membranes were incubated for 1h at RT. Membranes were subsequently washed and incubated with either horseradish peroxidase-conjugated sheep anti-mouse or donkey anti-rabbit (Amersham Biosciences) as secondary antibody for 1h at RT. Chemiluminescence detection was performed according to the manufacturer's protocol (ECL detection kit, Amersham Biosciences).

2.6 MICE

Six to eight week old female C57BL/6 mice were injected intramuscularly with 100μg of DNA, 50μg into each leg. Mice were immunized four times in a three-week interval and blood samples were taken two weeks after each immunization.

2.7 EVALUATION OF MICE SERA

2.7.1 SARS-CoV INDIRECT IMMUNOFLUORESCENCE TEST

25μl of 1:50 diluted serum is pipetted on each rectangle of the reagent tray. The BIOCHIP is applied on the reagent tray. The serum is incubated for 30min with the cells at room temperature. BIOCHIP is flushed with PBS-Tween and incubated for 5min in PBS-Tween in a cuvette while shaking. 20μl of 1:50 TRITC donkey anti-mouse antibody are pipetted on each rectangle of the reagent tray

and the BIOCHIP is applied and incubated for 30min at RT. Cells are then washed with PBS-Tween and incubated for 5min in PBS-Tween in the cuvette while shaking. The cover slips were evaluated under the fluorescence microscope.

2.7.2 ELISA WITH RECOMBINANT SOLUBLE S PROTEIN OF SARS-COV

Sera from 25 C57Bl/6 mice were used to set up a baseline for the S protein ELISA-based IgG antibody test. Each well of a Nunc immunoplate (Roskilde, Denmark) was coated with recombinant soluble, FLAG-tagged Spike protein (diluted 1:100) over night at 4°C and then blocked for 3h in PBS with 2% skim milk. The serum samples were 1:100 diluted and added to the wells of the coated plate in a total volume of 100µl and incubated at RT for 2h. After three washes with 0.05% Tween 20 in PBS, 100µl of diluted horseradish peroxidase-conjugated sheep anti-mouse IgG (1:10'000) was added to the wells and incubated at RT for 1h. After washing with washing buffer three times, 100µl of diluted 3,3',5,5'-tetramethylbenzidine (Zymed Laboratories, Inc.) was applied to each well and incubated at RT for 20min. 50µl of 1 M H_2SO_4 was added, and the absorbance at 450nm and 540nm of each well was measured. Each sample was tested in triplicate, and the mean absorbance for each serum was calculated.

3 RESULTS

3.1 CHARACTERIZATION OF HA-TAGGED AND GPI-ANCHORED S-PROTEINS COMPARED TO WILD TYPE SF PROTEIN

The wild type S-protein was genetically modified by two different strategies. (1) The S-protein leader sequence was exchanged by the influenza A/PR/8/34 HA leader sequence. The first 16 AA of the S-protein were replaced by the first 16 AA of the HA protein. The construct was named HASF. (2) The transmembrane (TM) and cytoplasmic (CP) domain of SF and HASF were replaced by the sequence for the GPI-anchor attachment.

The expression of the different SARS-CoV S-proteins was characterized by transfection of HEK293 T cells with plasmids encoding the indicated constructs (depicted in Fig. 6). All constructs included a Flag epitope, to allow antibody detection, as no commercially available antibody against the S-protein existed. The DNA sequence of each gene was confirmed. The cell lysates were analyzed by Western blotting. As shown in Fig. 7 lysates from 293T cells transfected with the different vectors revealed a protein band with a size of approximately 190kDa, which is the predicted size for the S-protein.

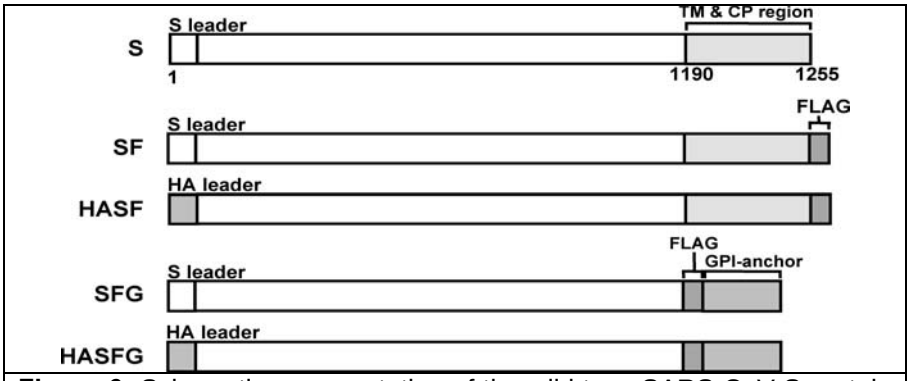

Figure 6: Schematic representation of the wild type SARS-CoV S-protein and the modified variants. Structures of the cDNAs used; SF: full length with a Flag-tag at the CT; HASF: S leader is replaced by the influenza HA leader; SFG: TM- and CP-region of the S-protein were replaced by the sequence for GPI-anchor; HASFG: HA leader and GPI-anchor.

The expression of SF was very weak, compared to HASF, and the expression efficiency was observed to be higher for HASFG than for SFG (Fig. 7). This led to the conclusion that the HA-tag might have an effect on the expression efficiency. According to their molecular weight, the S-GPI-fusion proteins run at a slower mobility than the full-length constructs (Fig. 7). This was explained by the exchange of the TM- and the CP-regions by the GPI-anchor sequence, which was encoded by a shorter sequence (depicted in Fig. 6).

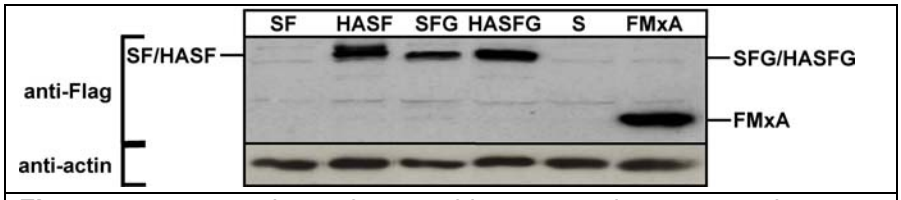

Figure 7: Expression of recombinant proteins; expression was determined by total protein extraction followed by Western blot analysis against the Flag-tag. S represents the S-protein without a tag, used here as a negative control, and FMxA stands for the MxA protein with a Flag epitope as positive control. Actin was detected as loading control.

An immunofluorescence assay with all different constructs showed the protein expression in individual cells (Fig. 8). Cells were permeabilized and expression of SF, HASF, SFG and HASFG in the whole cell was detected with an antibody against the Flag-epitope.

The expression levels of the individual constructs show significant differences in both analyses, western blotting and immuno-fluorescence. The expression level of HASF was higher than of SF, confirming the result from Fig. 8, identifying an effect of the HA-tag on the expression efficiency. The SFG-expression level was also inferior compared to HASFG, possibly because of the positive effect of the HA-tag. SFG displayed a higher expression level than SF, suggesting a positive impact of the GPI-anchor attachment sequence on the expression efficiency. In conclusion we state an influence on the expression level of the S-protein with exchange of any of the two genetic modifications used in this study. The HA-tag and the GPI-anchor signal sequence improved the expression of the protein and increased its potential as an antigen. Our finding was consistent with previous studies, which identified an increase in expression level by the influenza HA signal sequence on (Chao et al., 1987, Gething & Sambrook, 1982).

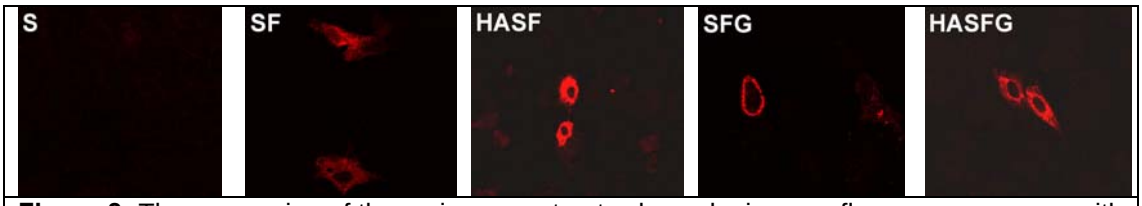

Figure 8: The expression of the various constructs shown by immunofluorescence assay with HEK293 T cells transfected with the plasmid encoding for the indicated protein. Cells were observed with a Zeiss Microscope equipped with a x40 magnification, 1.3 numerical aperture oil immersion lens.

3.2 Enhanced Expression of HA-Tagged SF

3.2.1 Western Blot Analysis

To confirm that the HASF construct showed an improved expression at the cell surface, a plasma membrane (PM) extraction was performed and the protein production was analyzed by Western blotting. To test overall expression levels of SF and HASF, we extracted total protein, as depicted in Fig. 9A. Quantitative analysis of the whole lysate showed a stronger expression of HASF compared to SF. To demonstrate the appearance of SF and HASF at the cell surface, equal amounts of proteins were loaded on the gel. SF and HASF both appear at the plasma membrane (Fig. 9B). We observed an increased amount of HASF at the plasma membrane, compared to SF. From these results we cannot conclude whether the difference between HASF and SF is higher in the PM-localization blot (Fig. 9B) than the total protein-blot (Fig. 9.A). Only a significant difference in the difference of expression level between HASF and SF of the two blots would confirm an effect of the HA-tag as a signal sequence. Ultimately the effect is explained by the altered sequence as sequence optimizing measure. However, the amount of HASF at the plasma membrane is significantly enhanced compared to SF, suggesting that HASF would be a more potent antigen than SF.
The bands with different mobility in Fig. 9B represent the multimeric and the monomeric form of the SF and HASF, respectively. Fig. 9B shows the same blot with the human transferrin receptor antibody (hTfR), which serves as loading

control and marker for membrane fractions. As shown in Fig. 9.B calnexin was detected as a marker for the ER, giving evidence that the plasma membrane extraction was not contaminated with membranes of the ER.

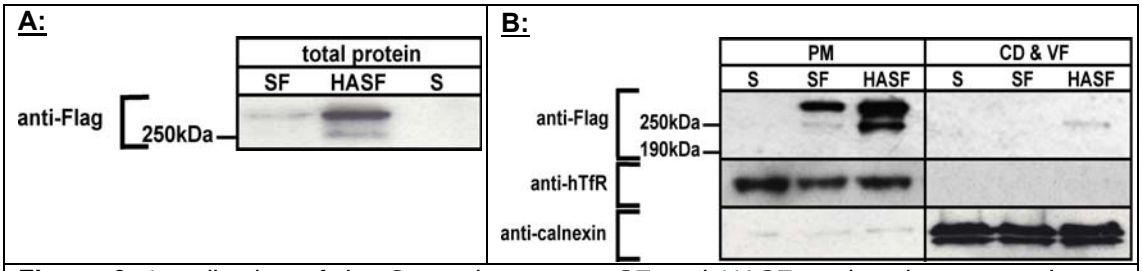

Figure 9: Localization of the S-protein mutants SF and HASF to the plasma membrane. Western blot analysis of HEK293 T cells transfected with the mammalian expression vector pVR1012 containing the desired fragment. Detection of the S-constructs by the Flag-tag. **A:** Total protein expression of SF and HASF. **B:** Plasma membrane extraction to show localization of SF and HASF. Detection of hTfR, loading control. Detection of calnexin, marker for the ER.

3.2.2 BIOINFORMATIC ANALYSIS

A bioinformatic study using the prediction software PSORT (Nakai & Horton, 1999, Nakai & Kanehisa, 1992) revealed a similar localization pattern of HASF and SF. PSORT is a program for detecting sorting signals in proteins and predicting their subcellular localization. Therefore it requests a full-length amino acid sequence and its sequence origin (gram-positive or gram-negative bacteria, yeast, animal or plant). PSORT functions with a simple algorithm -the k-nearest-neighbor method (Horton & Nakai, 1997). The predictive accuracy was assessed by ten-fold cross-validation, using 1531 Saccharomyces cerevisiae sequences encoded in nuclear DNA. The total accuracy of the prediction is 57% for these proteins.

As illustrated in Fig 10, SF and HASF were predicted to localize to intracellular membranes. 45% of the proteins localize in the ER, 33% in the Golgi and only 22% to the plasma membrane. This distribution is consistent with our previous data of the western blot analysis. The influenza glycoprotein HA was transported efficiently to the cell surface. Therefore, we compared the localization pattern of HA with the SARS-CoV S-proteins. HA was predicted to appear in equal amounts (33%) in the ER, the Golgi and the plasma membrane. Localization to the PM

was thus more efficient than of SF and HASF, suggesting the HA-sequence to contain additional protein signals relevant for the sorting to the cell surface. Both constructs will be used for a DNA vaccination study in mice.

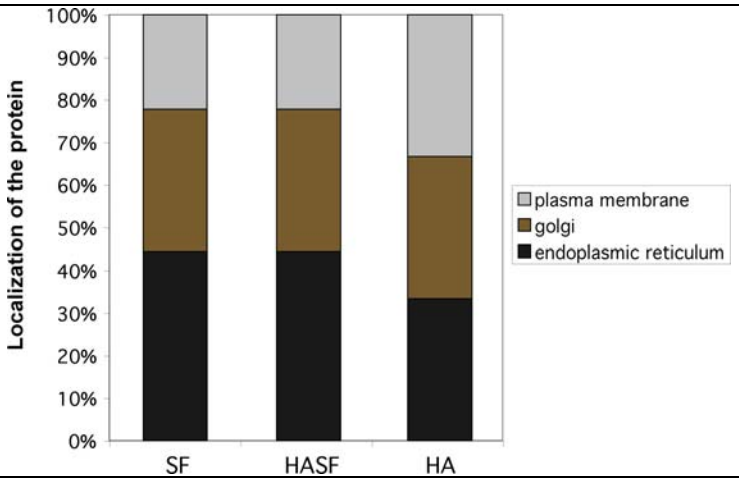

Figure 10: Cellular distribution of SF and HASF compared to the influenza A HA protein, using the PSORT prediction software from Kent Nakai (http://psort.ims.u-tokyo.ac.jp)

3.3 ISOLATION OF GPI-ANCHORED S-PROTEINS IN DIG'S

3.3.1 WESTERN BLOT ANALYSIS

Membrane rafts, defined as lipid-protein complexes insoluble in cold detergent solutions, because of their high lipid content and thus low buoyant density, can be isolated by density gradient ultracentrifugation. The low density allows DIGs to float in sucrose gradients upon extraction with Triton-X 100 at 4°C. This method allowed distinguishing between detergent-insoluble and detergent-soluble fractions to determine the co-fractionation of the overexpressed S-GPI proteins with other DIG-residing proteins. We compared the localization pattern of the S-GPI fusion proteins with the SF-protein and observed that GPI-constructs appeared in the detergent-insoluble fraction (DIF; Fig. 11). SF was not detected in this fraction, but in the detergent-soluble fraction (DSF; Fig. 11). The protein level of SFG in the DIF was lower than that of HASFG, suggesting a higher

amount of HASFG localizing in DIGs. However, total protein extracts showed a higher level of HASFG than SFG (Fig. 11). We further conclude, that this difference in localization to the DIGs originates from the HA-tag. The HA-tag is responsible for higher expression efficiency and thus more protein is available to be embedded into DIGs. The fraction of the detergent-soluble proteins showed the expression of the S protein and to a lower level of the S-GPI fusion proteins (Fig. 11).

SFG and HASFG were found in monomers and oligomers after the denaturing process. From this gel we could not conclude whether the band of a lower mobility represented a dimer or a trimer. The band with the oligomers indicates the high protein stability of the S-protein and the GPI-anchored S-protein complexes. Interestingly, the S-protein only appeared as oligomer, compared to the S-GPI fusion proteins, suggesting that the original S-protein sequence displayed a higher stability than the S-proteins with the GPI-anchor. The TM and CP region of the S-protein seemed to improve the stability of this protein. Fig. 11 showed the detection with anti-caveolin-1 and anti-hTfR as marker for DIGs and detergent-soluble membrane respectively. This suggested that the membranes were enriched for the marker proteins.

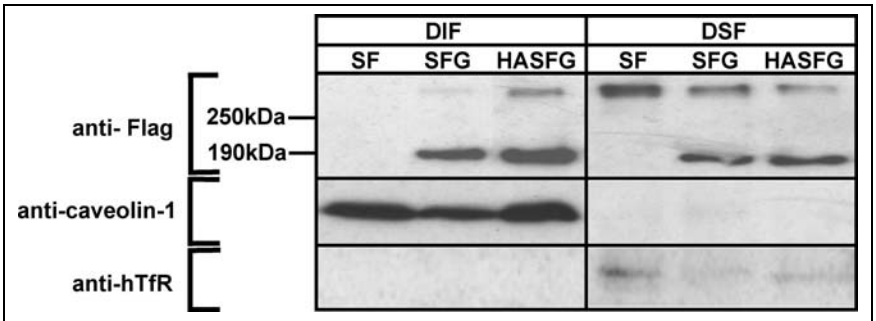

Figure 11: Isolation of GPI-anchored S-proteins in DIGs. Extraction of the detergent-insoluble fraction (DIF) and the detergent-soluble fraction (DSF) followed by Western blot analysis. SFG and HASFG were shown to co-localize in DIF.

3.3.2 BIOINFORMATIC ANALYSIS

In order to compare the sorting of the S-proteins attached to a GPI-anchor and the full length S-protein, a bioinformatic analysis was performed using the

PSORT prediction software (Fig. 12). SFG as well as HASFG were predicted to be transported to the cell surface to 67%. 33% remained to equal parts in the endoplasmic reticulum, vacuolar membranes and in mitochondria. The prediction with PSORT distinguished the S-protein sorted by the original pathway from the GPI-anchored S-protein by 45% (SF was sorted 45% less efficiently to the cell surface).

SFG as well as HASFG displayed an equal distribution to the different cellular compartments. This data indicated, that the sorting was not dependent on the S and the HA signal sequence at the N-terminus, but entirely dependent on the GPI-anchor attachment. In agreement we determined an enhanced expression of HASFG, compared to SFG and identified the presence of both recombinant proteins in DIGs. Therefore we speculate for an increased presentation of SFG and HASFG to the immune system. Both constructs will be used for a DNA vaccination study in mice.

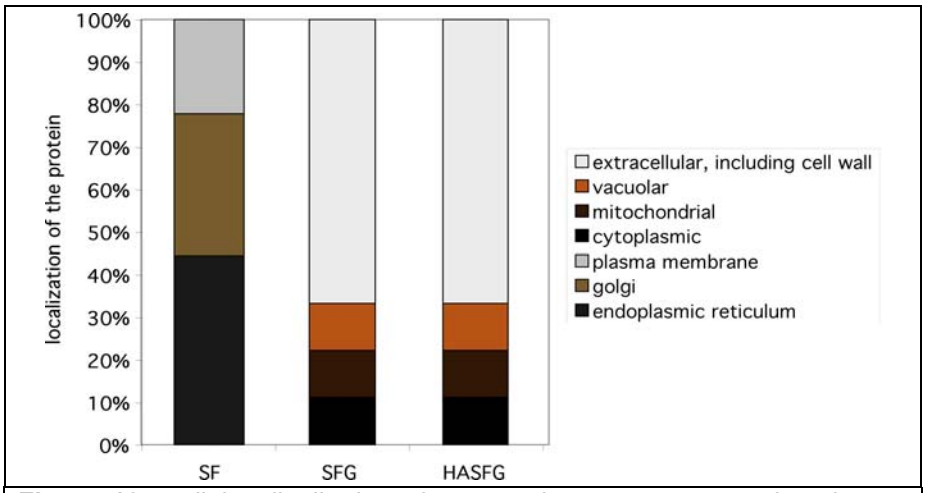

Figure 12: Cellular distribution of SFG and HASFG compared to the SF mutant, using the PSORT prediction software from Kent Nakai (http://psort.ims.u-tokyo.ac.jp).

3.4 Vaccination with HASF, SFG and HASFG significantly improved the Immune Response

In order to test the efficiency of the different S-protein constructs *in vivo*, mice were immunized with plasmid DNA (Fig. 13). Therefore, five mice per construct were immunized four times i.m. with a three-week interval with plasmid DNA

encoding for SF, HASF, SFG or HASFG. Five mice that received the empty vector served as background control. Serum samples were collected 7 days after each immunization. An ELISA was established to evaluate the humoral immune response evoked by the DNA encoding for SARS-CoV S-protein mutants, as described in materials and methods. Soluble S-protein (sSF) was chosen as coating material in the ELISA. Therefore HEK293T cells were transfected with pVR1012sSF and lysates were collected.

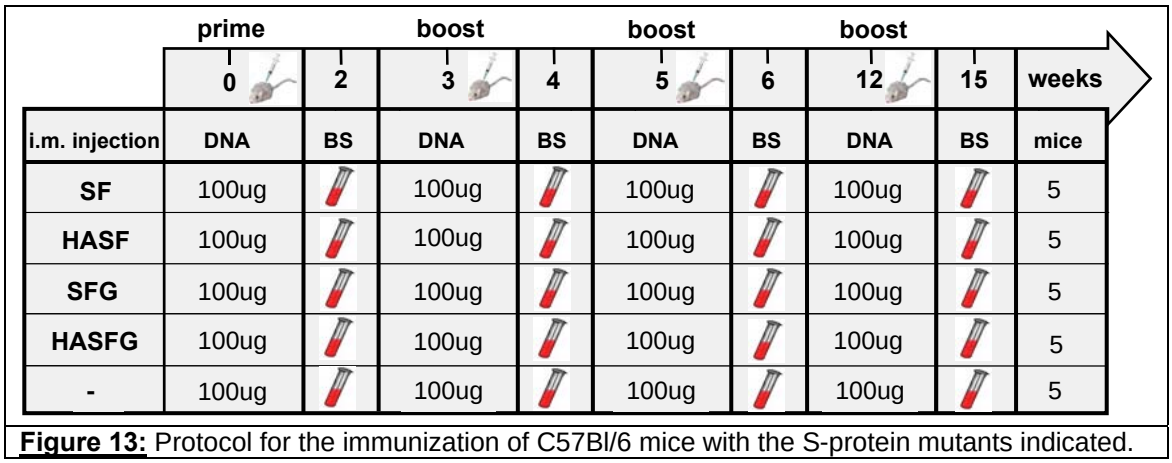

Figure 13: Protocol for the immunization of C57Bl/6 mice with the S-protein mutants indicated.

3.4.1 ELISA

ELISA analysis was performed to detect the S-protein specific antibodies of the sera. As shown in Fig. 14 all DNA plasmids produced antibodies binding the coating protein sSF. The immune response generated following immunization with p-SF was on the background level, together with the sera tested of the mice immunized with the empty vector. The antibody titer of mice immunized with p-HASF showed a two fold induction compared to the serum of the mice immunized with p-SF. Furthermore, p-HASFG induced a higher humoral immune response than p-SFG (0.5 versus 0.3). The ELISA results indicated, that p-HASFG displayed the best antibody response in comparison to the other vectors. p-HASF and p-SFG induced an equal level of S-protein specific antibodies. These data were consistent with the results from the expression analysis. Therefore, the improved antibody response of p-HASF compared to p-SF could be due to the enhanced expression of p-HASF shown in Fig. 9A and 9B. The

introduction of the GPI-anchor sequence was shown to be comparable with the introduction of the HA-tag. Both genetic modifications led to a similar improvement of the humoral immune response (comparing p-HASF and p-SFG). p-HASFG, including both genetic modifications, was the strongest antigen.

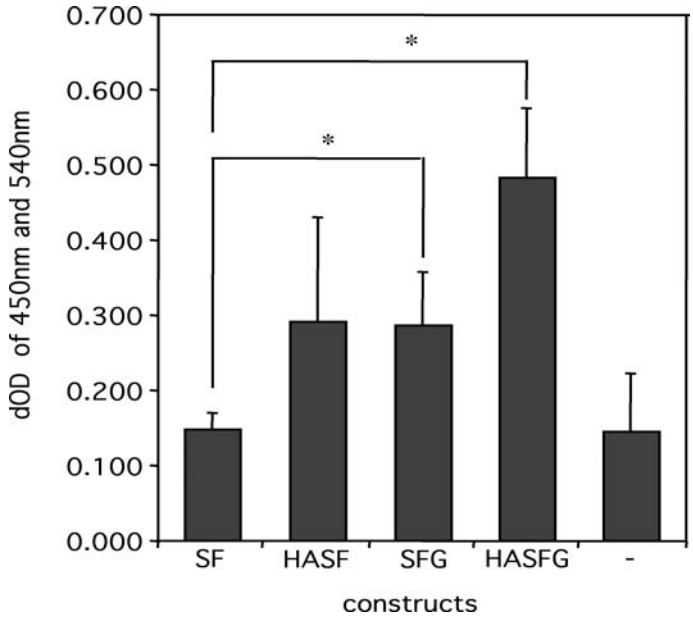

Figure 14: Immunization with SFG and HASFG significantly improved the immune response in C57BL/6 mice. Analysis of the sera by ELISA: Sera of C57BL/6 mice after the fourth i.m. immunization with the indicated expression plasmid encoding for the S-protein variants. The mice sera (1:100 diluted) were applied in triplicates and incubated for 1h. Anti-mouse antibody coated with HRPO was added in a 1:10'000 dilution. Absorbance was measured at 450nm and 540nm. The relative absorbance of 4 mice was substracted from the absorbance of the serum of non-immunized mice. Student t-test revealed: *p<0.05.

3.4.2 INDIRECT IMMUNOFLUORESCENCE ASSAY

In order to confirm the data obtained by the ELISA, an immunofluorescence assay was performed (Euroimmun AG). After the fourth i.m. immunization, serum samples of mice, were examined in a 1:50 dilution. The sera were applied to monkey cells, either infected or non-infected with SARS-CoV. Serum from a SARS-CoV infected patient served as positive control and serum from a healthy patient as negative control. Cells treated with positive control serum (hSARS-CoV) showed specific staining compared to cells treated with negative control serum (hmock). The fluorescent particles detected, were defined to be unspecific

(i.e. cell debris), as similar fluorescence signals were found on the slide with non-infected cells. Furthermore no compartmentalization and typical morphology could be observed. The serum from mice immunized with p-SF, p-HASF, p-SFG and p-HASFG showed specific fluorescence in some of the infected cells. Fig 15F and 15G showed an enhanced background staining. Cells treated with serum of p-HASFG-immunized mice showed augmented fluorescence, compared to the cells of p-SF-, p-HASF- or p-SFG-immunized mice. The non-infected cells did not provide the same staining for every slide. This might be explained by anti-mitochondrial or anti-nuclear antibodies (might be the case for mSFG and mHASFG, respectively) contained in the mice sera.

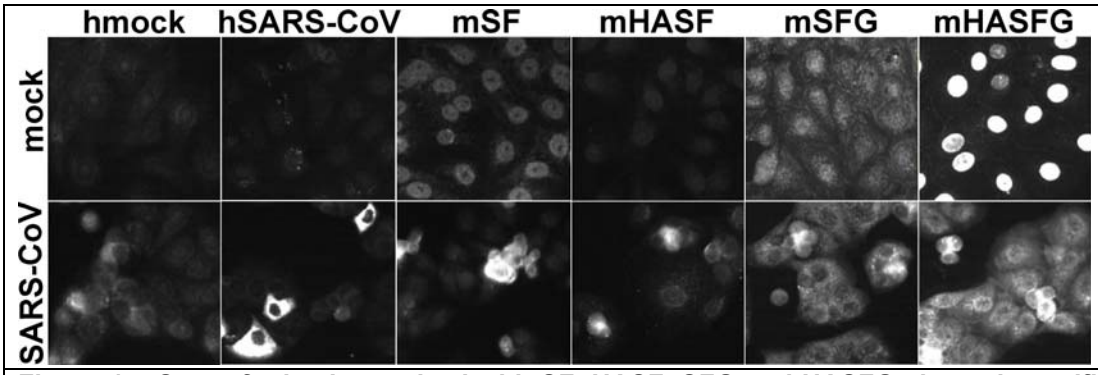

Figure 15: Sera of mice immunized with SF, HASF, SFG and HASFG showed specific interaction with SARS-CoV infected cells in an indirect immuno-fluorescence test (Euroimmun AG). Serum (1:50 dilution) was applied to the BIOCHIP containing SARS-CoV infected and non-infected cells. Upper panel: non-infected cells; lower panel: infected cells. Cells were stained with TRITC anti-mouse. Serum of a healthy patient and serum of a SARS-CoV infected patient served as negative and positive control, respectively; mSF-mHASFG are immunofluorescence pictures representing the cells incubated with sera of mice immunized with p-SF, p-HASF, p-SFG or p-HASFG.

The immunofluorescence data were consistent with the data we obtained with the ELISA. However we could not quantify a difference in fluorescence between SF- and HASF-serum and between SFG- and HASFG-serum. Together with the data extracted from the ELISA we identified the highest titer of SARS-CoV specific antibodies in the serum of mice immunized with p-HASFG. This finding confirmed our previous results, that both tags were required to significantly improve the antibody response.

4 DISCUSSION

The S-protein was identified to be the main antigen of SARS-CoV (Rota et al., 2003). Therefore we chose it as antigen in a DNA vaccine. DNA vaccinations have been tested for induction of cellular and humoral immune response against the SARS-CoV S-protein. Yang et al. (Yang et al., 2004) demonstrated that a DNA plasmid encoding the codon-optimized S-protein induced neutralizing antibodies, as well as a T-cell response. Protection from the SARS-CoV challenge in a murine model was mediated by the humoral immune response. Transfer of mice sera was sufficient to confer protection against SARS-CoV (Zhang et al., 2004). Therefore, DNA vaccination approaches with the SARS-CoV S gene might result in protection. Despite the fact that the S-protein represents the main target for vaccination, it is also known to be a weak antigen (Xiao et al., 2003). We therefore anticipated (1) the retention of the S protein through a retention signal, by a so far unknown mechanism (Lontok et al., 2004). (2) The interaction of the S-protein with other viral proteins withholding the S-protein inside the cell, as determined for S-proteins of other coronaviruses (Nguyen & Hogue, 1997). In this study we tried to overcome these limitations by genetic modifications.

S-proteins of other coronaviruses were identified to contain specific retention signals. Several responsible signal sequences were discovered. The infectious peritonitis virus S-protein was reported to be intracellularly retained in the ER because of its structure containing a dilysine motif (Vennema et al., 1993). The porcine coronavirus (Transmissible Gastroenteritis virus; TGEV) displayed a newly discovered sorting signal for intracellular localization (Schwegmann-Wessels et al., 2004). Retention of the coronavirus S-protein generally appears reasonable, considering the virus particle formation of this virus species intracellular. The budding process occurs at the cis-Golgi network/endoplasmic reticulum-Golgi intermediate compartment (ERGIC) (Hauri et al., 2000). This hypothesis is supported by the fact, that intracellular retention of the viral membrane proteins delays the time point of recognition of the infected cell by the

humoral and cellular defense systems. However, an increased level of the surface S-protein could promote syncytium formation and direct cell-to-cell spread of the infection (Lontok et al., 2004). The aim of this study was to optimize the synthesis, to increase the presentation of the S-protein as an antigen on the cell surface. In this study, the presentation of the S-protein on the cell surface was improved by two sequence modifications.

In order to enhance the expression and transport efficiency to the cell surface, the 5'-S-leader sequence at the amino terminal was replaced by the HA-leader sequence. Previous studies showed a different transport behavior for the full length HA-protein and the HA-protein missing the leader sequence. The HA-protein without a signal sequence was produced at low levels, located intracellularly, and was not glycosylated (Gething & Sambrook, 1982). The HA leader was thus increasing the transport efficiency through the ER, whereas truncated HA remained predominantly in the ER (Chao et al., 1987). In this study, the exchange of the S-leader sequence by the HA sequence (HASF), improved the overall expression efficiency in cell culture. If the over-expression of an intracellularly retained protein has exceeded a threshold value, the cellular interaction partners become saturated and are not able to retain the excess amount of the protein. This phenomenon has been reported for proteins that are retained intracellularly, e.g. in the endoplasmic reticulum-Golgi intermediate compartment (Hauri et al., 2000). This has to be taken in account for evaluation of transport efficiency caused by over-expression instead of specific targeting. We demonstrate an improved expression of HASF compared to SF and an increased expression of HASF at the plasma membrane compared to SF. This experimental result was consistent with the data of the studies mentioned above. The sequence of the HA leader was examined to be responsible for improved expression. Mice immunized with the DNA plasmid encoding for HASF (p-HASF) showed an enhanced S-specific antibody titer, compared to mice immunized with p-SF. We could not determine, whether the increased localization of HASF to the cell surface was due to the potency of the HA-leader sequence as a signal sequence, or whether the HA-tag was responsible for an enhanced expression

level due to optimized nucleotide sequence and thus enhanced translation efficiency. The insertion of the HA-leader sequence appeared to have a limited effect on trafficking of the S-protein, as the difference between SF and HASF expression in total protein extracts and PM-extracts was not significantly different. This observation was consistent with the data of Yang and co-workers (Yang et al., 2004). In that study, the SARS-CoV S-protein leader sequence was exchanged by the leader sequence derived from the interleukin-2 gene (IL-2). The IL-2 leader sequence did not alter the expression behavior of the S-protein (Yang et al., 2004). The data of the bioinformatic study using the software PSORT, did not determine any difference in the sorting of SF and HASF. The same analysis determining sorting of the GPI-anchored S-proteins revealed equal distribution of SFG and HASFG to diverse cellular compartments. This is an indication for the minor relevance of the leader sequence in trafficking. Thus, retention signals of the S-protein other than the leader sequence could be responsible for the weak difference in redistribution between SF and HASF, observed in Fig. 9A and 9B. Alternatively it might be an artefact. Lontok et al. identified a dibasic (KXHXX) intracellular localization signal at the very C-terminal amino acids, preceding the STOP codon of the SARS-CoV S-protein detected by the GPI-anchor attachment (Lontok et al., 2004).

The HA-protein itself is known to be a stronger antigen than the S-protein (Xiao et al., 2003). We speculate that the improvement of the S-protein as an antigen originates in the expression efficiency and the following improved presentation at the plasma membrane and thus to the immune system.

There is no information on viral interaction partners of the SARS-CoV S-protein during protein synthesis or virus assembly, which could affect the retention of the S-protein in an intracellular compartment. Nevertheless, this lack of information should be taken into account, since complex formation between the M-protein and the S-protein were shown to have an effect on the translocation of the S-proteins of other coronaviruses (Nguyen & Hogue, 1997). The interaction with other proteins may be important for the antigen presentation. Future analysis of these interactions should address the hypothesis comprehensively. The impact of

complex formations between the S-protein and cellular proteins was not examined in this study. Viral proteins were not considered as interaction partners of the S-protein, due to the lack of the other viral proteins in this vaccination strategy.

In order to facilitate the transport of the S-protein to the cell surface, we also designed an S-protein mutant in which the transmembrane and the cytoplasmic domain were exchanged by the sequence responsible for GPI-anchor attachment. This modification should allow targeting to lipid rafts (Brown & Waneck, 1992, Brown, 1992, Brown & Rose, 1992) and therefore increased the presentation on the cell surface. In addition it should prevent the involvement of the predicted dibasic retention signal. Furthermore, mice immunized with the truncated S-protein lacking the last 13 nucleotides, led to improved immune responses compared to the full length construct (Yang et al., 2004).
The attachment of the GPI-anchor sequence enabled the extraction of the S-protein from detergent-insoluble fractions, which included lipid rafts. Lipid rafts represent micro-domains presenting proteins in high density. Moreover these proteins are known to show an increased lateral mobility and an extended half-life of cell surface proteins (Premkumar et al., 2001). GPI-anchors are thus thought to potentate the possible immune response of an antigen (Bohme & Cross, 2002). Caveolae, the second kind of lipid-enriched membrane domains, display a highly organized structure containing caveolin-1 and are therefore visible under the electron microscope (50-70nm; Palade, 1953), compared to lipid rafts which do not contain any structures providing contrast. Most of the data obtained until now demonstrated the functional roles of lipid rafts based on membrane solubilization in suitable detergents and isolation of the lipid-enriched detergent resistant microdomains by density gradient ultracentrifugation. Only recently there have been major improvements in visualization of lipid rafts (Prior et al., 2003). Due to technical difficulties we could not perform lipid raft detection by microscopy. However, recently published data did show the existence of lipid rafts in living cells and also the presence of GPI-anchored proteins in these rafts.

Our results are interpreted taking in account the recent findings (Monastyrskaya et al., 2005, Wilson et al., 2004).

Our experimental data showed that the S-GPI proteins were associated with the detergent-insoluble membranes (DIF). The GPI-anchored S-proteins were thus present in lipid rafts. The preparation of DIFs by sucrose gradient flotation led to the co-extraction of caveolin-1, a characteristic protein of caveolae. The extraction of DIGs does not allow spatial discrimination of the two microdomain subtypes, lipid rafts and caveolae. The presence of caveolin-1 in DIF can be explained by the co-extraction of lipid rafts and caveolae by detergents and analysis by the sucrose gradient ultracentrifugation method. As shown in Fig. 10 the DIF fractions also contained caveolin-1. SFG as well as HASFG were detected in DIFs. SF did not show any co-localization with the GPI-anchor proteins in the DIGs, suggesting that the localization of the S-protein mutants in lipid rafts is entirely dependent on the GPI-anchor. Our experimental data were consistent with the data of other research groups, where GPI-anchored proteins were identified in lipid rafts (Bairoch & Apweiler, 1997, Brown & Waneck, 1992, Brown, 1992, Brown & Rose, 1992). SFG and HASFG also appear in the detergent-soluble fraction (DSF; Fig. 10). The presence of SFG and HASFG in the DSF could be explained by the over-expression. Over-expression of secretory proteins has been shown to affect the trafficking of these proteins (Nal et al., 2005). This may explain the presence of exogenous SFG and HASFG in this fraction.

SF as well as SFG and HASFG appeared as multimeric complexes despite denaturation by SDS-treatment. The oligomerization of the SARS-CoV S-protein was found to be very stable. The oligomers of the S-protein with the original TM and CP region displayed resistance to denaturating conditions as SDS and β-mercaptoethanol treatment. The stability of the SF-oligomers was higher than that of the GPI-anchored S-oligomers. Further experiments are required to show the improved stability of these proteins *in vivo*.

Our experimental data of mice sera were consistent with the results obtained by the cell culture study. The difference in the immune response between SF and HASF, and between SFG and HASFG, can be explained by the variations in the expression level, which might be comparable to the expression level observed in cell culture. In cell culture we have shown a higher protein expression for HASF than for SF and the same for HASFG and SFG. The enhanced expression was shown to be consistent with the improved immune response of HASF and HASFG compared to SF and SFG, respectively. The antibody titer of p-HASF immunized mice was twice as high as the titer of mice immunized with p-SF. The combination of the HA leader sequence and the GPI-anchor improved the expression and possibly also the antigen presentation, compared to the S-proteins containing only either the HA leader sequence or the GPI-anchor, *in vitro*. This subsequently led to a stronger humoral immune response in mice. The presence of both modifications in the S-protein (HASFG) increased the antibody titer three fold, compared to SF, as shown in Fig. 13.
The results of the ELISA experiment show a significant improvement of the immune response upon vaccination with p-HASFG. With these experimental data, we identified HASFG as a potent immunogen. The DNA vectors used in this study might display a synergistic effect in combination with a viral vector, a protein or an inactivated virus boost.

Taken together, with this DNA vaccination strategy to combat the SARS-CoV, we showed a significantly enhanced immune response in mice, immunized with HASFG. The immune response raised by the different recombinant proteins used in our study was dependent on (1) the expression level of the protein and (2) the sorting to the lipid-enriched microdomains. The sorting of the proteins in this study was dependent on the GPI-anchor signal sequence and the retention signal of the S protein. Therefore, HASFG displayed the strongest humoral immune response, containing the HA-leader for enhanced expression and the GPI-anchor for efficient antigen presentation on the cell surface.

Besides the humoral immune response, DNA vaccines raise also a cellular immune response (Kirman & Seder, 2003, Majumder et al., 2003, Wilson et al., 2003). However, our investigations did not allow identification of the cellular immune response, which might be induced by our vaccination protocol.

Our findings together with the results of other studies (Chao et al., 1987, Fanning et al., 2003, Gething & Sambrook, 1982) raise the question, whether the HA-leader and the GPI-anchor could be used as a model. We speculate that HA-tagged and GPI-anchored antigens may induce generally a higher immune response than conventional antigens. The exchange of the original leader sequence by the HA-leader enhances greatly the expression efficiency. The attachment of a GPI-anchor alters the trafficking of a given protein and directs it towards DIG's on the cell surface. This process is dependent on the GPI-anchor and not on the sequence of the target antigen. The improved immune response of the GPI-anchored S-proteins originated thus in the localization of the protein on the cell surface, in the export efficiency, the density of the antigen in a single raft domain and in the lateral mobility given by the anchor. These characteristics would provide an optimized presentation of the antigen to the immune system. We might therefore speculate, that any other given antigen, naturally not co-localizing with DIG's, could show an improved immune response upon attachment of the HA-leader and linkage to a GPI-anchor.

5 OUTLOOK

Up to date there has been no successful vaccination reported against the SARS-CoV. Preclinical trials of several studies showed protection upon mice challenge with the SARS-CoV, but the following clinical trials were all insufficient in their immune response. This should demonstrate the difficulties in vaccination development for this virus, taken into account the numerous attempts made in the past three years.

The results showed in this study identified the potential of the HA-tag and the GPI-anchor as genetic modifications increasing the humoral immune response. These two sequence modifications did not provide the necessary level of neutralizing antibodies for protection of mice. However, the potency of this vaccination strategy could be enhanced by the synergistic effect of a combination treatment. A synergistic effect could improve the humoral and cellular immune response. This combination treatment could consist of the DNA vaccine as a prime, and a viral vector, a protein or an inactivated virus as a boost. DNA priming and protein boosting have been shown to increase antibody responses (Coban et al., 2004, Konishi et al., 2003, Letvin et al., 1997).

Furthermore, the shut-off of the host cell protein synthesis after natural virus infection should be considered. This problem could be overcome by sequence optimization, which may concern the coding gene sequence, the non-coding mRNA leader sequence or the promoter/enhancer sequence. We may speculate about further improvement of our S-GPI anchor vaccine after sequence optimization.

PART II

6 INTRODUCTION

6.1 THE INTERFERON (IFN) SYSTEM

Interferon's (IFNs) were discovered as antiviral agents during studies on virus interference by Isaacs and Lindenmann in 1957 (Isaacs and Lindenmann, 1957). IFNs are a family of cytokines that act early in the innate immune response and represent the first line of defense after virus infection. IFNs are classified into two subtypes: the type I IFNs, which are also known as viral IFNs and include IFN-β, IFN-ω and several IFN-α genes. The type II IFN also known as immune IFN comprises a single gene that codes for IFN-γ. Recently, the type III IFNs a novel class of cytokines was discovered and named IFN-λ or interleukin (IL) 28/29. This new IFN family comprises three members: IFN-λ1, IFN-λ2 and IFN-λ3. The type II IFNs bind to a unique receptor. Despite this, they share many functional characteristics with IFN-α/β (Ank et al., 2006). The viral IFNs are induced by virus infection, whereas the type II IFN is induced by mitogenic or antigenic stimuli. Most types of virally infected cells are capable of synthesizing IFN-α/β in cell culture. However, plasmacytoid dentritic cells (pDCs) represent the natural IFN-α producing cells of the body (Diebold et al., 2003). IFN-α induces IFN-γ production in natural killer cells (NK) and T cells and stimulates their cytotoxic capacity (Matikainen, 2001)(Samuel, 2001). Furthermore IFN-α activates macrophages and stimulates dentritic cell maturation (Veckman, 2006).

IFNs are indispensable for vertebrates to control viral infections. Mice with a targeted deletion in the type I IFN receptor were unresponsive to IFN-α/β and succumb to viral infections despite having a normal adaptive immune system (Muller et al., 1994, Ryman et al., 2000). The disruption of a single IFN-induced

gene may cause complete loss of innate immunity against a particular type of virus. Inbred mice with a defect in their IFN-regulated *Mx1* gene show an increased susceptibility to influenza and influenza-like viruses (Lindenmann, 1964, Staeheli et al., 1988). Introduction of mouse or human Mx is sufficient to reconstitute partially resistance of susceptible mice (Pavlovic et al., 1995). Likewise, humans die of viral disease at an early age if they happen to acquire genetic defects in the IFN system (Dupuis et al., 2003).

IFNs can induce the synthesis of more than 400 cellular proteins, called IFN-stimulated genes (ISGs), including enzymes, signaling proteins, chemokines, transcription factors, heat shock proteins, and apoptotic proteins (Der et al., 1998).

6.1.1 GENE INDUCTION OF TYPE I IFN

Two events are required to trigger an effective anti-viral innate immune response: (1) the detection of the invading virus by pattern-recognition receptors (PRR) and (2) initiation of protein signaling cascades that regulate the synthesis of IFNs.

Viral infection is sensed by two independent receptor systems that trigger the production of type I IFN (Fig. 16). The type I IFNs exhibit a wide breath of biological activites: antiviral, antiproliferative, stimulation of cytotoxic activity on a variety of cells of the immune system (T cells, NK, monocytes, macrophages, and dentritic cells) (Pestka et al., 2004). These receptor systems localize to different compartments and recognize different viral particles as ligands. Toll-like receptors (TLR) represent one of the receptor systems that induce IFN-α/β as well as the newly discovered IFN-λ production (Ank et al., 2006). They are associated with the cell membrane in endosomes and and represent therefore the extracytoplasmic pathway for pathogen sensing. TLR7/8 are receptors for G/U rich single-stranded RNA (Heil et al., 2004) and TLR9 recognizes unmethylated CpG DNA present in DNA viruses (Bauer et al., 2001). TLR3 represents a more general sensor of viral infection through detection of double-stranded RNA, a by-product of viral replication and transcription for both RNA and DNA viruses (Alexopoulou et al., 2001). The TLR pathway induces IFN

production through several signaling proteins that ultimately lead to the activation of transcription factors ATF-2/c-Jun, NF-κB, IFN regulatory factor 3 (IRF3) and IRF7.

The second receptor system senses dsRNA by RNA helicases localized in the cytoplasm. Two such sensors have so far been described: the retinoic acid inducible gene I (RIG-I;(Yoneyama et al., 2004) and melanoma differentiation-associated gene5 (Mda5). RIG-I is essential for the production of IFNs in response to RNA viruses including paramyxoviruses, influenza virus and Japanese encephalitis virus (JEV), whereas Mda5 is critical for picornavirus detection (Kato et al., 2006). RIG-I and Mda5 activate NF-κB and IRFs through the recently identified adaptor protein MAVS (mitochondrial anti-viral signaling protein; (Andrejeva et al., 2004, Seth et al., 2005). How MAVS is regulated by RIG-I/Mda5 and how it activates downstream kinases remains largely unknown. The mitochondrial localization of MAVS seems to be essential for its signaling function, how mitochondria play a role in activation of kinases remains to be investigated. Synthetic dsDNA activates a MAVS dependent pathway, although a receptor responsible for DNA recognition has not been identified. Evidence for a TLR and RIG-I independent pathway in recognition of cytoplasmic DNA has recently been obtained (Ishii et al., 2006, Stetson & Medzhitov, 2006).

Plasmacytoid DCs (pDCs) mainly use mechanisms for the induction of IFNs that do not involve RIG-I (Kato et al., 2006). pDCs are specialized IFN producers and represent a major source of IFN-α in humans (Colonna et al., 2002). In pDCs, the TLR system appears to play a more important role in the induction of type I IFNs. This suggests that pDCs have developed specialized mechanisms for the detection of viruses. Moreover it is well known that pDCs are difficult to infect with viruses. Therefore, viral recognition in pDCs may mainly depend on endocytosis of viral particles rather than direct infection.

Secreted IFN-α/β interact with a receptor on the cell surface, resulting in the activation of the IFN-α/β signaling cascade. This activation ultimately results in expression of antiviral active proteins.

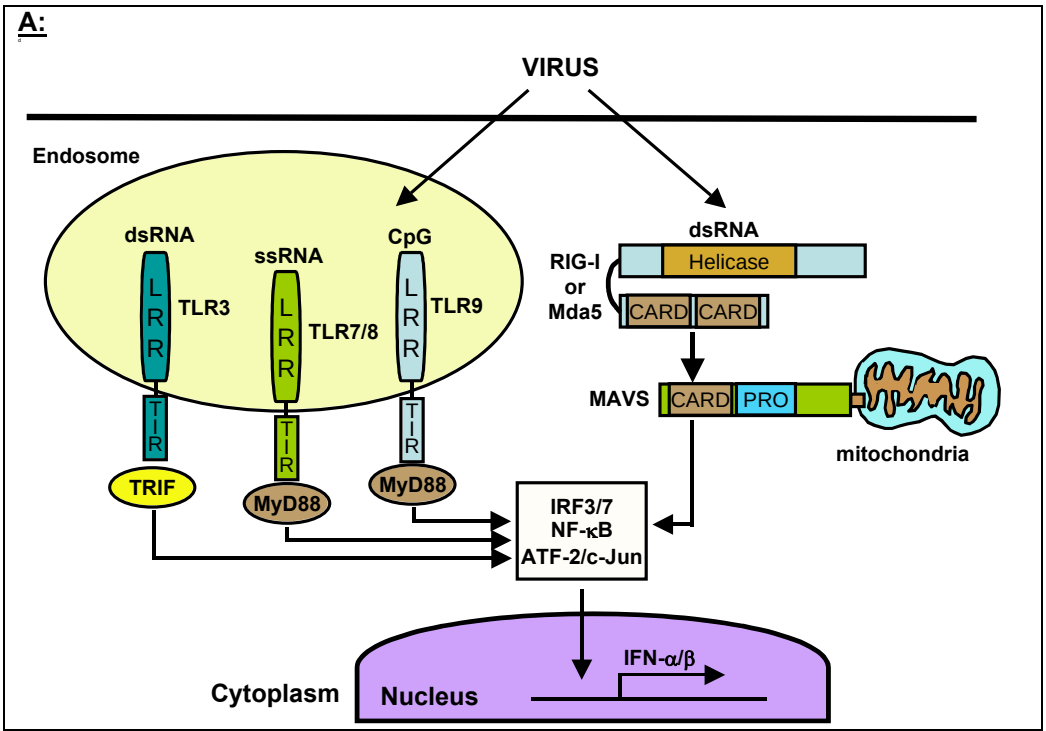

Figure 16.A: Two independent signaling pathways mediate the IFN-α/β synthesis: (1) TLR pathway: endosomal TLR3, 7, 8 and 9 activate IFR3/7, NF-κB and ATF-2/c-Jun. (2) dsRNA leads to activation of IRF3 and NF-κB by RIG-I and MAVS (adapted from Seth R. et al, Cell Research, 2006); **B:** Induction of IFN-α/β production in pDCs activated by TLR signaling (adapted from Haller O. et al, Virology, 2006).

6.1.2 IFN-α/β INDUCED SIGNAL TRANSDUCTION

Secreted IFN-α/β species can interact with the IFN-α/β receptor (IFNAR) on the surface of the infected cell or of neighboring cells. IFNAR sends a signal to the nucleus through the JAK-STAT pathway, which induces expression of genes with antiviral activities. Fig. 17 illustrates the individual steps in the IFN-α signaling pathway.

There are two subunits of the IFN-α/β receptor: IFNAR1 and IFNAR2 (Novick et al., 1994). IFNAR1 and IFNAR2 heterodimerise upon stimulation by IFN-α/β. The cytoplasmic tails of the two subunits of IFNAR are associated with the JAK tyrosine kinases Jak1 and Tyk2. Jak1, when bound to IFNAR2, can phosphorylate and activate Tyk2, bound to IFNAR1 (Gauzzi et al., 1996). Activated Tyk2 can then cross-phosphorylate Jak1. Activated Jak1 and Tyk2 are responsible for the sequential phosphorylation of IFNAR1 and two signal

transducer and activator of transcription proteins (STAT): STAT1 and STAT2. Phosphorylation of IFNAR1 by Jak1 allows the signal transducer molecule STAT2 to bind to the receptor. This results in phosphorylation of STAT2 creating a binding site for STAT1. Bound STAT1 is phophorylated and together with STAT2 dissociates from the receptor complex as a heterodimer (Leung et al., 1995). The P-STAT1/P-STAT2 complex interacts with IRF9 (p48) forming the IFN-stimulated gene factor (ISGF3) and translocates to the nucleus. ISGF3 facilitates transcription of IFN-stimulated genes (ISGs) by recognizing and binding to a sequence called the IFN-stimulated response element (ISRE).

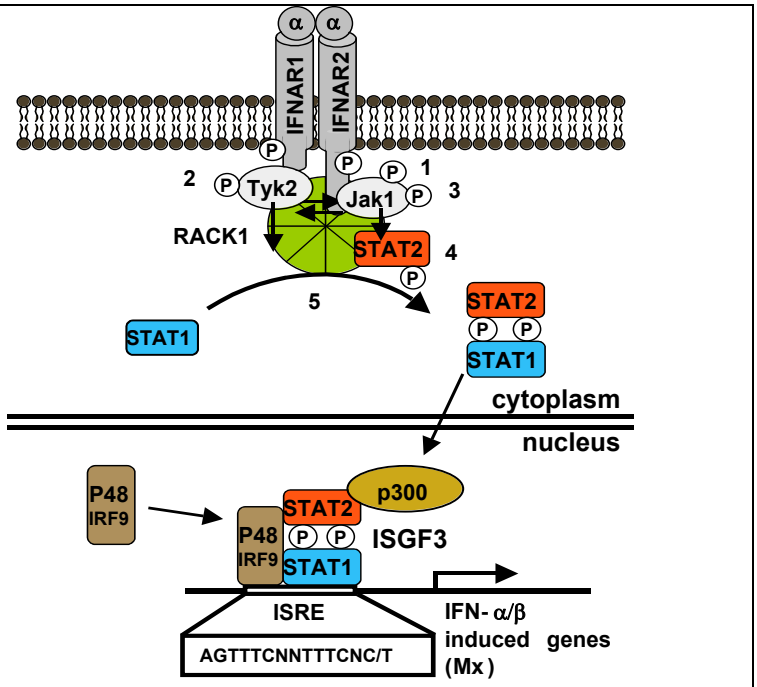

Figure 17: IFN-α/β signaling pathway. IFN-α triggers the IFN-receptor (IFNAR) and activates the signaling cascade resulting in activation of expression of IFN-inducible genes like Mx.

The receptor-activated kinase 1 (RACK1) is playing a pivotal role in this signaling mechanism. RACK1 is a scaffold associated with Tyk2 and Jak1 (Usacheva et al., 2003), as well as with IFNAR2 and STAT1 (Croze et al., 2000). The interaction between IFNAR and STAT1 is not direct, but mediated by RACK1 (Kubota et al., 2002, Stark et al., 1998). RACK1 is required for recruitment and activation of IFN-αinduced STAT1 activation and transduction of IFN-α signaling

(Yokota et al., 2003). Unlike the interaction between RACK1 and STAT1, RACK1 remains associated with the Janus kinases upon phosphorylation (Usacheva et al., 2003).

IFN-α/β mediated activation of ISGF3 leads to transcriptional stimulation of more than 100 cellular genes (Der et al., 1998). Among them are the well characterized IFN-inducible antiviral enzymes myxovirus resistance protein (Mx), protein kinase R (PKR) and 2'5'-oligoadenylate synthetase (OAS). PKR and 2'5'-OAS are not only transcriptionally activated by IFN-α/β but also directly by dsRNA (Sarkar & Sen, 2004).

6.1.3 Interferon Stimulated Genes (ISGs) with Antiviral Activity

6.1.3.1 Mx Proteins

Mx proteins are IFN-inducible GTPases that belong to the dynamin superfamily of large GTPases (Haller & Kochs, 2002) and display an antiviral activity. They were discovered in an inbred mouse strain that showed a high degree of resistance towards infection with influenza A virus. Two distinct Mx GTPases are expressed in humans, MxA and MxB. MxA is localized in the cytoplasm and displays, unlike MxB, antiviral activity. MxA has the ability to associate with viral nucleocapsids from different virus families including Orthomyxoviridae, Paramyxoviridae, Rhabdoviridae and Bunyaviridae, inhibiting their transport and/or biological properties, therefore blocking viral replication (Weber et al., 2000). Embryonic fibroblasts derived from transgenic mice expressing human MxA cDNA showed reduced susceptibility for influenza A and VSV (Pavlovic et al., 1995). MxA has no other known functions than the antiviral activity.

Mx GTPases are not constitutively present in the cells and their expression is not directly inducible by viruses or dsRNA (Bazzigher et al., 1992). Mouse and human Mx genes contain an ISRE in their upstream regulatory region (Horisberger et al., 1990) and are under tight transcriptional control, stimulated exclusively by IFN-α/β via the JAK-STAT signaling pathway (Dupuis et al., 2003).

Therefore, Mx is considered to be an excellent marker for IFN action in clinical settings (Roers et al., 1994).

After induction, Mx mRNA is rapidly accumulated and reaches highest levels at 5-10 hours post IFN-α induction and returning to basal levels within 24-48 hours post IFN-α induction (Aebi et al., 1989). Mx proteins appear to be very stable in cells. Accumulation of Mx proteins reaches its maximum between 24 and 48 hours post infection. The protein levels stay high for several days, the half-life of MxA exceeding 48 hours (Ronni et al., 1993, Ronni et al., 1995).

6.1.3.2 DS-RNA ACTIVATED PROTEIN KINASE R (PKR)

PKR is a serine/threonine protein kinase induced by dsRNA-mediated autophosphorylation. Activation of PKR results in phosphorylation and inactivation of the translation initiation factor eIF-2α (Williams, 1999). As a result, protein synthesis is blocked and viral replication inhibited.

6.1.3.3 2'5'-OLIGOADENYLATE SYNTHETASE (OAS)

Expression of OAS is strongly induced by IFN-α/β and requires the presence of dsRNA for activation (Hovanessian et al., 1977). Activated OAS catalyzes the polymerization of ATP into 2',5'-linked oligoadenylates of various lengths. These oligonucleotides bind and activate RNase L, a cellular endonuclease which degrades cellular and viral RNA (Malathi et al., 2005) and thus is responsible for the inhibition of viral replication (Rebouillat & Hovanessian, 1999).

6.1.4 VIRAL EVASION

Despite the fact that high vertebrates have developed an efficient innate and adaptive immune system, different viruses represent a continuous threat to humans, especially when no preventive measures, such as vaccination, are applied. Viruses developed counteracting measures, which allow the virus to escape the IFN system of the host organism (Basler et al., 2000, Goodbourn et al., 2000). Different virus families are characterized by the presence of specific viral IFN antagonists lacking homology with those from other families.

Nevertheless, viral IFN antagonists focus on either of the four strategies: **(1)** Viral **host shut-off**, **(2)** interference with the **IFN induction pathway** (IRF3 pathway), **(3)** interference with **IFN signaling** (JAK-STAT pathway) or **(4)** interference with the **IFN effector proteins** (PKR pathway) (Weber et al., 2003).

6.1.4.1 VIRAL HOST CELL SHUT-OFF

Host shut-off is a virus-mediated inhibition of the cellular machinery at a transcriptional level. It has been proposed for some viruses, that the main reason of the host shut-off is suppression of the IFN production (Ferran & Lucas-Lenard, 1997, Lyles, 2000, Stojdl et al., 2003). Inhibition of the innate immune response facilitates the infection of the host cell. The production of inducible genes (like IFN production) is blocked by the inhibitory effect of the virus on the host gene transcription. The housekeeping genes display the decline in mRNA much later in infection (Billecocq et al., 2004). This is beneficial to the virus, as viruses depend on a functional cellular environment and cannot afford to disturb the entire cellular metabolism, risking the loss of the host.

This general block of transcription in the host cell is a strategy only used by viruses with a lytic replication cycle. The mechanisms by which the host cell is shut off are very diverse. The NSs protein of the Rift Valley Fever Virus (RVFV) impairs proper assembly of the RNA Polymerase II (Le May et al., 2004), whereas the influenza A NS1 protein can bind to cellular mRNAs and impair their post-transcriptional processing and nuclear export (Chen et al., 1999, Fortes et al., 1994, Li et al., 2001).

6.1.4.2 VIRAL INTERFERENCE WITH THE IFN INDUCTION PATHWAY

A prominent target to counteract the IFN system is the dsRNA, a characteristic by-product of viral replication. Proteins from many unrelated viruses inhibit activation of IRF3. They prevent IFN-α/β production by initial phosphorylation of IRF3 and subsequently, its dimerization and translocation to the nucleus. Examples are the VP35 protein of Ebola virus (Basler et al., 2003), and the NS1/NS2 complex of respiratory syncytial virus (RSV) (Bossert et al., 2003). Simian Virus 5 (SV5) V protein also inhibits activation of IRF3 (He et al., 2002,

Poole et al., 2002). Influenza and poxviruses encode dsRNA binding proteins NS1 and E3L that prevent IRF3 activation (Garcia-Sastre et al., 1998b, Talon et al., 2000, Wang et al., 2000), at least in part by sequestering dsRNA and preventing stimulation of cellular sensors of dsRNA, such as RIG-I and Mda5 (Garcia-Sastre & Biron, 2006). Hepatitis C virus blocks the TLR3 and RIG-I mediated activation of IFN by cleavage of MAVS and TRIF by the viral NS3/4A protease (Meylan et al., 2005).

6.1.4.3 INHIBITION OF IFN-α/β SIGNALING

Many viruses suppress the specific IFN signaling pathway to prevent ISG expression (Fig. 18). Poxviruses secrete a soluble form of the IFNAR that sequesters type I IFN before it can bind to the natural IFNAR (Symons et al., 1995). The V protein of SV5 and Mumps viruses (MuV) inhibits the JAK-STAT pathway by inducing the degradation of STAT1 (Didcock et al., 1999b). MuV V promotes disruption of the IFN receptor RACK1 interaction by binding to RACK1 with a high affinity, resulting in the subsequent release of STAT1 from IFNAR (Kubota et al., 2002). The measles virus (MeV) shows suppression of Jak1 phosphorylation induced by IFN-α. RACK1 was found to act as interaction partners of two viral proteins: MeV and MeC.

The scaffold protein RACK1 can associate with various viral proteins, including adenovirus E1A protein (Sang et al., 2001), Epstein-Barr virus BZLF1 protein (Baumann et al., 2000), human immunodeficiency virus-1 Nef protein (Gallina et al., 2001), and influenza A virus M1 protein (Reinhardt & Wolff, 2000). In the latter, RACK1 acts as a scaffold for the phosphorylation of influenza A M1 by PKC (Reinhardt & Wolff, 2000).

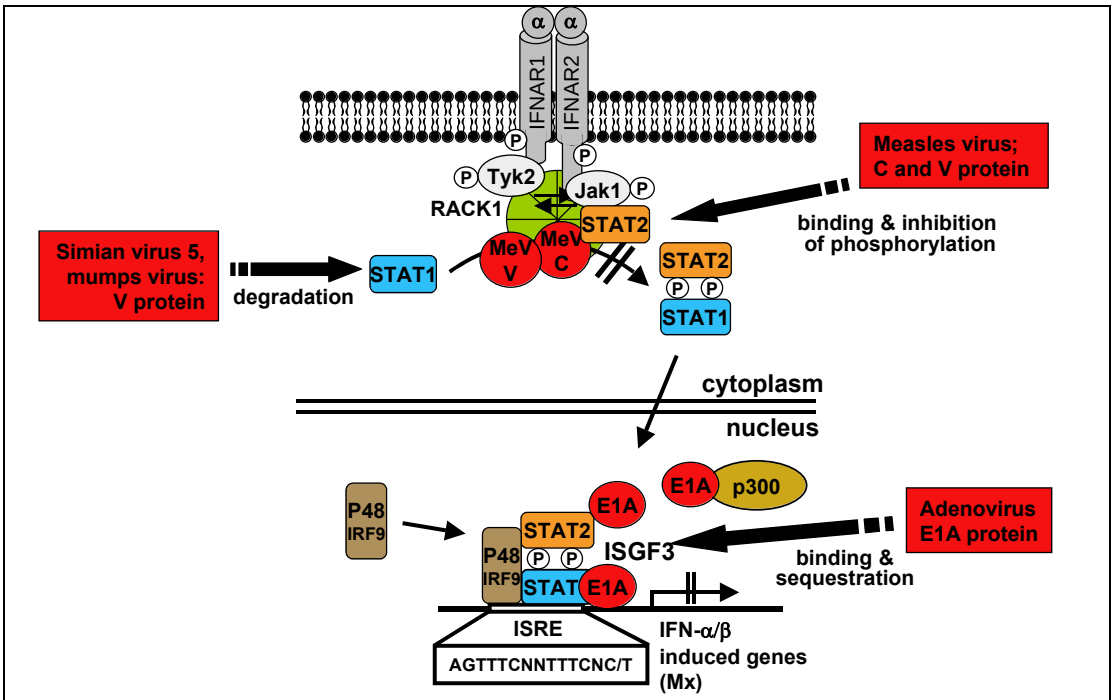

Figure 18: Viral interference in the IFN-α/β signaling pathway. Degradation of STAT1 by SV5 V protein; Inhibition of phosphorylation of Jak1 and Tyk2 by measles virus V- and C-protein and binding of the adenoviral E1A protein and sequestration of the ISGF3 complex.

6.1.4.4 INHIBITION OF IFN EFFECTOR PROTEINS

An efficient way to escape the IFN response is to directly inhibit the IFN effector proteins. All viruses with the capacity to sequester dsRNA are able to prevent activation of PKR or the 2'5'-OAS/RNase L system (Bergmann et al., 2000). The influenza NS1 protein inhibits activation of 2'5'-OAS by sequestering dsRNA away from the antiviral enzyme (Min & Krug, 2006). Furthermore influenza NS1 inhibits two cellular proteins that are required for the 3'-end processing of cellular pre-mRNAs: the cleavage and polyadenylation specificity factor (CPSF) and poly(A)-binding protein II (PABII) (Chen et al., 1999, Nemeroff et al., 1998). Herpesvirus, a complex DNA virus expresses an inhibitor of the PKR antiviral pathway, the ICP34.5 protein. ICP34.5 recruits a cellular phosphatase to dephosphorylate eIF-2α, and thus release the translational block by PKR (He et al., 1997). Moreover herpes simplex virus is able to generate 2'-5'-oligoadenylate derivatives that bind to and inhibit RNase L and thus prevent degradation of RNA (Cayley et al., 1984).

6.2 INFLUENZA A VIRUS

Influenza viruses are negative stranded, segmented, enveloped RNA viruses containing helical ribonucleocapsid (viral ribonucleoprotein; vRNP) and belong to the *Orthomyxoviridae* family (Lamb & Takeda, 2001). Virus particles are approximately 100nm in diameter and of spherical shape (Fujiyoshi et al., 1994). The genome of this virus comprises eight negative-stranded RNA segments, which direct the synthesis of 11 viral proteins in infected cells, as shown in Table 4. Four of these proteins, the nucleoprotein (NP), which encapsidates the viral RNA, and the three subunits of the polymerase (PB1, PB2 and PA) are associated with each of the viral genomic RNAs forming vRNPs. Three of the proteins: hemagglutinin (HA), neuraminidase (NA), and the ion channel (M2), are transmembrane proteins, and the two structural components, the matrix (M1) and nuclear export protein (NEP), are internal components of the viral particle. NS1 and the recently discovered facilitator of apoptosis PB1-F2 are besides the polymerase polyprotein the only non-structural proteins encoded by the viral genome (Lamb et al., 1985, O'Neill et al., 1998).

Segment	Size(nt)	**Protein**	Function
1	2341	**PB2**	Transcriptase (Polymerase): cap binding
2	2341	**PB1**	Transcriptase (Polymerase): elongation
3	2233	**PA**	Transcriptase: protease activity (?)
4	1778	**HA**	Haemagglutinin: receptor binding; fusion activity
5	1565	**NP**	Nucleoprotein: binds RNA; part of transcriptase complex; nuclear/cytoplasmic transport of vRNA.
6	1413	**NA**	Neuraminidase: release of virus.
7	1027	**M1**	Matrix protein: major structural component of virion.
		M2	Integral membrane protein - ion channel (H+).
8	890	**NS1**	Non-structural protein 1: effects on cellular RNA transport, splicing, translation; anti-IFN protein.
		NEP	Nuclear export protein: nucleus+cytoplasm; active in mRNA export from nucleus.
		PB1-F2	Facilitator of apoptosis: protein inducing cellular apoptosis.

Table 4: Genome of the Influenza virus. 11 viral genes are divided into 8 RNA segments, encoding for the proteins described.

The emergence of new influenza strains in the human population occurs via transmission from animal species, most notably birds. Transmission to humans is most commonly thought to occur through an intermediate such as swine (Webster et al., 1992). Typically, human and avian influenza viruses are quite different and are not cross-infectious. However, pigs can become infected with both types of viruses, and it has been proposed that they act as a ‘mixing vessel’

for the transmission of avian influenza viruses to humans. Occasionally, direct avian-human transmission can occur, as demonstrated in the case of the recent H5N1 virus.

6.2.1 INFLUENZA VIRUS LIFE CYLCE

Influenza virus particles bind to cell surface sialic acid, ubiquitously present on glycoproteins or glycolipids. The specificity of the sialic acid (avian: α2,3-linked sialic acid or human: α2,6-linked sialic acid) and preferred binding of a particular strain of influenza virus to a specific sialic acid receptor are important determinants for species-specific restriction of influenza viruses (Matrosovich & Klenk, 2003).

Influenza viruses infect cells via multiple endocytic pathways, with both calthrin-mediated and clathrin- and caveolin-independent pathway(s). Both pathways lead to viral fusion with similar efficiency (Lakadamyali et al., 2004, Sieczkarski & Whittaker, 2002). Viruses taking the clathrin-mediated pathway enter cells via the *de novo* formation of clathrin-coated pits at viral binding sites, a process that is dependent on dynamin, a cellular GTPase (GTP phosphohydrolase; (Roy et al., 2000). After internalization, the viruses are trafficked via early endosomes to late endosomes, where the acid pH~5.0 generated in these organelles by the vacuolar proton ATPase, induces a conformational change in the viral HA. This conformational change triggers viral fusion with the endosome and leads to the release of the viral genome (Hernandez et al., 1996, Skehel & Wiley, 2000). In the acidic pH of the endosome, the cleaved HA undergoes conformational changes causing fusion of viral and endosomal membranes (Colman & Lawrence, 2003). Virus particles containing uncleaved HA can bind and be endocytosed but cannot undergo fusion and are therefore non-infectious. The ion channel M2 opens up in the acidic pH of the endosome, acidifies the internal virion core, and thereby enables the release of vRNP from M1 into the cell cytoplasm. vRNPs are then imported into the nucleus through nuclear pores using nuclear transport signals of NP (Neumann et al., 2000).

Influenza viruses are one of a few RNA viruses to undergo replication and transcription in the nucleus of their host cell (Whittaker & Helenius, 1998). In the nucleus, the vRNPs serve as templates for the production of two forms of positive-sense RNA: viral messenger RNA (mRNA) and complementary RNA (cRNA; Krug et al., influenza viruses, Plenum Press, New York, USA, 1989). The synthesis of mRNA is catalyzed by the viral RNA-dependent RNA polymerase (comprising the three subunits PA, PB1 and PB2), which is part of the incoming vRNP complex. Viral mRNAs are processed in an analogous fashion to eukaryotic mRNAs. They are capped (contain a methylated 5'-guanosine residue) by a process called cap-snatching and polyadenylated (contain a sequence of polyadenylic acid at their 3'-end), and are exported from the nucleus for translation by cytoplasmic ribosomes. In the cap-snatching process, cellular, nuclear RNA fragments are cleaved at their 5' ends by a virus-encoded, cap-dependent endonuclease that is part of the RNA polymerase. The resulting 10- to 13-nucleotide-long capped fragments serve as primers for the initiation of viral mRNA synthesis (Plotch et al., 1981). The viral cRNA is neither capped nor polyadenylated, and remains in the nucleus, where it serves as a template for the production of negative-sense genomic RNA (viral RNA; vRNA). The nuclear export of viral mRNA utilizes the 'translocation machinery' of the host cell and is controlled by NS1 (Chen & Krug, 2000). Many viral proteins (NP, M1, NEP and the polymerases) are imported into the nucleus upon synthesis for the final stages of replication and for vRNP assembly.

vRNPs containing minus-strand vRNA, NP, the three polymerase proteins and NEP are transported out of the nucleus through the chromosome region maintenance 1 (CRM1) protein together with M1 (Neumann et al., 2000). How M1 and vRNP, individually or jointly are transported to the budding site remains unclear. Cytoskeletal components, particularly microfilaments, interact with the NP of the vRNP and the M1 complex and thereby may facilitate the transport of these components to the assembly site (Avalos et al., 1997).

M1 is central to the assembly. M1 proteins bind to vRNPs and the plasma membrane to form a shell beneath the virus envelope (Nayak et al., 2004). The

structural organization of M1 in the virion and its involvement in multiple interactions with other viral proteins and RNP support the assumption that budding of negative-strand RNA viruses is orchestrated by this protein (Garoff et al., 1998).

For the final budding step, it has recently been shown that the viral components come together at the detergent-insoluble glycolipid-enriched domains (DIGs), or lipid rafts (Scheiffele et al., 1999, Zhang & Lamb, 1996). The final release of viruses from the cell surface relies on the action of the viral NA. NA (sialidase) acts as a receptor-destroying enzyme, by removing sialic acid (the viral receptor) from the surface of host cells (Colman & Lawrence, 2003). Without this step, the newly assembled virus particles would immediately re-bind to their receptor and not be released into the extra-cellular space. Instead, they would remain attached to the cell in large clumps. NA is therefore important for the efficient release of viruses. The establishment of a productive infection is dependent on both NA and HA.

6.2.2 INFLUENZA MATRIX PROTEIN M1

M1 is the most abundant protein (3000 molecules/virion) in the virus particle and a major structural component of the virion. M1 has multiple regulatory functions during the infectious cycle, which include the dissociation of M1 from RNP from the viral shell to enable transcription. This step is required for the release of viral RNP into the cytoplasm of the infected host cell. Dissociation is triggered by transport of H^+ ions across the viral membrane by M2 (Bui et al., 1996, Helenius, 1992, Martin & Helenius, 1991). Furthermore, M1 mediates inhibition of viral transcription (Hankins et al., 1990, Perez & Donis, 1998, Watanabe et al., 1996, Ye et al., 1989). It also has been shown that M1 is transported during early viral replication from the cytoplasm into the nucleus, via a nuclear localization signal (NLS) (Ye et al., 1989), where M1 associates with newly synthesized RNPs (Bui et al., 1996, Rey & Nayak, 1992). The transport of RNP from the nucleus to the cytoplasm requires the binding of M1 to RNP, which also prevents RNP from reentering the nucleus (Huang et al., 2001, Martin & Helenius, 1991).

It has been shown that M1 is the major virus assembly organizer and the major driving force in the budding process (Gomez-Puertas et al., 2000). Interactions of M1 with HA, NA, M2, NEP and host cell lipid membranes occur on the cytoplasmic side of the membrane as part of the process of virion maturation and budding at the cell surface (Enami & Enami, 1996, Lamb et al., 1985, Ruigrok et al., 2000, Yasuda et al., 1993, Zhang & Lamb, 1996).

M1 becomes phosphorylated during influenza virus infection. Protein kinase C (PKC) is proposed to be the M1-phosphorylating enzyme, whereas the receptor activated kinase C1 (RACK1) is thought to be the scaffold for this phosphorylation (Reinhardt & Wolff, 2000). The phosphorylation status is thought to determine the different regulatory roles of M1. To date there is no information about the different regulatory functions of M1 in its different activated states.

6.3 AIM OF THIS PROJECT

The basis of this project is the observation of the down-regulation of MxA of M1-transfected A549 cells by immunofluorescence. This led to the hypothesis, that influenza A may have the ability to counteract the innate immune response by M1, an alternative mechanism to NS1. The aim of this study was to identify the M1-protein as an antagonist of the IFN-α signaling pathway and to identify the interaction partners of M1 in the signaling cascade.

7 MATERIALS AND METHODS

7.1 CELL CULTURE AND TRANSFECTION

Human embryonal kidney cells (HEK293), human lung carcinoma cells (A549) and African green monkey kidney cells (Vero E6) were cultured at 37°C and 5% CO_2 in Dulbecco's Modified Eagle Medium (DMEM, Gibco) containing 10% fetal calf serum (FCS). The cells were split every second day before reaching confluency.

A549 cells were transfected with Lipofectamine™ 2000 as described in chapter 3.

7.2 VIRUS INFECTION WITH INFLUENZA A/WSN/33

Influenza A/WSN/33 virus (WSN) is a mouse adapted H1N1 human strain. A549 and Vero E6 cells were splitted 10-12h previous to the infection. Cells displayed about 95% confluency at the time of infection. Cells were infected with 10 multiplicities of infection (MOI). The virus stock had a titer of $3.16x10^8$ TCID/ml, equaling $3.16x10^8$ TCID/ml / 1.44 = $2.195x10^8$ virus/ml. The culture medium was exchanged (DMEM, 2%FCS, 20mM Hepes) at time of infection. For exogenous IFN-α stimulation upon infection 1000 U/ml Roferon (Roche) was applied to the cells in fresh DMEM medium. Cells were harvested 6-48h post infection, depending on the experiment, and protein expression and cell viability were analyzed.

7.3 DUAL-LUCIFERASE® REPORTER ASSAY

Luciferase reporter assays were performed in 12 well plates with infected or transfected HEK293 or Vero cells. Assays were performed with the dual-Luciferase® reporter system kit (Promega) according to the manufacturer's instructions: Cells co-transfected with 0.6μg/well p(9-27)4tkD(-39)lucter (a

plasmid encoding the firefly luciferase (FFL) under the control of an ISRE) and 0.04μg/well pRL-TK (a plasmid encoding the *renilla reniformis* Luciferase, expressed constitutively under the control of the HSV tyrosine kinase promoter) as an internal control were rinsed with PBS and then incubated for 15min in an appropriate amount of passive lysis buffer (PLB, for a 12 well plate 250μl). 10μl of cell lysate were added to 50μl of LARII. Luminescence of FFL was measured in a Sirius Luminometer (Berthold detection systems). 50μl of Stop&Glo reagent were added and the luminescence of RRL was measured.

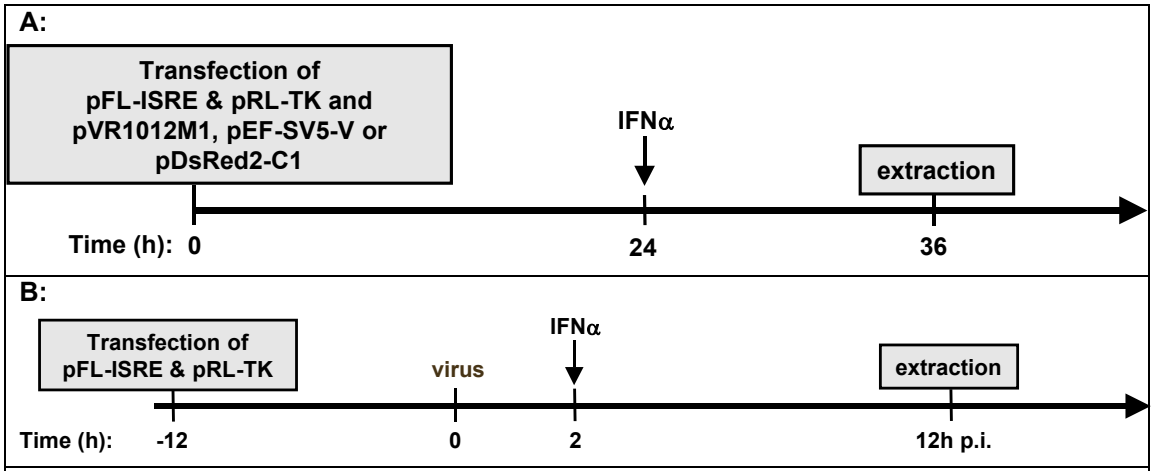

Fig. 19.A and B: Time scale of how cells were treated before the luciferase reporter assay was performed. A: cells were transfected with M1, SV5 V or RFP, and the luciferase constructs, stimulated with IFN-α 24h later and extracted another 12h (36h post transfection) for a luciferase reporter assay. B: cells were transfected with the luciferase constructs and infected with influenza A/WSN/33 12h later. 2h p.i. the cells were stimulated with IFN-α and another 10h later cells were extracted for a luciferase reporter assay.

7.4 PROTEIN EXTRACTION

A549 cells were washed twice in ice cold phosphate-buffered saline (PBS, Gibco) and cells were lysed in Ripa buffer (20mM Tris-HCl, 135mM NaCl, 2mM EDTA, 1% Triton X-100, 0.1% SDS, 0,5% Deoxycholat, 10% glycerol and protease inhibitors) for 10min on ice. The cells were then scraped from the dish and transferred into an eppendorf tube. The lysate was centrifuged at 13000rpm and 4°C for 5min. Protein concentration was measured by BCA (Micro BCA protein assay reagent kit; Pierce).

7.5 ANTIBODIES AND WESTERN BLOTTING

For Western blotting, infected cells were diluted in SDS Laemmli buffer and boiled at 95°C for 10min. Samples were electrophoresed by SDS-PAGE, and the proteins were transferred onto nitrocellulose membranes (Hybond^{TM}-ECL^{TM}). Membranes were blocked with 5% skim milk TBS-T buffer (20mM Tris-HCl pH7.5, 0.5 M NaCl, 0.05% Tween 20) and rabbit anti-STAT1, rabbit anti-phospho-STAT1, rabbit anti-phospho-STAT2, rabbit anti-phospho-Tyk2 and rabbit anti-phospho-Jak1 (Cell Signaling) antibodies as well as the anti-cortactin (Santa Cruz) antibody were diluted 1:1000 in 5% skim milk TBS/Tween buffer. Membranes were incubated for 1h at RT or at 4°C overnight, subsequently washed 4 times 5min in TBS-Tween and incubated with horseradish peroxidase-conjugated donkey anti-rabbit (Amersham Biosciences) antibody as secondary antibody for 1h at RT. Chemiluminescence detection was performed according to the manufacturer's protocol (ECL detection kit, Amersham Biosciences) after washing the membranes 4 times with milk TBS-T buffer for 5min and 2 times with TBS-buffer for 5min.

7.6 CO-IMMUNOPRECIPITATION

30 μl total volume of protein L-agarose (Santa Cruz) or protein A-agarose (Sigma-Aldrich), were washed for each lysate three times with the extraction buffer (with protease inhibitors). 2 μg antibody was added to the beads (1:1 diluted in extraction buffer) and incubated on a turning row at 4°C for 1-3h. The bead-AB mix was washed three times with extraction buffer to get rid of soluble AB, which would compete with the bead-AB mix for the proteins. Unspecific AB-binding sites were blocked with 0.5% BSA (10% BSA in PBS stock solution; 1.5μl/30μl bead-AB volume) for 30min-1h at 4°C. The blocked bead-AB mix was washed 3 times with extraction buffer and extracted proteins were added and incubated for 1-2h at 4°C. The remaining proteins were selected by washing the beads 2 times with extraction buffer with protease inhibitors. Finally the beads are centrifuged at 2500rpm for 1min, the supernatant is discarded and the beads

are boiled in SDS-loading buffer for 10min at 95°C and analyzed by Western blotting.

7.7 STATISTICS

Numerical data were analyzed for statistical significance using the Student *t* test with tail = 2 and type = paired (1).

8 RESULTS

8.1 INHIBITORY EFFECT OF INFLUENZA A ON THE IFN-α/β SIGNALING

8.1.1 INFLUENZA INFECTION DECREASES THE RESPONSIVENESS OF ISRE IN A REPORTER ASSAY

The effect of influenza A on the IFN-α/β signaling cascade was measured indirectly using a transient co-transfection method including p(9-27)4tkD(-39)lucter that expresses the firefly luciferase (FFL) under the control of an ISRE (King & Goodbourn, 1998). As an additional control a second plasmid pRL-TK encoding the *renilla reniformis* luciferase (RRL) was expressed constitutively under the control of the HSV tyrosine kinase promoter. These constructs have been tested by co-transfection in HEK293 cells and stimulation with exogenous IFN-α. The expression level of FFL depended linearly on the level of IFN-α added to the cells and the activity of the IFN-α/β signaling pathway.

In order to determine the effect of influenza on the production of FFL and RRL, HEK293 cells and Vero cells were infected with influenza. The experimental design of the co-transfection and infection experiment is summarized in Fig. 19A. Dividing the activity of RRL normalized the activity of FFL. As shown in Fig. 19B the IFN-α dependent FFL activity was decreased by 80% in influenza-infected HEK293 cells, compared to non-infected cells. This result indicated that influenza A reduced the responsiveness of the ISRE-promoter and therefore decreased FFL activity. Lysates of infected, non-stimulated cells showed limited increase in FFL activity, compared to lysates of non-infected cells. This finding indicated that (1) the IFN-α treatment stimulated the ISRE-regulated FFL activity, (2) influenza activated the IFN-α signaling pathway in the absence of exogenous IFN-α and (3) influenza effectively blocked the activation of the IFN-α signaling upon exogenous IFN-α stimulation. The mechanism of induction by influenza virus

infection is known to be mediated by the interaction of dsRNA and TLR3, leading to the production of IFN-α/β (Alexopoulou et al., 2001, Matsumoto et al., 2004).

The same experiment was performed with Vero cells, lacking the IFN-α genes. As shown in Fig. 19C, FFL activity was equal in non-stimulated, infected and non-infected Vero cells, as IFN-α could not be induced endogenously as for infected HEK293 cells. A decrease in FFL activity of more than 50% was detected in infected, IFN-α stimulated Vero cells, compared to non-infected, IFN-α stimulated cells. The difference in IFN-α dependent FFL activity in influenza-infected HEK293 and Vero cells was due to a different efficiency in infectivity of the two cell lines.

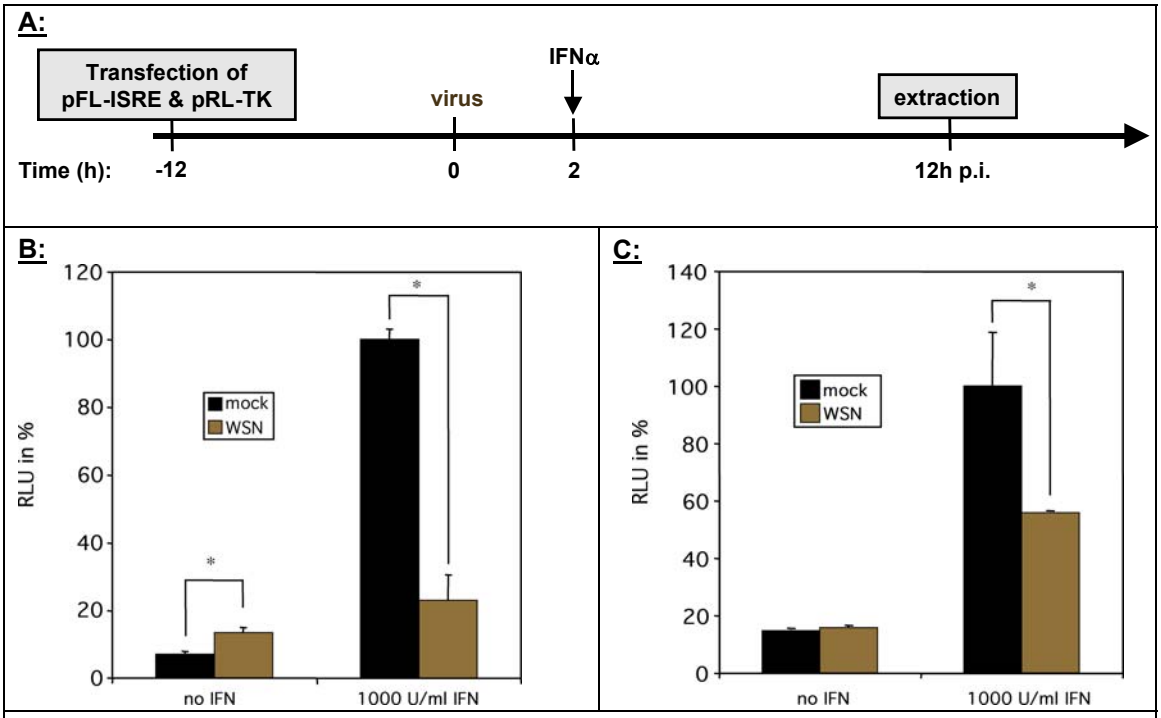

Figure 19: Inhibitory effect of influenza A on the IFN-α signaling pathway in HEK293 cells (B) or Vero cells (C). **A:** time line of experimental set up. Cells were transfected with a plasmid coding for the FFL and another plasmid encoding the RRL 12h ahead of influenza infection. The FFL was under control of an ISRE, whereas the RRL was ubiquitously expressed. Influenza-infected cells were stimulated with IFN-α 2h p.i. and luciferase activity was measured 12h p.i. Graphs show the values of 3 independent experiments. p values: p>0.009; p>0.0004; p>0.005.

8.2 INHIBITORY EFFECT OF INFLUENZA M1 ON THE IFN-α/β SIGNALING

8.2.1 OVEREXPRESSION OF M1 DECREASES THE RESPONSIVENESS OF ISRE IN A REPORTER ASSAY

In order to define the viral protein responsible for the inhibitory activity of the influenza virus, a transient co-transfection method was used to measure FFL activity upon transfection with the M1-protein. The M1-protein was expressed under the control of the CMV gene promoter by the plasmid pVR1012-M1. FFL and RRL were co-expressed by the plasmids introduced in the experiment above. In order to determine the effect of the M1-protein on the production of the FFL, the impact of pVR1012-M1 was compared to the empty vector pVR1012.

HEK293 cells were transfected and 24h later exogenously stimulated with IFN-α. Cell lysates were collected 12h post stimulation (Fig. 20A). As depicted in Fig. 20B, in IFN-α stimulated cells, the FFL activity was inhibited by 60% in pVR1012-M1 transfected cells. The inhibition of FFL activity in stimulated cells did not show a significant difference in cells transfected with 0.6μg pVR1012-M1 than in cells transfected with 0.3μg pVR1012-M1 (compare gray bar with brown bar).

The difference of the FFL activity for the non-stimulated cells transfected with either pVR1012 or pVR1012-M1 was not significant. ($p>0.223$). The inhibitory effect of the M1-protein on the IFN-α signaling, compared to pVR1012 appeared to be dependent on exogenous IFN-α.

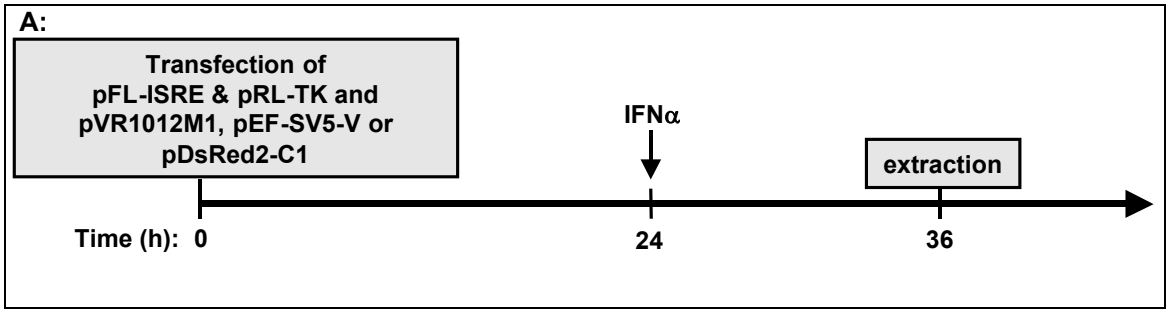

B:

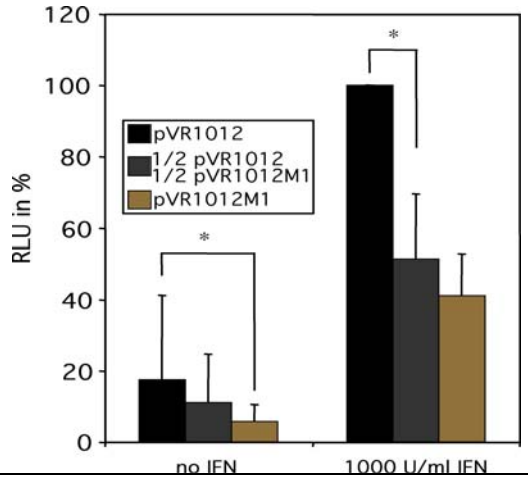

Figure 20: A: Time line to show the experimental set up for the reporter assay. **B:** Overexpression of M1 decreases the responsiveness of ISRE in a reporter assay. HEK293 cells were co-transfected with pVR1012, pVR1012 and pVR1012M1, or pVR1012M1 and the plasmids encoding FFL and RRL. Cells were stimulated with IFN-α and luciferase activity was measured. p values: p>0.223; p>0.005.

8.2.2 OVEREXPRESSION OF M1 DECREASES THE RESPONSIVENESS OF ISRE IN A REPORTER ASSAY SIMILAR TO THE SV5 V-PROTEIN

In order to prove the specificity of the inhibitory activity of the M1-protein, the effect of over-expressed M1 was compared to two control proteins: red fluorescent protein (RFP) and simian virus 5 (SV5) V-protein. The experimental set up was the same as in Fig. 20A. Cells were transfected and a saturating amount of IFN-α was added 24h post transfection. Cells were harvesed 12h post stimulation.

RFP was expressed under the control of a CMV promoter of the expression plasmid pDsRed1-C2 and was not expected to have any effect on the IFN-α signaling cascade. The SV5 V-protein was shown previously to be a strong IFN-α signaling inhibitor (Didcock et al., 1999a, Didcock et al., 1999b) and served as positive control. As shown in Fig. 21, M1 inhibited the FFL activity by 80% compared to the RFP indicating a specific inhibition of the IFN-α/β signaling pathway by the M1-protein. Similar to the M1-protein, the SV5 V-protein inhibited the IFN-α/β signaling pathway also by 80%. Thus, the V-protein and the M1-protein were shown to affect the IFN-α/β signaling equally well. Since the V-

protein is known to be a potent inhibitor of the type I IFN signaling pathway, we concluded that M1 could be a strong and specific inhibitor of the type I IFN signaling pathway.

Non-stimulated Vero cells showed a statistically significant difference in the FFL activity between RFP and the M1-protein ($p>0.0004$) as well as between the V-protein and the M1-protein ($p>0.00035$). The M1-protein showed a weak IFN-α independent inhibition of the FFL activity, compared to the IFN-α stimulated cells. This observation may be explained by a toxic effect of the plasmid backbone containing CpG-rich sequences, which could lead to non-specific activation of the IFN-α/β pathway. This finding was confirmed by the result of the non-stimulated cells in Fig. 20B. The FFL activity did not show a significant difference in cells transfected with pVR1012-M1 or pVR1012, possibly due to the identical backbone of the two plasmids. The IFN-α independent effect of the plasmid backbone on the activity of FFL was not observed in lysates of IFN-α treated cells. The effect might be overruled by the excess amount of IFN-α added.

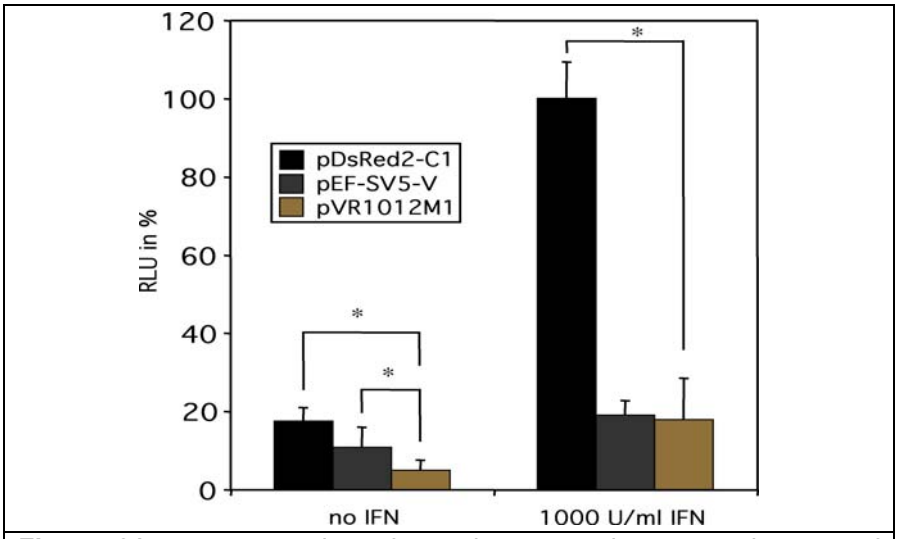

Figure 21: Overexpression of M1 decreases the responsiveness of ISRE in a reporter system, similar to the SV5 V-protein. Vero cells were co-transfected with pDsRed2-C1 encoding RFP, pEF-SV5-V encoding the V-protein, pVR1012-M1 encoding the M1-protein and the plasmids encoding the FFL and RRL. Cells were stimulated with IFN-α and luciferase activity was measured.

8.3 INFLUENZA A INHIBITS MXA

In order to independently confirm the effects of influenza on the type I IFN signaling pathway, MxA protein levels were measured in infected A549 cells. It has been shown previously that the MxA production is tightly regulated by a type I IFN-stimulated response element (ISRE). As depicted in Figure 22A, the MxA expression increased from 6h to 24h after IFN-α stimulation. The time frame from 18h to 24h was chosen to identify the effect of influenza A on the MxA production. Fig. 22B shows the experimental set up of the MxA detection experiment. A549 cells were infected and IFN-α stimulated 2, 4 or 6h p.i. Stimulated cells were harvested 18h post stimulation and non-stimulated cells were harvested 20, 22 or 24h p.i.

Analysis of non-infected A549 cells (Fig. 22C; lane1) did not show any MxA, confirming data (Haller & Kochs, 2002) that MxA expression in absence of IFN-α pathway activators is minimal. Analysis of infected cells revealed, that MxA was induced upon infection, but remained at a very low level. Comparing lane2 to lane4, the level of MxA protein was shown to decrease with time p.i.. MxA is known to be stable for several days (Aebi et al., 1989). The observed decrease of the MxA protein level cannot be explained by general protein instability, suggesting that MxA is degraded upon influenza A infection.

Fig. 22C showed A549 cells infected with influenza A and stimulated with IFN-α 2, 4 or 6h p.i. MxA was highly induced by IFN-α stimulation in non-infected cells. Interestingly, infection and IFN-α stimulation together showed a strong inhibition of MxA expression (lane2). The level of MxA transcripts was shown to be lower, the later infected cells were stimulated with IFN-α (lane2-4).

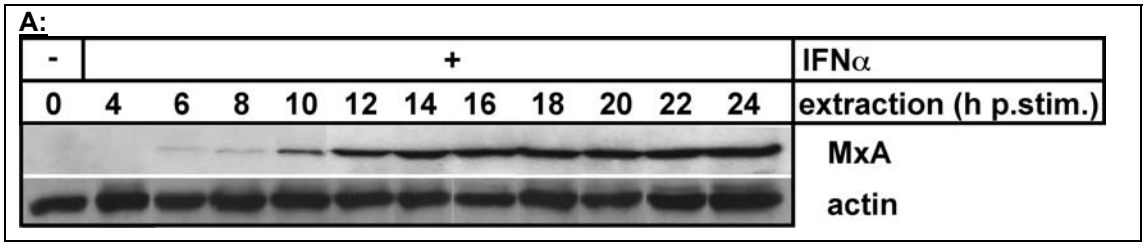

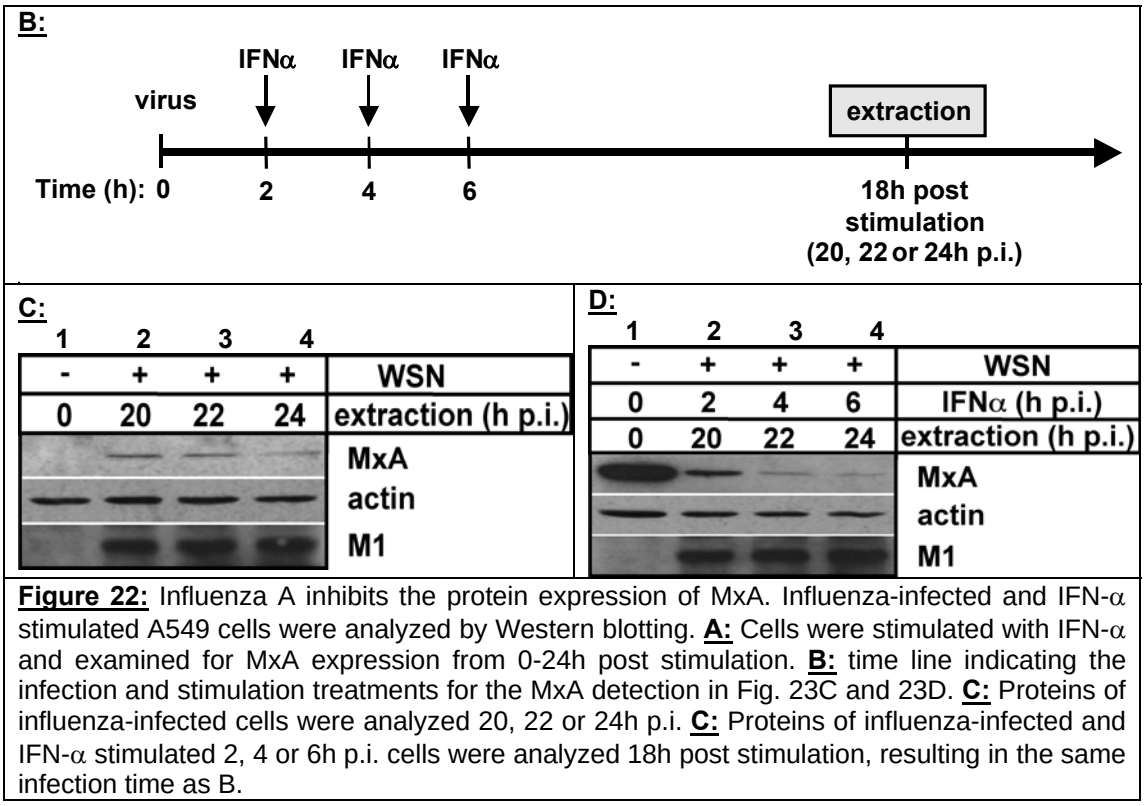

Figure 22: Influenza A inhibits the protein expression of MxA. Influenza-infected and IFN-α stimulated A549 cells were analyzed by Western blotting. **A:** Cells were stimulated with IFN-α and examined for MxA expression from 0-24h post stimulation. **B:** time line indicating the infection and stimulation treatments for the MxA detection in Fig. 23C and 23D. **C:** Proteins of influenza-infected cells were analyzed 20, 22 or 24h p.i. **C:** Proteins of influenza-infected and IFN-α stimulated 2, 4 or 6h p.i. cells were analyzed 18h post stimulation, resulting in the same infection time as B.

8.3.1 INFLUENZA INFECTION OR OVEREXPRESSION OF M1 INHIBIT THE EXPRESSION OF MXA

The Western blot analysis was confirmed by an immunofluorescence experiment, detecting the IFN-α induced expression of MxA in influenza-infected A549 cells (Fig. 23A). Influenza-infected cells showed an inhibited expression of MxA compared to non-infected cells. Furthermore, the immunofluorescence experiment of A549 cells overexpressing M1 revealed a suppressed MxA expression (Fig. 23B). MxA was equally expressed in A549 cells overexpressing GFP. Therefore, M1 was repeatedly shown to be responsible for the interference with the IFN-α signaling pathway.

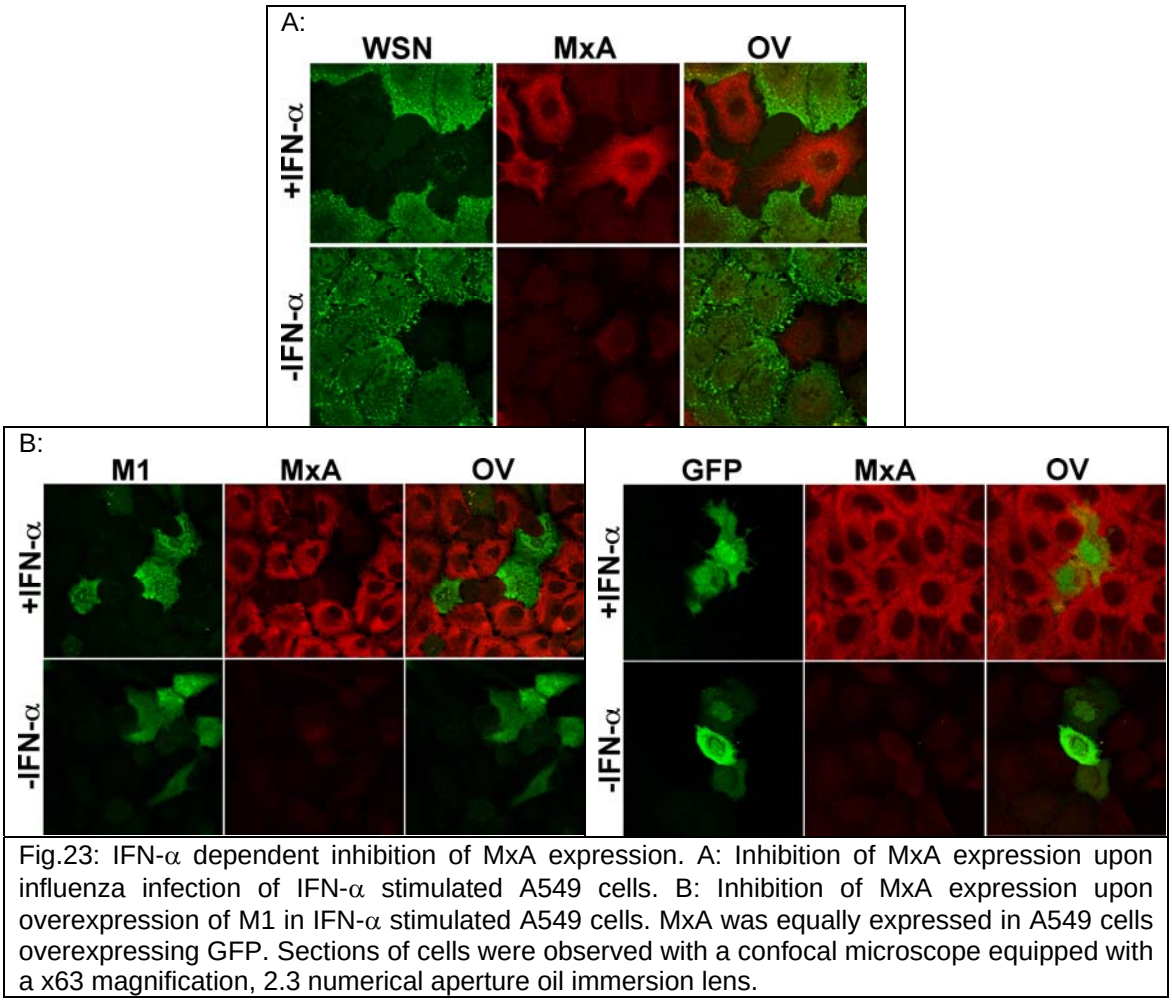

Fig.23: IFN-α dependent inhibition of MxA expression. A: Inhibition of MxA expression upon influenza infection of IFN-α stimulated A549 cells. B: Inhibition of MxA expression upon overexpression of M1 in IFN-α stimulated A549 cells. MxA was equally expressed in A549 cells overexpressing GFP. Sections of cells were observed with a confocal microscope equipped with a x63 magnification, 2.3 numerical aperture oil immersion lens.

8.4 Inhibition of STAT1 Phosphorylation by Influenza A

8.4.1 Influenza A did not Affect the Stability of IFN-α/β Signaling Proteins at Early Stages After Infection

In order to examine the expression of IFN-α signaling proteins upon influenza-infection, a time course analysis was performed. A549 cells were infected, proteins were extracted up to 18h p.i., and analyzed by Western blotting. Total cell lysates of A549 cells were harvested and protein levels of STAT1, STAT2, Jak1 and Tyk2 were determined. These proteins have been shown to play an

essential role in viral interference with the IFN-α signaling by other viruses and represent potential targets for influenza A.

To test whether the virus affects the stability of the signaling proteins we determined the total protein amount. As shown in Fig. 24, the level of signaling proteins remained constant up to 15h p.i. At 18h p.i., a weak decrease in the STAT2 protein level was observed. In order to exclude the effect of virally induced protein degradation and apoptosis, an infection time of 12h was chosen for all further experiments.

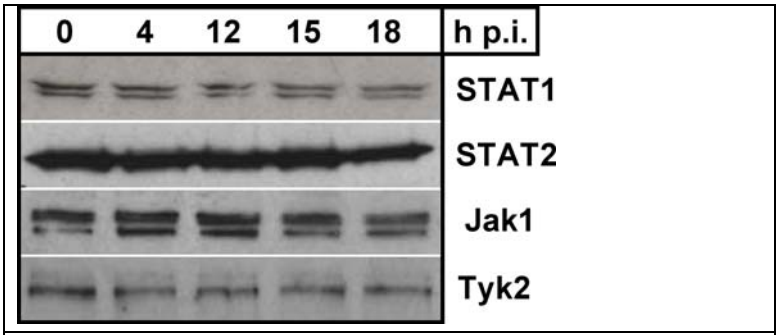

Figure 24: Stability of the IFN signaling proteins upon influenza infection. A549 cells were infected and harvested at the indicated time points and total proteins were extracted. Lysates were subjected to Western blot analysis and examined for total amounts of STAT1, STAT2, Jak1 and Tyk2.

8.4.2 Influenza A Leads to the Inhibition of P-STAT1, but Does not Affect the Protein Level of STAT1

To examine whether the influenza M1-protein antagonizes the IFN-α signaling by interfering with the phosphorylation and subsequent activation of STAT1, we performed a Western blot analysis with influenza infected, IFN-α stimulated A549 cells. In a first experiment, the maximal phosphorylation of STAT1 was determined between 15 to 30min after IFN-α stimulation (Fig. 25A).

As shown in Fig. 25B, IFN-α induced phosphorylation of STAT1 in influenza A infected cells (lane4) was dramatically suppressed at 20min treatment compared to the uninfected control cells (lane3). The protein level of total STAT1 remained equal for all cell lysates. STAT1 was not degraded in influenza A infected A549

cells. Concluding, IFN-α dependent STAT1 phosphorylation was inhibited by infection with influenza A.

Interestingly, longer exposure of the membranes of Fig. 25B (30min versus 1min), showed IFN-α independent P-STAT1 in influenza-infected A549 cells. This effect was explained by the induction of the type I IFN pathway mediated by the interaction of dsRNA with TLR3 (Alexopoulou et al., 2001, Matsumoto et al., 2004). The IFN-α/β signaling cascade was suggested to be induced by extra cellular dsRNA or virus particles sensed at the cell surface, before viral infection. Upon infection, the M1-protein was thought to act as IFN-α/β signaling antagonist, inhibiting the antiviral activity.

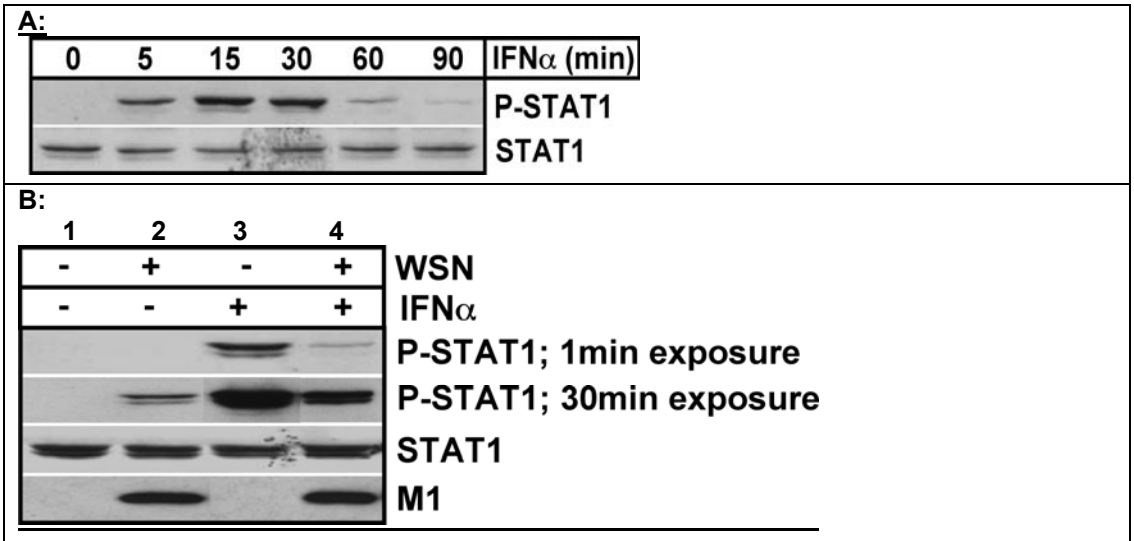

Figure 25: IFN-α dependent inhibition of P-STAT1 upon infection with influenza. A549 cells were harvested and lysates of extracted proteins were subjected to Western blot analysis and examined for STAT1 and P-STAT1. **A:** Determination of the time frame of maximal P-STAT1 upon IFN-α stimulation. **B:** Inhibition of P-STAT1 upon influenza infection and IFN-α stimulation (lane3 & 4; 1min exposure) and induction of IFN-α signaling upon influenza infection (lane 1 & 2; 30min exposure). A549 cells were stimulated with IFN-α for 20min 12h p.i.

8.4.3 Overexpression of M1 Leads to the Inhibition of Nuclear Translocation of STAT1

Inhibition of STAT1 phosphorylation impairs its transport into the nucleus, as heterodimers with P-STAT2 are not built and thus not translocated into the nucleus. In order to confirm this hypothesis, an immunofluorescence experiment

was performed with A549 cells overexpressing M1. Cells were stimulated with IFN-α and M1 and STAT1 were detected. Fig. 26A showed IFN-α dependent nuclear translocation of STAT1 in M1-negative A549 cells, whereas cells expressing M1 showed no STAT1-translocation into the nucleus. Cells overexpressing GFP were not impaired in nuclear translocation of STAT1, as depicted in Fig. 26B. This result showed that the STAT1 translocation into the nucleus was inhibited by M1 and supports the finding of the Western blot analysis displaying a decreased protein amount of P-STAT1.

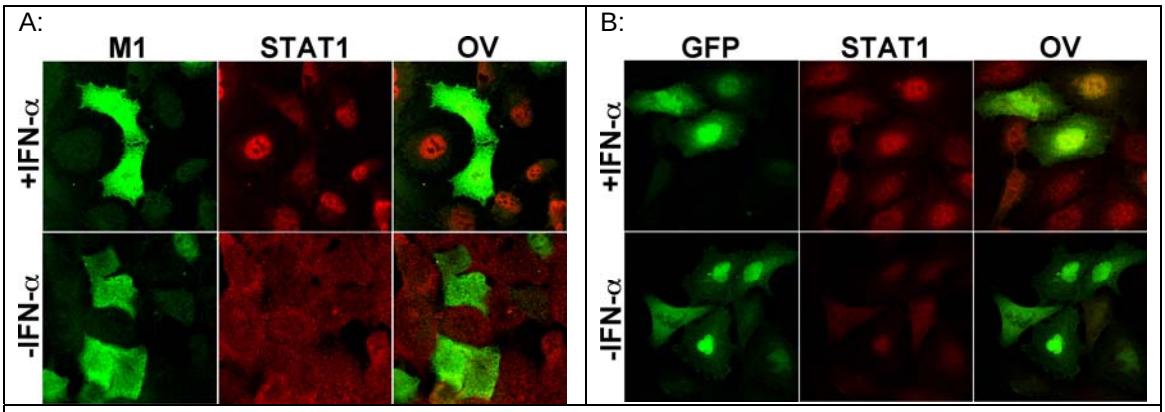

Fig. 26: A: IFN-α dependent inhibition of STAT1 translocation into the nucleus in A549 cells overexpressing the M1-protein. B: Overexpression of GFP did not impair the nuclear translocation of STAT1. Sections of cells were observed with a confocal microscope equipped with a x63 magnification, 2.3 numerical aperture oil immersion lens.

8.5 Inhibition of Tyk2 Phosphorylation by Influenza A

In order to further explore the molecular mechanism by which influenza A suppressed the type I IFN signaling pathway, the proteins upstream of STAT1 in the signaling were investigated. Tyk2 is located upstream of STAT1 in the IFN-α/β signaling and is directly responsible for the STAT1 phosphorylation (Leung et al., 1995). Therefore, Tyk2 was chosen as the second signaling protein to be examined. A549 cells were infected with influenza A and Tyk2 and phosphorylated Tyk2 (P-Tyk2) were analyzed by Western blotting. As depicted in Fig. 26, P-Tyk2 was suppressed upon influenza A infection in IFN-α stimulated cells (lane4), compared to the Tyk2 phosphorylation in non-infected cells (lane3).

Tyk2 phosphorylation was not detected in non-stimulated protein extracts (lane 1 & 2). The protein level of total Tyk2 protein remained equal for all cell lysates (lane 1-4).

Influenza A was shown to inhibit the phosphorylation of Tyk2 and therefore also STAT1 phosphorylation. It remains to be seen whether direct binding of M1 to Tyk2 causes this inhibition, or whether RACK1 was recruited by M1, resulting in the destruction of the receptor complex and therefore impairing the Tyk2 phosphorylation by Jak1.

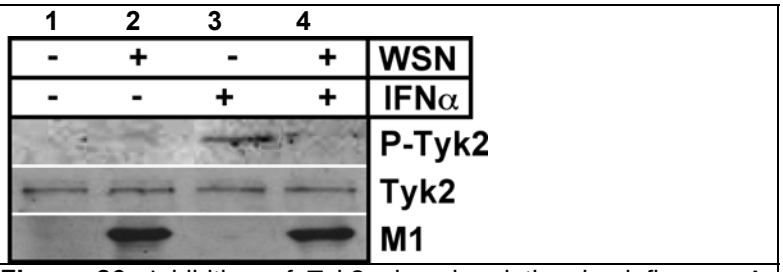

Figure 26: Inhibition of Tyk2 phosphorylation by influenza A infection of A549 cells. 12h p.i. cells were stimulated with IFN-α for 10min, harvested and proteins extracted. Lysates were subjected to Western blot analysis and examined for Tyk2 and P-Tyk2.

8.6 Inhibition of STAT2 and Jak1 Phosphorylation by Influenza A

As STAT2 is phosphorylated upon Tyk2 phosphorylation, it was assumed that the level of STAT2 phosphorylation (P-STAT2) might also be reduced. In order to determine the effect of influenza A on STAT2/P-STAT2, A549 cells were infected with influenza and proteins analyzed by Western blotting. In Fig. 27A, total STAT2 was detected equally in all cell lysates, STAT2 was thus not degraded by influenza. Analogous to P-STAT1, P-STAT2 was detected in non-infected/stimulated (lane2) cells. This finding indicated the induction of the IFN-α/β signaling cascade upon influenza infection. In influenza-infected cells, P-STAT2 was inhibited upon IFN-α stimulation (lane4), compared to non-stimulated cells (lane3).

Furthermore, the phosphorylation status of Jak1 was assessed and the inhibition of its phosphorylation upon infection and stimulation identified. As shown in Fig. 27B, phosphorylated Jak1 (P-Jak1) was detected in all cell lysates. P-Jak1 was shown in non-stimulated cells unlike the other IFN-α signaling proteins. This could either be explained by unspecific binding of the anti-P-Jak1 antibody to unphosphorylated Jak1 or by a basal phosphorylation status of Jak1 in non-stimulated cells. However, in analogy to the other IFN-α signaling proteins, P-Jak1 did not increase upon IFN-α stimulation in influenza-infected cells (lane 2 and 4), indicating the interference with the IFN-α/β signaling pathway by an infecting virus. The protein level of Jak1 was equal for all cell lysates.

Our data suggested that influenza A inhibited phosphorylation of STAT2 and Jak1. Further analysis will provide insight on mechanism of interference and on interaction partners of the virus in the type I IFN signaling pathway.

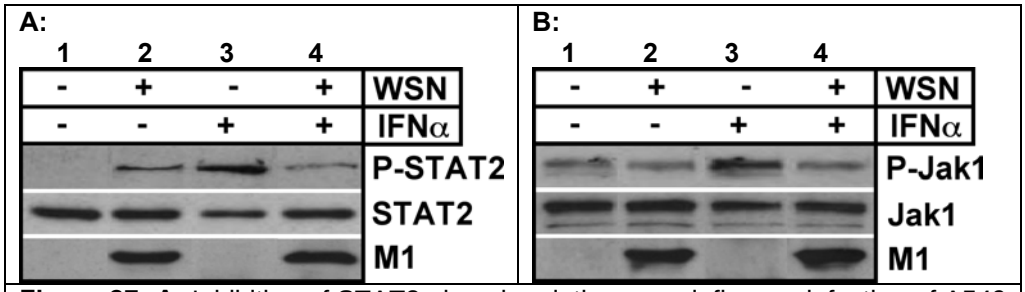

Figure 27: A: Inhibition of STAT2 phosphorylation upon influenza infection of A549 cells. Cells were stimulated with IFN-α for 20min. **B:** Inhibition of Jak1 phosphorylation upon influenza infection of A549 cells. Cells were stimulated with IFN-α for 10min. **A&B:** harvested 12h p.i. and proteins were extracted. Lysates were subjected to Western blot analysis and examined for STAT2, P-STAT2, Jak1 and P-Jak1.

8.7 PHOSPHORYLATION OF IFN-α/β SIGNALING PROTEINS UPON M1 TRANSFECTION

In order to exclude the negative regulation of the IFN-α signaling proteins through other viral proteins, a transfection of pVR1012-M1 was performed in HEK293 cells. SV5 V-protein and RFP were used as positive and negative control, respectively. pVR1012 (empty vector: e.v.) served as another negative

control, which enabled to determine the effect of an overexpressed protein on the IFN-α/β signaling in the transfected cell.

As shown in Fig. 28A, the phosphorylation of STAT1 was impaired upon transfection with M1 (lane1), compared to the cells transfected with RFP (lane3) or the empty vector (lane4). The transfection with SV5-V showed a significant decrease in the amount of P-STAT1. This finding was consistent with the data from literature, where SV5 V-protein was proposed to degrade STAT1, with the consequence of a decreased level of P-STAT1 (Didcock et al., 1999b). P-STAT2 was decreased after M1-transfection compared to the empty vector, but equal to SV5 V and RFP.

These findings confirmed the negative regulation of the IFN-α/β signaling pathway by M1. The inhibitory effect was confirmed to be dependent on the M1-protein, as the phosphorylation and thus activation of the signaling proteins was decreased by transfection of pVR1012-M1.

As depicted in Fig. 28B, the phosphorylation of Tyk2 was inhibited the amount of P-Tyk2 was higher in IFN-α stimulated cells transfected with 1/5xM1 than with 1xM1. The negative regulation of M1 on the IFN-α signaling pathway was hereby shown to correlate with the amount of M1 in the cell.

Furthermore non-stimulated, transfected HEK293 cells were observed for the phosphorylation of the IFN-α/β signaling proteins, as shown in Fig. 28C. These cells were not expected to display any phosphorylated IFN-α/β signaling proteins. However, P-STAT2 and P-STAT1 were detected 24h post transfection for all transfections. This finding indicated a toxic effect of the plasmids on the cells. The toxic effect led to the induction of endogenous IFN-α production and thus activation of the type I IFN signaling pathway. The amount of phosphorylated STAT's was higher upon transfection with pVR1012, than upon transfection with pEFSV5-V or pDsRed1-C2. The plasmid pVR1012 was thus identified to be more toxic to the cells than pDsRed1-C2. pEFSV5-V and pVR1012-M1 showed a similar effect on the phosphorylation level of the lysates of IFN-α induced, transfected cells (Fig. 28A). The level of phosphorylation upon transfection with pEFSV5-V in the non-stimulated cells was higher than with pVR1012-M1 (Fig.

28C). The plasmid pEFSV5-V displayed also a toxic effect. Transfection with pVR1012-M1 revealed the lowest level of STAT-phosphorylation. This result confirmed the data of the IFN-α stimulated, transfected cells depicted in Fig. 28C. pVR1012 induced the IFN-α production by its backbone, but pVR1012 coding for the M1-protein inhibited the activation of the IFN-α/β signaling pathway, suggesting a specific inhibitory effect of viral M1-protein.

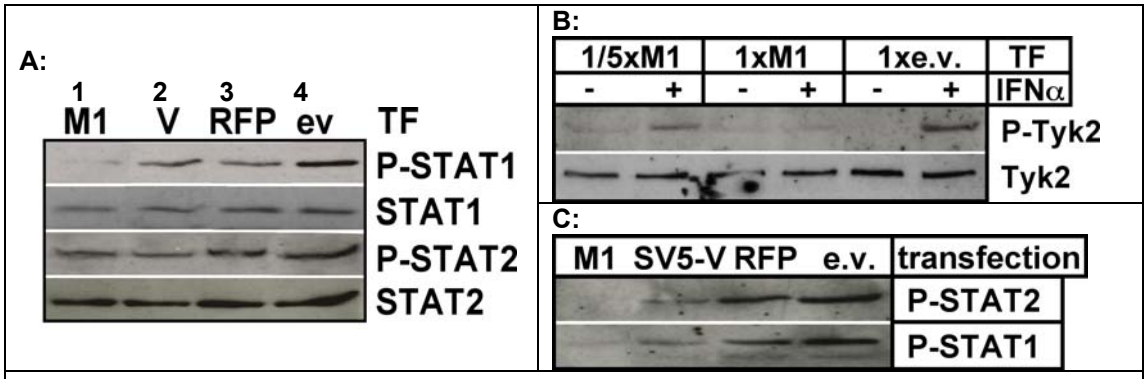

Figure 28: Phosphorylation of IFN-α signaling proteins upon overexpression of M1 in HEK293 cells. Cells were harvested and proteins were analyzed by Western blotting detecting P-Jak1, P-Tyk2, P-STAT2 or P-STAT1. A: Cells were transfected with pVR1012M1, pEFSV5-V, pDsRed1-C2 or pVR1012 and stimulated with IFN-α for 10 or 20min. B: HEK293 cells were transfected with 1/5 or 1 volume of pVR1012M1, or pVR1012 and stimulated with IFN-α for 10min. C: Cells were transfected with pVR1012M1, pEFSV5-V, pDsRed1-C2 or pVR1012.

8.8 JAK1, TYK2, STAT2 AND RACK1 AS INTERACTION PARTNERS OF M1

The previous experiments gave evidence for a negative regulation of the IFN-α/β signaling pathway by the influenza A M1-protein. Interaction partners of M1 in this negative regulation were still unknown and had thus to be identified by a co-immunoprecipitation experiment. Jak1, Tyk2, STAT2 and STAT1 were the first to be studied. They were shown to be inhibited in their phosphorylation and thus likely to be interaction partners of M1.

A co-immunoprecipitation analysis was done in influenza-infected cells. Jak1, Tyk2, STAT1 or STAT2 were precipitated and M1 was detected in immunoprecipitates. The immunoprecipitation was shown in this direction only,

as for the precipitation of the M1-protein with detection of the IFN-α/β signaling proteins no bands were detected.

Lysates were precipitated with an unspecific antibody in order to detect unspecific binding of M1 to the Protein-A agarose beads. As depicted in Fig. 29, M1 was detected after infection in immunoprecipitation analysis with Jak1, Tyk2, STAT2 and RACK1. Precipitation of Tyk2 displayed a strong band with the specific antibody only. The precipitation with Jak1 and STAT2 showed a stronger band with the specific antibody (anti-Jak1 or anti-STAT2, respectively; lane3), than the band with the unspecific antibody (anti-myosin; lane4). Therefore the interaction between Jak1-M1 and STAT2-M1 was determined to be specific. Immunoprecipitation with STAT1 did not reveal any band, indicating that there was no binding between STAT1-M1. Furthermore a co-immunoprecipitation experiment between RACK1 and M1 was performed. M1 and RACK1 were shown to be interaction partners in a yeast-two-hybrid assay (Reinhardt & Wolff, 2000). The precipitation of M1 along with RACK1 would be expected. The RACK1 precipitation was done with lysates of infected HEK293 cells, as depicted in Fig. 29. Specific interaction of M1 with RACK1 was identified (lane3). The interaction resulted in a band with the specific antibody (anti-RACK1) only, which led to the conclusion that the beads for RACK1 (protein-L agarose beads) did not interact unspecifically with M1 as did the protein-A agarose beads, used for the other IFN-α signaling proteins.

Thus, M1 was suggested to interact with Jak1, Tyk2, STAT2 and RACK1. The phosphorylation of Jak1, Tyk2 and STAT2 was inhibited and the binding of STAT1 to the receptor complex and thus the phosphorylation of STAT1 blocked. Therefore, the activation of the IFN-α/β signaling cascade was impaired by M1.

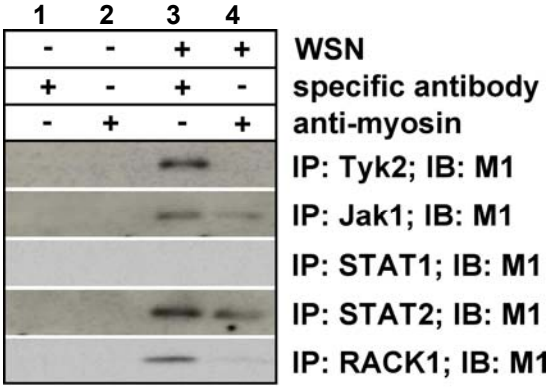

Figure 29: Co-immunoprecipitation revealed Jak1, Tyk2 and RACK1 as interaction partners of the M1-protein. Cells were harvested and proteins were extracted 12h p.i.. Western blot analysis was performed detecting M1. A co-immunoprecipitation was performed with HEK293 cells using specific antibodies (sAB) to precipitate Jak1, Tyk2, STAT1, STAT2 and RACK1 and anti-myosin as unspecific antibody to determine unspecific binding of M1 to the beads.

9 DISCUSSION

The type I IFN system is a highly evolved system that protects humans and animals from viral infection and plays an important role in the establishment of the antiviral state upon infection of a cell. Signaling induced by IFN-α/β and derived from the IFN receptor through the JAK-STAT pathway, mediates rapid and robust transcriptional induction of genes encoding antiviral proteins. The interplay between IFN and virus might affect viral pathogenicity, clearance and host immunity. Viruses encoding IFN antagonists often display increased virulence. Using various strategies, DNA and RNA viruses can inhibit IFN induced host defense mechanisms. Some viruses reduce the basal levels of particular molecules of the Jak-STAT pathway and others inactivate components of the Jak-STAT pathway.

It was previously reported that the influenza A NS1 protein repressed the antiviral response by multiple mechanisms. These mechanisms included the inhibition of the IFN inducible enzymes PKR and OAS (Bergmann et al., 2000, Tan & Katze, 1998) and the blocking of IFN-β production by preventing NF-κB, IRF3, and IRF7 activation (Smith et al., 2001, Talon et al., 2000, Wang et al., 2000). The generation of a recombinant influenza A/PR/8/34 virus lacking the NS1 gene (delNS1) impaired its ability to replicate in MDCK cells, reducing the viral growth by three logs compared to the wild type virus. As the delNS1 influenza virus deletion mutant was only partially attenuated (Garcia-Sastre et al., 1998b), it was assumed that additional influenza virus genes contributed to the virus mediated block of the antiviral-response (Geiss et al., 2002).

The scaffold protein RACK1 was shown in literature to act as a scaffold for the IFN receptor complex (Yokota et al., 2003) and for the phosphorylation of the influenza A M1-protein (Reinhardt & Wolff, 2000). These findings suggested the M1-protein as a potent antagonist of the IFN-α signaling pathway. We hypothesized that RACK1 may be the target protein for a negative regulation of the IFN-α/β signaling by the M1-protein. In the present study, we show the negative regulation of the innate immune response; more precisely the IFN-α

induced antiviral response following influenza A infection in various cell lines. Influenza A was found to have acquired the ability, to target the JAK-STAT signaling cascade for evading the IFN response. The IFN-α signaling pathway was examined by infection with influenza and transfection of the M1 protein. The data presented here demonstrate that the M1-protein of influenza is an antagonist of the IFN-α signaling pathway.

The influenza virus infection and the overexpression of M1 reduced the IFN-α/β stimulated transcription of the FFL reporter gene upon addition of excess amounts of IFN-α. The FFL activity was inhibited by 80% in HEK293 cells and by 50% in Vero cells. The difference in the suppression between the two cell lines may be explained by the infection efficiency, which was higher for the HEK293 cells. Non-stimulated, infected HEK293 cells showed a weak, but significant increase in FFL activity, compared to non-infected cells (Fig. 20A). Such a response is considered to be an indirect effect involving an intermediary IFN release. Influenza A has been shown to induce the expression of the antiviral protein Mx (Lee et al., 2000). This mechanism of induction is known to be mediated by interaction of dsRNA with TLR3 and leads to the production of type I IFNs (Alexopoulou et al., 2001, Matsumoto et al., 2004). This induction in FFL activity was not observed in Vero cells, as they do not possess the genes for type I IFNs.

The FFL reporter assay demonstrated a reduction in ISRE-promoter activity in IFN-α induced M1 transfected cells, when compared with induced RFP transfected cells. The M1-protein displayed antagonistic activity similar to the SV5 V-protein, which is known to be a strong inhibitor of the IFN-α signaling pathway (Didcock et al., 1999a, Didcock et al., 1999b). The M1-protein is the most abundant protein in the influenza A virus. A virus particle includes about 3000 molecules of the M1-protein and the amount increases rapidly upon infection. It is assumed that the IFN-α/β signaling pathway was suppressed very efficiently, considering the excess amount of M1 in the infected cell. The strength

of M1 as an IFN-α/β antagonist may be a combination of the abundance of the protein and its potency as an inhibitor.

The result of the reporter gene assay was independently confirmed by the detection of lower protein levels of MxA in IFN-α stimulated, influenza infected cells. MxA is a key effector in the IFN-α/β signaling pathway and known to be specifically induced by type I IFNs in mammals (for review see Haller and Kochs, 2002).

For efficient replication, most viruses have evolved the ability to code for IFN antagonistic molecules, capable of blocking one or more steps in the IFN system. The JAK-STAT pathway is a frequent point of interference by viruses, as it induces the activation of many antiviral genes (Sen, 2001). Some paramyxoviruses, such as SV5 and parainfluenza virus type 2 (HPIV2) have been shown to block IFN signal transduction by targeting the STAT1 and STAT2 proteins respectively for degradation (Didcock et al., 1999a, Didcock et al., 1999b, Parisien et al., 2001). Rabies virus has been shown to inhibit the translocation of activated STAT1 in the nucleus (Brzozka et al., 2006). Measles virus was shown to inhibit the antiviral activity by suppression of Jak1 phosphorylation, and Sendai virus (SeV) and Japanese encephalitis virus (JEV) were shown to interfere with the JAK-STAT signaling through the blocking of Tyk2 phosphorylation (Komatsu et al., 2000, Lin et al., 2004). Since approximately 400 genes are known to be transcriptionally stimulated by type I IFNs (Der et al., 1998), it is perhaps not surprising that for most viruses, the exact mechanism involved in blocking these complex signal transduction pathways remain to be fully elucidated. Indeed, despite intensive studies, the detailed mechanism of action responsible for the IFN antagonistic properties of the influenza NS1 protein remains to be elucidated (Garcia-Sastre, 2004).

The phosphorylation analysis of the IFN-α/β signaling proteins in influenza-infected cells gave evidence for the interference of the M1-protein with the JAK-STAT pathway. Phosphorylation of Jak1, Tyk2, STAT1 and STAT2 were suppressed upon IFN-α stimulation in influenza-infected cells and Tyk2, STAT1 and STAT2 in M1 transfected cells. Jak1 and Tyk2, bound to IFN receptor

complex, initiate the IFN-α/β signaling cascade. The suppression of the IFN-α/β signaling cascade was proposed to inhibit the phosphorylation of STAT1 and STAT2 as a consequence of inhibited phosphorylation of Jak1 and Tyk2. This finding is similar to the mechanism of IFN-α/β signaling suppression found in tick-borne encephalitis (TBE) viruses. TBE blocks the IFN-α signaling by inhibition of Jak1 and Tyk2 phosphorylation (Best et al., 2005), which suppresses the downstream signaling of IFN-α/β. The transcript level of total Jak1, Tyk2, STAT1 and STAT2 remained constant, showing that influenza infection did not induce proteolysis in this time frame.

The actual interference of the M1-protein with the IFN-α/β signaling pathway was examined by a co-immunoprecipitation experiment, where Jak1, Tyk2, STAT2 and RACK1 were identified to be interaction partners of M1 in influenza infected cells. The experimental procedure did not allow to determine whether the interaction between the five proteins was direct or indirect. Future studies are required to determine the details of the protein interaction. Moreover, the observation did not allow us to determine whether the IFN-α stimulation of infected cells led to a single type of interaction complex: M1 with Jak1, Tyk2, STAT2 and RACK1 and eventually other, currently unknown proteins, or whether the interaction between the signaling kinases Jak1, Tyk2, STAT2 and M1, and between the scaffold RACK1 and M1 were independent interactions. If the interactions with the M1-protein were independent from each other, they may also function independently in infected cells. One function would be the negative regulation of the IFN-α/β signaling and the other function would be the phosphorylation of the M1-protein by PKC (Reinhardt & Wolff, 2000).

Taken together, the complex interplay between M1 and the IFN-α/β signaling proteins could be narrowed down to two possible models (illustrated in Fig. 30): (A) Upon influenza infection the scaffold protein RACK1 associated to the IFN receptor complex is recruited by M1. The receptor complex would thereby be destroyed and the signaling cascade of IFN-α/β blocked. The suppression of the IFN-α/β signaling, caused by the defective receptor complex would be a

secondary effect of the need of M1 phosphorylation. Jak1 and Tyk2 were identified as interaction partners of M1 because the interaction with RACK1 was maintained. (B) Upon influenza infection, M1 binds to Jak1, Tyk2 and RACK1 on the IFN-α receptor complex. The membrane-associated complex is not destroyed. The interaction can lead to the inhibition of the IFN-α/β signaling only, and the phosphorylation of M1 would be an independent reaction, or the phosphorylation of M1 occurs at the IFN-α/β receptor complex, thereby masking the phosphorylation sites of Jak1 and Tyk2.

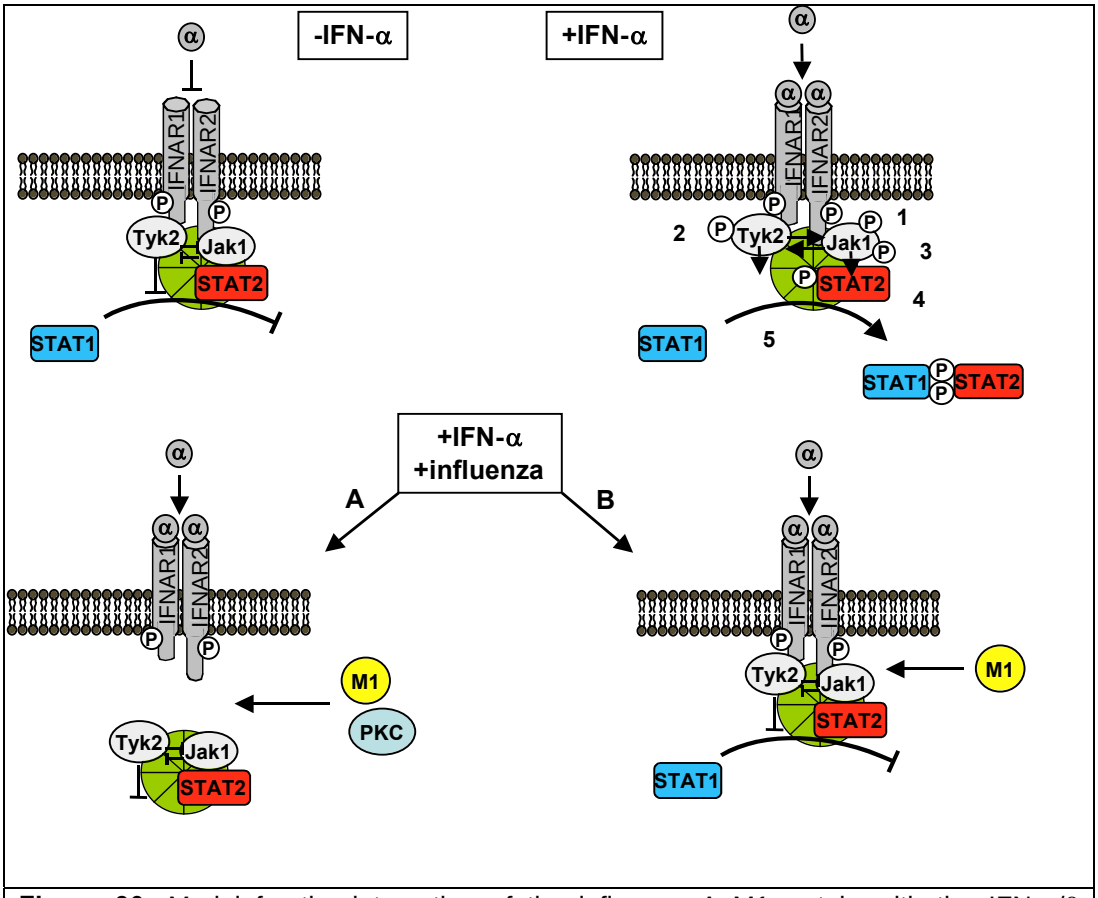

Figure 30: Model for the interaction of the influenza A M1-protein with the IFN-α/β signaling proteins. Two different models could explain the negative regulation of the IFN-α/β signaling pathway by M1: (A) The scaffold protein RACK1 is recruited by M1 for its phosphorylation by PKC. This leads to the destruction of the IFN receptor complex and thus the block of the IFN-α/β signaling pathway. As M1 was precipitated with the kinases Jak1 and Tyk2, they were expected to bind the M1-phosphorylation complex. (B) M1 binds to the IFN receptor complex directly or indirectly binding Jak1, Tyk2 and RACK1 and blocks thereby phosphorylation of Jak1, Tyk2 and STAT2, and binding of STAT1. *In vivo,* the situation could be either of the two models or a combination of them.

In addition to the inhibitory effect of the M1-protein on the IFN-α/β signaling pathway, an independent effect was observed by the detection of MxA in infected A549 cells. Analysis of MxA by Western blotting showed a significant decrease in MxA protein content (Fig. 22B), if A549 cells were infected with influenza A and proteins were extracted 20h to 24h later. This phenomenon was observed without IFN-α stimulation. The effect was thus not a consequence of the time gap between influenza infection and IFN-α stimulation of the cells. MxA remains stable in the cells for several days after synthesis (Aebi et al., 1989). Therefore, our observation led to the conclusion that MxA was actively degraded by influenza A. The influenza A polymerase A subunit (PA) was shown to induce proteolysis upon infection of a cell (Hara et al., 2001, Sanz-Ezquerro et al., 1995). PA may be responsible for the degradation of MxA. Further experiments remain to be done in order to proof this hypothesis. This proteolytic activity would represent the third protein of influenza A, displaying antagonistic activity against the innate immune response. This indicates the importance of the suppression of the IFN system for the virulence of the influenza A virus, as it was previously described for other viruses.

This study elucidated the M1-protein as second influenza protein, interfering with the innate immune response. Until now, the influenza virus displays two proteins counteracting the innate immune response, the NS1 protein by suppression of the IFN-α/β production, and the M1-protein by inhibition of the expression of IFN inducible genes. This additional strategy against the innate immune system enables the virus to replicate in cells stimulated by paracrine or endocrine secreted IFN-α. The virus displays an enhanced virulence and is therefore well prepared to counteract the host cell defense. The identification of an IFN antagonist protein in influenza A represents an important step in understanding influenza virus-host interactions since inhibition of the IFN system is known to play an important role in pathogenicity, immunogenicity, persistence and tissue/host tropism (Didcock et al., 1999a, Garcia-Sastre et al., 1998a).

Experimental data have shown the importance of adaptive immune response, especially the antibody response upon influenza virus infection (Graham et al., 1994). The importance of a potent antibody response for viral clearance might be a consequence of the efficient suppression of IFN-α/β induction/signaling by influenza virus.

10 OUTLOOK

This study showed an alternative mechanism of influenza to counteract the innate immune system. We identified the influenza protein M1 as interaction partner of several IFN-α signaling proteins.

An interesting approach for the future would be to find out whether M1-protein *de novo* synthesis is required for the negative regulation of the innate immune response in influenza infected cells. Therefore cells could be infected with inactivated, but morphologically intact virus (inactivation by UV light, which destroys the RNA, but not the proteins). As the viral protein synthesis would be blocked, a possible effect upon infection would originate in the antagonistic activity of M1 protein brought into the cell by the virus particle. It remains to be examined whether the amount of M1-protein brought into the cell by infection is sufficient for IFN-α signaling suppression.

This study identified influenza A to contain a proteolytic activity, responsible for the degradation of MxA. It was speculated that the polymerase subunit PA of influenza A encodes a proteolytic activity (Perales et al., 2000, Sanz-Ezquerro et al., 1995). Our finding together with this hypothesis would present an interesting investigation for a future project.

It is known from literature that M1 is phosphorylated by PKC, and that M1 has different functions depending on its phosphorylation status. It would be interesting to know whether the phosphorylation status of M1 is related to its activity in IFN-α signaling cascade.

11 REFERENCES

Aebi, M., Fah, J., Hurt, N., Samuel, C. E., Thomis, D., Bazzigher, L., Pavlovic, J., Haller, O. & Staeheli, P. (1989). cDNA structures and regulation of two interferon-induced human Mx proteins. *Mol Cell Biol* **9**, 5062-72.

Alcami, A. (2003). Viral mimicry of cytokines, chemokines and their receptors. *Nat Rev Immunol* **3**, 36-50.

Alexopoulou, L., Holt, A. C., Medzhitov, R. & Flavell, R. A. (2001). Recognition of double-stranded RNA and activation of NF-kappaB by Toll-like receptor 3. *Nature* **413**, 732-8.

Amara, R. R., Villinger, F., Altman, J. D., Lydy, S. L., O'Neil, S. P., Staprans, S. I., Montefiori, D. C., Xu, Y., Herndon, J. G., Wyatt, L. S., Candido, M. A., Kozyr, N. L., Earl, P. L., Smith, J. M., Ma, H. L., Grimm, B. D., Hulsey, M. L., Miller, J., McClure, H. M., McNicholl, J. M., Moss, B. & Robinson, H. L. (2001). Control of a mucosal challenge and prevention of AIDS by a multiprotein DNA/MVA vaccine. *Science* **292**, 69-74.

Andrejeva, J., Childs, K. S., Young, D. F., Carlos, T. S., Stock, N., Goodbourn, S. & Randall, R. E. (2004). The V proteins of paramyxoviruses bind the IFN-inducible RNA helicase, mda-5, and inhibit its activation of the IFN-beta promoter. *Proc Natl Acad Sci U S A* **101**, 17264-9.

Ank, N., West, H. & Paludan, S. R. (2006). IFN-lambda: Novel Antiviral Cytokines. *J Interferon Cytokine Res* **26**, 373-9.

Ashraf, H. (2003). WHO declares Beijing to be free of SARS. *Lancet* **361**, 2212.

Avalos, R. T., Yu, Z. & Nayak, D. P. (1997). Association of influenza virus NP and M1 proteins with cellular cytoskeletal elements in influenza virus-infected cells. *J Virol* **71**, 2947-58.

Bairoch, A. & Apweiler, R. (1997). The SWISS-PROT protein sequence database: its relevance to human molecular medical research. *J Mol Med* **75**, 312-6.

Baron, W., Decker, L., Colognato, H. & ffrench-Constant, C. (2003). Regulation of integrin growth factor interactions in oligodendrocytes by lipid raft microdomains. *Curr Biol* **13**, 151-5.

Basler, C. F., Mikulasova, A., Martinez-Sobrido, L., Paragas, J., Muhlberger, E., Bray, M., Klenk, H. D., Palese, P. & Garcia-Sastre, A. (2003). The Ebola virus VP35 protein inhibits activation of interferon regulatory factor 3. *J Virol* **77**, 7945-56.

Basler, C. F., Wang, X., Muhlberger, E., Volchkov, V., Paragas, J., Klenk, H. D., Garcia-Sastre, A. & Palese, P. (2000). The Ebola virus VP35 protein functions as a type I IFN antagonist. *Proc Natl Acad Sci U S A* **97**, 12289-94.

Bauer, S., Kirschning, C. J., Hacker, H., Redecke, V., Hausmann, S., Akira, S., Wagner, H. & Lipford, G. B. (2001). Human TLR9 confers responsiveness to bacterial DNA via species-specific CpG motif recognition. *Proc Natl Acad Sci U S A* **98**, 9237-42.

Baumann, M., Gires, O., Kolch, W., Mischak, H., Zeidler, R., Pich, D. & Hammerschmidt, W. (2000). The PKC targeting protein RACK1 interacts with the Epstein-Barr virus activator protein BZLF1. *Eur J Biochem* **267**, 3891-901.

Baumgartner, M., Angelisova, P., Setterblad, N., Mooney, N., Werling, D., Horejsi, V. & Langsley, G. (2003). Constitutive exclusion of Csk from Hck-positive membrane microdomains permits Src kinase-dependent proliferation of Theileria-transformed B lymphocytes. *Blood* **101**, 1874-81.

Bazzigher, L., Pavlovic, J., Haller, O. & Staeheli, P. (1992). Mx genes show weaker primary response to virus than other interferon-regulated genes. *Virology* **186**, 154-60.

Bergmann, M., Garcia-Sastre, A., Carnero, E., Pehamberger, H., Wolff, K., Palese, P. & Muster, T. (2000). Influenza virus NS1 protein counteracts PKR-mediated inhibition of replication. *J Virol* **74**, 6203-6.

Best, S. M., Morris, K. L., Shannon, J. G., Robertson, S. J., Mitzel, D. N., Park, G. S., Boer, E., Wolfinbarger, J. B. & Bloom, M. E. (2005). Inhibition of interferon-stimulated JAK-STAT signaling by a tick-borne flavivirus and identification of NS5 as an interferon antagonist. *J Virol* **79**, 12828-39.

Billecocq, A., Spiegel, M., Vialat, P., Kohl, A., Weber, F., Bouloy, M. & Haller, O. (2004). NSs protein of Rift Valley fever virus blocks interferon production by inhibiting host gene transcription. *J Virol* **78**, 9798-806.

Bisht, H., Roberts, A., Vogel, L., Bukreyev, A., Collins, P. L., Murphy, B. R., Subbarao, K. & Moss, B. (2004). Severe acute respiratory syndrome coronavirus spike protein expressed by attenuated vaccinia virus protectively immunizes mice. *Proc Natl Acad Sci U S A* **101**, 6641-6.

Bohme, U. & Cross, G. A. (2002). Mutational analysis of the variant surface glycoprotein GPI-anchor signal sequence in Trypanosoma brucei. *J Cell Sci* **115**, 805-16.

Boothroyd, J. C., Paynter, C. A., Cross, G. A., Bernards, A. & Borst, P. (1981). Variant surface glycoproteins of Trypanosoma brucei are synthesised with cleavable hydrophobic sequences at the carboxy and amino termini. *Nucleic Acids Res* **9**, 4735-43.

Bossert, B., Marozin, S. & Conzelmann, K. K. (2003). Nonstructural proteins NS1 and NS2 of bovine respiratory syncytial virus block activation of interferon regulatory factor 3. *J Virol* **77**, 8661-8.

Bredenbeek, P. J., Pachuk, C. J., Noten, A. F., Charite, J., Luytjes, W., Weiss, S. R. & Spaan, W. J. (1990). The primary structure and expression of the second open reading frame of the polymerase gene of the coronavirus MHV-A59; a highly conserved polymerase is expressed by an efficient ribosomal frameshifting mechanism. *Nucleic Acids Res* **18**, 1825-32.

Brown, D. (1993). The tyrosine kinase connection: how GPI-anchored proteins activate T cells. *Curr Opin Immunol* **5**, 349-54.

Brown, D. & Waneck, G. L. (1992). Glycosyl-phosphatidylinositol-anchored membrane proteins. *J Am Soc Nephrol* **3**, 895-906.

Brown, D. A. (1992). Interactions between GPI-anchored proteins and membrane lipids. *Trends Cell Biol* **2**, 338-43.

Brown, D. A. & Rose, J. K. (1992). Sorting of GPI-anchored proteins to glycolipid-enriched membrane subdomains during transport to the apical cell surface. *Cell* **68**, 533-44.

Brzozka, K., Finke, S. & Conzelmann, K. K. (2006). Inhibition of interferon signaling by rabies virus phosphoprotein P: activation-dependent binding of STAT1 and STAT2. *J Virol* **80**, 2675-83.

Bui, M., Whittaker, G. & Helenius, A. (1996). Effect of M1 protein and low pH on nuclear transport of influenza virus ribonucleoproteins. *J Virol* **70**, 8391-401.

Casimiro, D. R., Chen, L., Fu, T. M., Evans, R. K., Caulfield, M. J., Davies, M. E., Tang, A., Chen, M., Huang, L., Harris, V., Freed, D. C., Wilson, K. A., Dubey, S., Zhu, D. M., Nawrocki, D., Mach, H., Troutman, R., Isopi, L., Williams, D., Hurni, W., Xu, Z., Smith, J. G., Wang, S., Liu, X., Guan, L., Long, R., Trigona, W., Heidecker, G. J., Perry, H. C., Persaud, N., Toner, T. J., Su, Q., Liang, X., Youil, R., Chastain, M., Bett, A. J., Volkin, D. B., Emini, E. A. & Shiver, J. W. (2003). Comparative immunogenicity in rhesus monkeys of DNA plasmid, recombinant vaccinia virus, and replication-defective adenovirus vectors expressing a human immunodeficiency virus type 1 gag gene. *J Virol* **77**, 6305-13.

Cayley, P. J., Davies, J. A., McCullagh, K. G. & Kerr, I. M. (1984). Activation of the ppp(A2'p)nA system in interferon-treated, herpes simplex virus-infected cells and evidence for novel inhibitors of the ppp(A2'p)nA-dependent RNase. *Eur J Biochem* **143**, 165-74.

Cebecauer, M., Cerny, J. & Horejsi, V. (1998). Incorporation of leucocyte GPI-anchored proteins and protein tyrosine kinases into lipid-rich membrane domains of COS-7 cells. *Biochem Biophys Res Commun* **243**, 706-10.

Chao, C. C., Bird, P., Gething, M. J. & Sambrook, J. (1987). Posttranslational translocation of influenza virus hemagglutinin across microsomal membranes. *Mol Cell Biol* **7**, 3842-5.

Chen, Z. & Krug, R. M. (2000). Selective nuclear export of viral mRNAs in influenza-virus-infected cells. *Trends Microbiol* **8**, 376-83.

Chen, Z., Li, Y. & Krug, R. M. (1999). Influenza A virus NS1 protein targets poly(A)-binding protein II of the cellular 3'-end processing machinery. *Embo J* **18**, 2273-83.

Coban, C., Philipp, M. T., Purcell, J. E., Keister, D. B., Okulate, M., Martin, D. S. & Kumar, N. (2004). Induction of Plasmodium falciparum transmission-blocking antibodies in nonhuman primates by a combination of DNA and protein immunizations. *Infect Immun* **72**, 253-9.

Colman, P. M. & Lawrence, M. C. (2003). The structural biology of type I viral membrane fusion. *Nat Rev Mol Cell Biol* **4**, 309-19.

Cox, G. J., Zamb, T. J. & Babiuk, L. A. (1993). Bovine herpesvirus 1: immune responses in mice and cattle injected with plasmid DNA. *J Virol* **67**, 5664-7.

Croze, E., Usacheva, A., Asarnow, D., Minshall, R. D., Perez, H. D. & Colamonici, O. (2000). Receptor for activated C-kinase (RACK-1), a WD motif-containing protein, specifically associates with the human type I IFN receptor. *J Immunol* **165**, 5127-32.

Delmas, B. & Laude, H. (1990). Assembly of coronavirus spike protein into trimers and its role in epitope expression. *J Virol* **64**, 5367-75.

Der, S. D., Zhou, A., Williams, B. R. & Silverman, R. H. (1998). Identification of genes differentially regulated by interferon alpha, beta, or gamma using oligonucleotide arrays. *Proc Natl Acad Sci U S A* **95**, 15623-8.

Didcock, L., Young, D. F., Goodbourn, S. & Randall, R. E. (1999a). Sendai virus and simian virus 5 block activation of interferon-responsive genes: importance for virus pathogenesis. *J Virol* **73**, 3125-33.

Didcock, L., Young, D. F., Goodbourn, S. & Randall, R. E. (1999b). The V protein of simian virus 5 inhibits interferon signalling by targeting STAT1 for proteasome-mediated degradation. *J Virol* **73**, 9928-33.

Diebold, S. S., Montoya, M., Unger, H., Alexopoulou, L., Roy, P., Haswell, L. E., Al-Shamkhani, A., Flavell, R., Borrow, P. & Reis e Sousa, C. (2003). Viral infection switches non-plasmacytoid dendritic cells into high interferon producers. *Nature* **424**, 324-8.

Donnelly, J., Berry, K. & Ulmer, J. B. (2003). Technical and regulatory hurdles for DNA vaccines. *Int J Parasitol* **33**, 457-67.

Donnelly, J. J., Ulmer, J. B., Shiver, J. W. & Liu, M. A. (1997). DNA vaccines. *Annu Rev Immunol* **15**, 617-48.

Dupuis, S., Jouanguy, E., Al-Hajjar, S., Fieschi, C., Al-Mohsen, I. Z., Al-Jumaah, S., Yang, K., Chapgier, A., Eidenschenk, C., Eid, P., Al Ghonaium, A., Tufenkeji, H., Frayha, H., Al-Gazlan, S., Al-Rayes, H., Schreiber, R. D., Gresser, I. & Casanova, J. L. (2003). Impaired response to interferon-alpha/beta and lethal viral disease in human STAT1 deficiency. *Nat Genet* **33**, 388-91.

Egan, M. A., Megati, S., Roopchand, V., Garcia-Hand, D., Luckay, A., Chong, S. Y., Rosati, M., Sackitey, S., Weiner, D. B., Felber, B. K., Pavlakis, G. N., Israel, Z. R., Eldridge, J. H. & Sidhu, M. K. (2005). Rational design of a plasmid DNA vaccine capable of eliciting cell-mediated immune responses to multiple HIV antigens in mice. *Vaccine*.

Enami, M. & Enami, K. (1996). Influenza virus hemagglutinin and neuraminidase glycoproteins stimulate the membrane association of the matrix protein. *J Virol* **70**, 6653-7.

Epstein, S. L., Kong, W. P., Misplon, J. A., Lo, C. Y., Tumpey, T. M., Xu, L. & Nabel, G. J. (2005). Protection against multiple influenza A subtypes by vaccination with highly conserved nucleoprotein. *Vaccine* **23**, 5404-10.

Fanning, S. L., Czesny, B., Sedegah, M., Carucci, D. J., van Gemert, G. J., Eling, W. & Williamson, K. C. (2003). A glycosylphosphatidylinositol anchor signal sequence enhances the immunogenicity of a DNA vaccine encoding Plasmodium falciparum sexual-stage antigen, Pfs230. *Vaccine* **21**, 3228-35.

Ferran, M. C. & Lucas-Lenard, J. M. (1997). The vesicular stomatitis virus matrix protein inhibits transcription from the human beta interferon promoter. *J Virol* **71**, 371-7.

Fleck, F. (2003). WHO says SARS outbreak is over, but fight should go on. *Bmj* **327**, 70.

Fortes, P., Beloso, A. & Ortin, J. (1994). Influenza virus NS1 protein inhibits pre-mRNA splicing and blocks mRNA nucleocytoplasmic transport. *Embo J* **13**, 704-12.

Foster, L. J., De Hoog, C. L. & Mann, M. (2003). Unbiased quantitative proteomics of lipid rafts reveals high specificity for signaling factors. *Proc Natl Acad Sci U S A* **100**, 5813-8.

Frana, M. F., Behnke, J. N., Sturman, L. S. & Holmes, K. V. (1985). Proteolytic cleavage of the E2 glycoprotein of murine coronavirus: host-dependent differences in proteolytic cleavage and cell fusion. *J Virol* **56**, 912-20.

Fujiyoshi, Y., Kume, N. P., Sakata, K. & Sato, S. B. (1994). Fine structure of influenza A virus observed by electron cryo-microscopy. *Embo J* **13**, 318-26.
Fynan, E. F., Robinson, H. L. & Webster, R. G. (1993). Use of DNA encoding influenza hemagglutinin as an avian influenza vaccine. *DNA Cell Biol* **12**, 785-9.
Gallagher, T. M. & Buchmeier, M. J. (2001). Coronavirus spike proteins in viral entry and pathogenesis. *Virology* **279**, 371-4.
Gallina, A., Rossi, F. & Milanesi, G. (2001). Rack1 binds HIV-1 Nef and can act as a Nef-protein kinase C adaptor. *Virology* **283**, 7-18.
Gao, W., Tamin, A., Soloff, A., D'Aiuto, L., Nwanegbo, E., Robbins, P. D., Bellini, W. J., Barratt-Boyes, S. & Gambotto, A. (2003). Effects of a SARS-associated coronavirus vaccine in monkeys. *Lancet* **362**, 1895-6.
Garcia-Sastre, A. (2004). Identification and characterization of viral antagonists of type I interferon in negative-strand RNA viruses. *Curr Top Microbiol Immunol* **283**, 249-80.
Garcia-Sastre, A. & Biron, C. A. (2006). Type 1 interferons and the virus-host relationship: a lesson in detente. *Science* **312**, 879-82.
Garcia-Sastre, A., Durbin, R. K., Zheng, H., Palese, P., Gertner, R., Levy, D. E. & Durbin, J. E. (1998a). The role of interferon in influenza virus tissue tropism. *J Virol* **72**, 8550-8.
Garcia-Sastre, A., Egorov, A., Matassov, D., Brandt, S., Levy, D. E., Durbin, J. E., Palese, P. & Muster, T. (1998b). Influenza A virus lacking the NS1 gene replicates in interferon-deficient systems. *Virology* **252**, 324-30.
Garoff, H., Hewson, R. & Opstelten, D. J. (1998). Virus maturation by budding. *Microbiol Mol Biol Rev* **62**, 1171-90.
Gauzzi, M. C., Velazquez, L., McKendry, R., Mogensen, K. E., Fellous, M. & Pellegrini, S. (1996). Interferon-alpha-dependent activation of Tyk2 requires phosphorylation of positive regulatory tyrosines by another kinase. *J Biol Chem* **271**, 20494-500.
Geiss, G. K., Salvatore, M., Tumpey, T. M., Carter, V. S., Wang, X., Basler, C. F., Taubenberger, J. K., Bumgarner, R. E., Palese, P., Katze, M. G. & Garcia-Sastre, A. (2002). Cellular transcriptional profiling in influenza A virus-infected lung epithelial cells: the role of the nonstructural NS1 protein in the evasion of the host innate defense and its potential contribution to pandemic influenza. *Proc Natl Acad Sci U S A* **99**, 10736-41.
Gething, M. J. & Sambrook, J. (1982). Construction of influenza haemagglutinin genes that code for intracellular and secreted forms of the protein. *Nature* **300**, 598-603.
Gomez-Puertas, P., Albo, C., Perez-Pastrana, E., Vivo, A. & Portela, A. (2000). Influenza virus matrix protein is the major driving force in virus budding. *J Virol* **74**, 11538-47.
Goodbourn, S., Didcock, L. & Randall, R. E. (2000). Interferons: cell signalling, immune modulation, antiviral response and virus countermeasures. *J Gen Virol* **81**, 2341-64.
Graham, M. B., Braciale, V. L. & Braciale, T. J. (1994). Influenza virus-specific CD4+ T helper type 2 T lymphocytes do not promote recovery from experimental virus infection. *J Exp Med* **180**, 1273-82.
Haller, O. & Kochs, G. (2002). Interferon-induced mx proteins: dynamin-like GTPases with antiviral activity. *Traffic* **3**, 710-7.

Hankins, R. W., Nagata, K., Kato, A. & Ishihama, A. (1990). Mechanism of influenza virus transcription inhibition by matrix (M1) protein. *Res Virol* **141**, 305-14.
Hara, K., Shiota, M., Kido, H., Ohtsu, Y., Kashiwagi, T., Iwahashi, J., Hamada, N., Mizoue, K., Tsumura, N., Kato, H. & Toyoda, T. (2001). Influenza virus RNA polymerase PA subunit is a novel serine protease with Ser624 at the active site. *Genes Cells* **6**, 87-97.
Hauri, H. P., Kappeler, F., Andersson, H. & Appenzeller, C. (2000). ERGIC-53 and traffic in the secretory pathway. *J Cell Sci* **113 (Pt 4)**, 587-96.
He, B., Gross, M. & Roizman, B. (1997). The gamma(1)34.5 protein of herpes simplex virus 1 complexes with protein phosphatase 1alpha to dephosphorylate the alpha subunit of the eukaryotic translation initiation factor 2 and preclude the shutoff of protein synthesis by double-stranded RNA-activated protein kinase. *Proc Natl Acad Sci U S A* **94**, 843-8.
He, B., Paterson, R. G., Stock, N., Durbin, J. E., Durbin, R. K., Goodbourn, S., Randall, R. E. & Lamb, R. A. (2002). Recovery of paramyxovirus simian virus 5 with a V protein lacking the conserved cysteine-rich domain: the multifunctional V protein blocks both interferon-beta induction and interferon signaling. *Virology* **303**, 15-32.
Heil, F., Hemmi, H., Hochrein, H., Ampenberger, F., Kirschning, C., Akira, S., Lipford, G., Wagner, H. & Bauer, S. (2004). Species-specific recognition of single-stranded RNA via toll-like receptor 7 and 8. *Science* **303**, 1526-9.
Helenius, A. (1992). Unpacking the incoming influenza virus. *Cell* **69**, 577-8.
Hermanson, G., Whitlow, V., Parker, S., Tonsky, K., Rusalov, D., Ferrari, M., Lalor, P., Komai, M., Mere, R., Bell, M., Brenneman, K., Mateczun, A., Evans, T., Kaslow, D., Galloway, D. & Hobart, P. (2004). A cationic lipid-formulated plasmid DNA vaccine confers sustained antibody-mediated protection against aerosolized anthrax spores. *Proc Natl Acad Sci U S A* **101**, 13601-6.
Hernandez, L. D., Hoffman, L. R., Wolfsberg, T. G. & White, J. M. (1996). Virus-cell and cell-cell fusion. *Annu Rev Cell Dev Biol* **12**, 627-61.
Horejsi, V. (2003). The roles of membrane microdomains (rafts) in T cell activation. *Immunol Rev* **191**, 148-64.
Horisberger, M. A., McMaster, G. K., Zeller, H., Wathelet, M. G., Dellis, J. & Content, J. (1990). Cloning and sequence analyses of cDNAs for interferon- and virus-induced human Mx proteins reveal that they contain putative guanine nucleotide-binding sites: functional study of the corresponding gene promoter. *J Virol* **64**, 1171-81.
Horton, P. & Nakai, K. (1997). Better prediction of protein cellular localization sites with the k nearest neighbors classifier. *Proc Int Conf Intell Syst Mol Biol* **5**, 147-52.
Hovanessian, A. G., Brown, R. E. & Kerr, I. M. (1977). Synthesis of low molecular weight inhibitor of protein synthesis with enzyme from interferon-treated cells. *Nature* **268**, 537-40.
Huang, X., Liu, T., Muller, J., Levandowski, R. A. & Ye, Z. (2001). Effect of influenza virus matrix protein and viral RNA on ribonucleoprotein formation and nuclear export. *Virology* **287**, 405-16.
Ishii, K. J., Coban, C., Kato, H., Takahashi, K., Torii, Y., Takeshita, F., Ludwig, H., Sutter, G., Suzuki, K., Hemmi, H., Sato, S., Yamamoto, M., Uematsu, S., Kawai,

T., Takeuchi, O. & Akira, S. (2006). A Toll-like receptor-independent antiviral response induced by double-stranded B-form DNA. *Nat Immunol* **7**, 40-8.
Kapadia, S. U., Rose, J. K., Lamirande, E., Vogel, L., Subbarao, K. & Roberts, A. (2005). Long-term protection from SARS coronavirus infection conferred by a single immunization with an attenuated VSV-based vaccine. *Virology* **340**, 174-82.
Kato, H., Takeuchi, O., Sato, S., Yoneyama, M., Yamamoto, M., Matsui, K., Uematsu, S., Jung, A., Kawai, T., Ishii, K. J., Yamaguchi, O., Otsu, K., Tsujimura, T., Koh, C. S., Reis e Sousa, C., Matsuura, Y., Fujita, T. & Akira, S. (2006). Differential roles of MDA5 and RIG-I helicases in the recognition of RNA viruses. *Nature* **441**, 101-5.
King, P. & Goodbourn, S. (1998). STAT1 is inactivated by a caspase. *J Biol Chem* **273**, 8699-704.
Kirman, J. R. & Seder, R. A. (2003). DNA vaccination: the answer to stable, protective T-cell memory? *Curr Opin Immunol* **15**, 471-6.
Komatsu, T., Takeuchi, K., Yokoo, J., Tanaka, Y. & Gotoh, B. (2000). Sendai virus blocks alpha interferon signaling to signal transducers and activators of transcription. *J Virol* **74**, 2477-80.
Kong, W. P., Xu, L., Stadler, K., Ulmer, J. B., Abrignani, S., Rappuoli, R. & Nabel, G. J. (2005). Modulation of the immune response to the severe acute respiratory syndrome spike glycoprotein by gene-based and inactivated virus immunization. *J Virol* **79**, 13915-23.
Konishi, E., Terazawa, A. & Imoto, J. (2003). Simultaneous immunization with DNA and protein vaccines against Japanese encephalitis or dengue synergistically increases their own abilities to induce neutralizing antibody in mice. *Vaccine* **21**, 1826-32.
Krokhin, O., Li, Y., Andonov, A., Feldmann, H., Flick, R., Jones, S., Stroeher, U., Bastien, N., Dasuri, K. V., Cheng, K., Simonsen, J. N., Perreault, H., Wilkins, J., Ens, W., Plummer, F. & Standing, K. G. (2003). Mass spectrometric characterization of proteins from the SARS virus: a preliminary report. *Mol Cell Proteomics* **2**, 346-56.
Kubota, T., Yokosawa, N., Yokota, S. & Fujii, N. (2002). Association of mumps virus V protein with RACK1 results in dissociation of STAT-1 from the alpha interferon receptor complex. *J Virol* **76**, 12676-82.
Lai, M. M. & Cavanagh, D. (1997). The molecular biology of coronaviruses. *Adv Virus Res* **48**, 1-100.
Lakadamyali, M., Rust, M. J. & Zhuang, X. (2004). Endocytosis of influenza viruses. *Microbes Infect* **6**, 929-36.
Lamb, R. A. & Takeda, M. (2001). Death by influenza virus protein. *Nat Med* **7**, 1286-8.
Lamb, R. A., Zebedee, S. L. & Richardson, C. D. (1985). Influenza virus M2 protein is an integral membrane protein expressed on the infected-cell surface. *Cell* **40**, 627-33.
Laude, A. J. & Prior, I. A. (2004). Plasma membrane microdomains: organization, function and trafficking. *Mol Membr Biol* **21**, 193-205.
Le May, N., Dubaele, S., Proietti De Santis, L., Billecocq, A., Bouloy, M. & Egly, J. M. (2004). TFIIH transcription factor, a target for the Rift Valley hemorrhagic fever virus. *Cell* **116**, 541-50.
Lee, J. Y., Hirono, I. & Aoki, T. (2000). Cloning and analysis of expression of Mx cDNA in Japanese flounder, Paralichthys olivaceus. *Dev Comp Immunol* **24**, 407-15.

Letvin, N. L., Montefiori, D. C., Yasutomi, Y., Perry, H. C., Davies, M. E., Lekutis, C., Alroy, M., Freed, D. C., Lord, C. I., Handt, L. K., Liu, M. A. & Shiver, J. W. (1997). Potent, protective anti-HIV immune responses generated by bimodal HIV envelope DNA plus protein vaccination. *Proc Natl Acad Sci U S A* **94**, 9378-83.

Leung, S., Qureshi, S. A., Kerr, I. M., Darnell, J. E., Jr. & Stark, G. R. (1995). Role of STAT2 in the alpha interferon signaling pathway. *Mol Cell Biol* **15**, 1312-7.

Li, W., Greenough, T. C., Moore, M. J., Vasilieva, N., Somasundaran, M., Sullivan, J. L., Farzan, M. & Choe, H. (2004). Efficient replication of severe acute respiratory syndrome coronavirus in mouse cells is limited by murine angiotensin-converting enzyme 2. *J Virol* **78**, 11429-33.

Li, Z., Stahl, G. & Farabaugh, P. J. (2001). Programmed +1 frameshifting stimulated by complementarity between a downstream mRNA sequence and an error-correcting region of rRNA. *Rna* **7**, 275-84.

Lin, R. J., Liao, C. L., Lin, E. & Lin, Y. L. (2004). Blocking of the alpha interferon-induced Jak-Stat signaling pathway by Japanese encephalitis virus infection. *J Virol* **78**, 9285-94.

Lindenmann, J. (1964). Inheritance of Resistance to Influenza Virus in Mice. *Proc Soc Exp Biol Med* **116**, 506-9.

Liu, M. A. (2003). DNA vaccines: a review. *J Intern Med* **253**, 402-10.

Lontok, E., Corse, E. & Machamer, C. E. (2004). Intracellular targeting signals contribute to localization of coronavirus spike proteins near the virus assembly site. *J Virol* **78**, 5913-22.

Lorenzen, N. & LaPatra, S. E. (2005). DNA vaccines for aquacultured fish. *Rev Sci Tech* **24**, 201-13.

Lyles, D. S. (2000). Cytopathogenesis and inhibition of host gene expression by RNA viruses. *Microbiol Mol Biol Rev* **64**, 709-24.

MacGregor, R. R., Boyer, J. D., Ugen, K. E., Lacy, K. E., Gluckman, S. J., Bagarazzi, M. L., Chattergoon, M. A., Baine, Y., Higgins, T. J., Ciccarelli, R. B., Coney, L. R., Ginsberg, R. S. & Weiner, D. B. (1998). First human trial of a DNA-based vaccine for treatment of human immunodeficiency virus type 1 infection: safety and host response. *J Infect Dis* **178**, 92-100.

Majumder, B., Gray, B., McBurney, S., Schaefer, T. M., Dentchev, T., Mahalingam, S., Reinhart, T. A. & Ayyavoo, V. (2003). Attenuated nef DNA vaccine construct induces cellular immune response: role in HIV-1 multiprotein vaccine. *Immunol Lett* **89**, 207-14.

Malathi, K., Paranjape, J. M., Bulanova, E., Shim, M., Guenther-Johnson, J. M., Faber, P. W., Eling, T. E., Williams, B. R. & Silverman, R. H. (2005). A transcriptional signaling pathway in the IFN system mediated by 2'-5'-oligoadenylate activation of RNase L. *Proc Natl Acad Sci U S A* **102**, 14533-8.

Martin, K. & Helenius, A. (1991). Nuclear transport of influenza virus ribonucleoproteins: the viral matrix protein (M1) promotes export and inhibits import. *Cell* **67**, 117-30.

Matrosovich, M. & Klenk, H. D. (2003). Natural and synthetic sialic acid-containing inhibitors of influenza virus receptor binding. *Rev Med Virol* **13**, 85-97.

Matsumoto, M., Funami, K., Oshiumi, H. & Seya, T. (2004). Toll-like receptor 3: a link between toll-like receptor, interferon and viruses. *Microbiol Immunol* **48**, 147-54.

Matsuyama, S., Ujike, M., Morikawa, S., Tashiro, M. & Taguchi, F. (2005). Protease-mediated enhancement of severe acute respiratory syndrome coronavirus infection. *Proc Natl Acad Sci U S A* **102**, 12543-7.

Megede, J. Z., Otten, G. R., Doe, B., Liu, H., Srivastava, R., Greer, C., Legg, H., Tang, T., Polo, J. M., Donnelly, J. J., Ulmer, J. B. & Barnett, S. W. (2006). Evaluation of human immunodeficiency virus type 1 subtype C gag, pol, and gagpol DNA and alphavirus replicon vaccines. *Vaccine* **24**, 2755-63.

Menon, A. K., Mayor, S., Ferguson, M. A., Duszenko, M. & Cross, G. A. (1988). Candidate glycophospholipid precursor for the glycosylphosphatidylinositol membrane anchor of Trypanosoma brucei variant surface glycoproteins. *J Biol Chem* **263**, 1970-7.

Meylan, E., Curran, J., Hofmann, K., Moradpour, D., Binder, M., Bartenschlager, R. & Tschopp, J. (2005). Cardif is an adaptor protein in the RIG-I antiviral pathway and is targeted by hepatitis C virus. *Nature* **437**, 1167-72.

Min, J. Y. & Krug, R. M. (2006). The primary function of RNA binding by the influenza A virus NS1 protein in infected cells: Inhibiting the 2'-5' oligo (A) synthetase/RNase L pathway. *Proc Natl Acad Sci U S A* **103**, 7100-5.

Moelling, K. (1998). Naked DNA--the poor man's gene therapy? *Gene Ther* **5**, 573-4.

Monastyrskaya, K., Hostettler, A., Buergi, S. & Draeger, A. (2005). The NK1 receptor localizes to the plasma membrane microdomains, and its activation is dependent on lipid raft integrity. *J Biol Chem* **280**, 7135-46.

Montgomery, D. L., Donnelly, J. J., Shiver, J. W., Liu, M. A. & Ulmer, J. B. (1994). Protein expression in vivo by injection of polynucleotides. *Curr Opin Biotechnol* **5**, 505-10.

Moran, P. & Caras, I. W. (1994). Requirements for glycosylphosphatidylinositol attachment are similar but not identical in mammalian cells and parasitic protozoa. *J Cell Biol* **125**, 333-43.

Muller, U., Steinhoff, U., Reis, L. F., Hemmi, S., Pavlovic, J., Zinkernagel, R. M. & Aguet, M. (1994). Functional role of type I and type II interferons in antiviral defense. *Science* **264**, 1918-21.

Nakai, K. & Horton, P. (1999). PSORT: a program for detecting sorting signals in proteins and predicting their subcellular localization. *Trends Biochem Sci* **24**, 34-6.

Nakai, K. & Kanehisa, M. (1992). A knowledge base for predicting protein localization sites in eukaryotic cells. *Genomics* **14**, 897-911.

Nal, B., Chan, C., Kien, F., Siu, L., Tse, J., Chu, K., Kam, J., Staropoli, I., Crescenzo-Chaigne, B., Escriou, N., van der Werf, S., Yuen, K. Y. & Altmeyer, R. (2005). Differential maturation and subcellular localization of severe acute respiratory syndrome coronavirus surface proteins S, M and E. *J Gen Virol* **86**, 1423-34.

Nayak, D. P., Hui, E. K. & Barman, S. (2004). Assembly and budding of influenza virus. *Virus Res* **106**, 147-65.

Nemeroff, M. E., Barabino, S. M., Li, Y., Keller, W. & Krug, R. M. (1998). Influenza virus NS1 protein interacts with the cellular 30 kDa subunit of CPSF and inhibits 3'end formation of cellular pre-mRNAs. *Mol Cell* **1**, 991-1000.

Neumann, G., Hughes, M. T. & Kawaoka, Y. (2000). Influenza A virus NS2 protein mediates vRNP nuclear export through NES-independent interaction with hCRM1. *Embo J* **19**, 6751-8.

Nguyen, V. P. & Hogue, B. G. (1997). Protein interactions during coronavirus assembly. *J Virol* **71**, 9278-84.

Niemann, H., Boschek, B., Evans, D., Rosing, M., Tamura, T. & Klenk, H. D. (1982). Post-translational glycosylation of coronavirus glycoprotein E1: inhibition by monensin. *Embo J* **1**, 1499-504.

Novick, D., Cohen, B. & Rubinstein, M. (1994). The human interferon alpha/beta receptor: characterization and molecular cloning. *Cell* **77**, 391-400.

O'Neill, R. E., Talon, J. & Palese, P. (1998). The influenza virus NEP (NS2 protein) mediates the nuclear export of viral ribonucleoproteins. *Embo J* **17**, 288-96.

Opstelten, D. J., Raamsman, M. J., Wolfs, K., Horzinek, M. C. & Rottier, P. J. (1995a). Coexpression and association of the spike protein and the membrane protein of mouse hepatitis virus. *Adv Exp Med Biol* **380**, 291-7.

Opstelten, D. J., Raamsman, M. J., Wolfs, K., Horzinek, M. C. & Rottier, P. J. (1995b). Envelope glycoprotein interactions in coronavirus assembly. *J Cell Biol* **131**, 339-49.

Otten, G. R., Schaefer, M., Doe, B., Liu, H., Srivastava, I., Megede, J., Kazzaz, J., Lian, Y., Singh, M., Ugozzoli, M., Montefiori, D., Lewis, M., Driver, D. A., Dubensky, T., Polo, J. M., Donnelly, J., O'Hagan, D. T., Barnett, S. & Ulmer, J. B. (2005). Enhanced potency of plasmid DNA microparticle human immunodeficiency virus vaccines in rhesus macaques by using a priming-boosting regimen with recombinant proteins. *J Virol* **79**, 8189-200.

Parisien, J. P., Lau, J. F., Rodriguez, J. J., Sullivan, B. M., Moscona, A., Parks, G. D., Lamb, R. A. & Horvath, C. M. (2001). The V protein of human parainfluenza virus 2 antagonizes type I interferon responses by destabilizing signal transducer and activator of transcription 2. *Virology* **283**, 230-9.

Parton, R. G. & Hancock, J. F. (2004). Lipid rafts and plasma membrane microorganization: insights from Ras. *Trends Cell Biol* **14**, 141-7.

Pavlovic, J., Arzet, H. A., Hefti, H. P., Frese, M., Rost, D., Ernst, B., Kolb, E., Staeheli, P. & Haller, O. (1995). Enhanced virus resistance of transgenic mice expressing the human MxA protein. *J Virol* **69**, 4506-10.

Perales, B., Sanz-Ezquerro, J. J., Gastaminza, P., Ortega, J., Santaren, J. F., Ortin, J. & Nieto, A. (2000). The replication activity of influenza virus polymerase is linked to the capacity of the PA subunit to induce proteolysis. *J Virol* **74**, 1307-12.

Perez, D. R. & Donis, R. O. (1998). The matrix 1 protein of influenza A virus inhibits the transcriptase activity of a model influenza reporter genome in vivo. *Virology* **249**, 52-61.

Plotch, S. J., Bouloy, M., Ulmanen, I. & Krug, R. M. (1981). A unique cap(m7GpppXm)-dependent influenza virion endonuclease cleaves capped RNAs to generate the primers that initiate viral RNA transcription. *Cell* **23**, 847-58.

Poole, E., He, B., Lamb, R. A., Randall, R. E. & Goodbourn, S. (2002). The V proteins of simian virus 5 and other paramyxoviruses inhibit induction of interferon-beta. *Virology* **303**, 33-46.

Powell, K. (2004). DNA vaccines--back in the saddle again? *Nat Biotechnol* **22**, 799-801.

Premkumar, D. R., Fukuoka, Y., Sevlever, D., Brunschwig, E., Rosenberry, T. L., Tykocinski, M. L. & Medof, M. E. (2001). Properties of exogenously added GPI-anchored proteins following their incorporation into cells. *J Cell Biochem* **82**, 234-45.

Prior, I. A., Muncke, C., Parton, R. G. & Hancock, J. F. (2003). Direct visualization of Ras proteins in spatially distinct cell surface microdomains. *J Cell Biol* **160**, 165-70.

Rajcani, J., Mosko, T. & Rezuchova, I. (2005). Current developments in viral DNA vaccines: shall they solve the unsolved? *Rev Med Virol* **15**, 303-25.

Rebouillat, D. & Hovanessian, A. G. (1999). The human 2',5'-oligoadenylate synthetase family: interferon-induced proteins with unique enzymatic properties. *J Interferon Cytokine Res* **19**, 295-308.

Reinhardt, J. & Wolff, T. (2000). The influenza A virus M1 protein interacts with the cellular receptor of activated C kinase (RACK) 1 and can be phosphorylated by protein kinase C. *Vet Microbiol* **74**, 87-100.

Rey, O. & Nayak, D. P. (1992). Nuclear retention of M1 protein in a temperature-sensitive mutant of influenza (A/WSN/33) virus does not affect nuclear export of viral ribonucleoproteins. *J Virol* **66**, 5815-24.

Robinson, H. L. (1997). Nucleic acid vaccines: an overview. *Vaccine* **15**, 785-7.

Robinson, H. L. & Torres, C. A. (1997). DNA vaccines. *Semin Immunol* **9**, 271-83.

Roers, A., Hochkeppel, H. K., Horisberger, M. A., Hovanessian, A. & Haller, O. (1994). MxA gene expression after live virus vaccination: a sensitive marker for endogenous type I interferon. *J Infect Dis* **169**, 807-13.

Ronni, T., Melen, K., Malygin, A. & Julkunen, I. (1993). Control of IFN-inducible MxA gene expression in human cells. *J Immunol* **150**, 1715-26.

Ronni, T., Sareneva, T., Pirhonen, J. & Julkunen, I. (1995). Activation of IFN-alpha, IFN-gamma, MxA, and IFN regulatory factor 1 genes in influenza A virus-infected human peripheral blood mononuclear cells. *J Immunol* **154**, 2764-74.

Rota, P. A., Oberste, M. S., Monroe, S. S., Nix, W. A., Campagnoli, R., Icenogle, J. P., Penaranda, S., Bankamp, B., Maher, K., Chen, M. H., Tong, S., Tamin, A., Lowe, L., Frace, M., DeRisi, J. L., Chen, Q., Wang, D., Erdman, D. D., Peret, T. C., Burns, C., Ksiazek, T. G., Rollin, P. E., Sanchez, A., Liffick, S., Holloway, B., Limor, J., McCaustland, K., Olsen-Rasmussen, M., Fouchier, R., Gunther, S., Osterhaus, A. D., Drosten, C., Pallansch, M. A., Anderson, L. J. & Bellini, W. J. (2003). Characterization of a novel coronavirus associated with severe acute respiratory syndrome. *Science* **300**, 1394-9.

Roy, A. M., Parker, J. S., Parrish, C. R. & Whittaker, G. R. (2000). Early stages of influenza virus entry into Mv-1 lung cells: involvement of dynamin. *Virology* **267**, 17-28.

Ruigrok, R. W., Barge, A., Durrer, P., Brunner, J., Ma, K. & Whittaker, G. R. (2000). Membrane interaction of influenza virus M1 protein. *Virology* **267**, 289-98.

Ryman, K. D., Klimstra, W. B., Nguyen, K. B., Biron, C. A. & Johnston, R. E. (2000). Alpha/beta interferon protects adult mice from fatal Sindbis virus infection and is an important determinant of cell and tissue tropism. *J Virol* **74**, 3366-78.

Samuel, C. E. (2001). Antiviral actions of interferons. *Clin Microbiol Rev* **14**, 778-809, table of contents.

Sang, N., Severino, A., Russo, P., Baldi, A., Giordano, A., Mileo, A. M., Paggi, M. G. & De Luca, A. (2001). RACK1 interacts with E1A and rescues E1A-induced yeast growth inhibition and mammalian cell apoptosis. *J Biol Chem* **276**, 27026-33.

Sanz-Ezquerro, J. J., de la Luna, S., Ortin, J. & Nieto, A. (1995). Individual expression of influenza virus PA protein induces degradation of coexpressed proteins. *J Virol* **69**, 2420-6.

Sargiacomo, M., Sudol, M., Tang, Z. & Lisanti, M. P. (1993). Signal transducing molecules and glycosyl-phosphatidylinositol-linked proteins form a caveolin-rich insoluble complex in MDCK cells. *J Cell Biol* **122**, 789-807.

Sarkar, S. N. & Sen, G. C. (2004). Novel functions of proteins encoded by viral stress-inducible genes. *Pharmacol Ther* **103**, 245-59.

Scheiffele, P., Rietveld, A., Wilk, T. & Simons, K. (1999). Influenza viruses select ordered lipid domains during budding from the plasma membrane. *J Biol Chem* **274**, 2038-44.

Schroeder, R., London, E. & Brown, D. (1994). Interactions between saturated acyl chains confer detergent resistance on lipids and glycosylphosphatidylinositol (GPI)-anchored proteins: GPI-anchored proteins in liposomes and cells show similar behavior. *Proc Natl Acad Sci U S A* **91**, 12130-4.

Schwegmann-Wessels, C., Al-Falah, M., Escors, D., Wang, Z., Zimmer, G., Deng, H., Enjuanes, L., Naim, H. Y. & Herrler, G. (2004). A novel sorting signal for intracellular localization is present in the S protein of a porcine coronavirus but absent from severe acute respiratory syndrome-associated coronavirus. *J Biol Chem* **279**, 43661-6.

Sen, G. C. (2001). Viruses and interferons. *Annu Rev Microbiol* **55**, 255-81.

Seth, R. B., Sun, L., Ea, C. K. & Chen, Z. J. (2005). Identification and characterization of MAVS, a mitochondrial antiviral signaling protein that activates NF-kappaB and IRF 3. *Cell* **122**, 669-82.

Shiver, J. W., Fu, T. M., Chen, L., Casimiro, D. R., Davies, M. E., Evans, R. K., Zhang, Z. Q., Simon, A. J., Trigona, W. L., Dubey, S. A., Huang, L., Harris, V. A., Long, R. S., Liang, X., Handt, L., Schleif, W. A., Zhu, L., Freed, D. C., Persaud, N. V., Guan, L., Punt, K. S., Tang, A., Chen, M., Wilson, K. A., Collins, K. B., Heidecker, G. J., Fernandez, V. R., Perry, H. C., Joyce, J. G., Grimm, K. M., Cook, J. C., Keller, P. M., Kresock, D. S., Mach, H., Troutman, R. D., Isopi, L. A., Williams, D. M., Xu, Z., Bohannon, K. E., Volkin, D. B., Montefiori, D. C., Miura, A., Krivulka, G. R., Lifton, M. A., Kuroda, M. J., Schmitz, J. E., Letvin, N. L., Caulfield, M. J., Bett, A. J., Youil, R., Kaslow, D. C. & Emini, E. A. (2002). Replication-incompetent adenoviral vaccine vector elicits effective anti-immunodeficiency-virus immunity. *Nature* **415**, 331-5.

Sieczkarski, S. B. & Whittaker, G. R. (2002). Influenza virus can enter and infect cells in the absence of clathrin-mediated endocytosis. *J Virol* **76**, 10455-64.

Simmons, G., Gosalia, D. N., Rennekamp, A. J., Reeves, J. D., Diamond, S. L. & Bates, P. (2005). Inhibitors of cathepsin L prevent severe acute respiratory syndrome coronavirus entry. *Proc Natl Acad Sci U S A* **102**, 11876-81.

Simmons, G., Reeves, J. D., Rennekamp, A. J., Amberg, S. M., Piefer, A. J. & Bates, P. (2004). Characterization of severe acute respiratory syndrome-associated

coronavirus (SARS-CoV) spike glycoprotein-mediated viral entry. *Proc Natl Acad Sci U S A* **101**, 4240-5.
Simons, K. & Ikonen, E. (1997). Functional rafts in cell membranes. *Nature* **387**, 569-72.
Skehel, J. J. & Wiley, D. C. (2000). Receptor binding and membrane fusion in virus entry: the influenza hemagglutinin. *Annu Rev Biochem* **69**, 531-69.
Smith, E. J., Marie, I., Prakash, A., Garcia-Sastre, A. & Levy, D. E. (2001). IRF3 and IRF7 phosphorylation in virus-infected cells does not require double-stranded RNA-dependent protein kinase R or Ikappa B kinase but is blocked by Vaccinia virus E3L protein. *J Biol Chem* **276**, 8951-7.
Smith, J. M., Amara, R. R., Wyatt, L. S., Ellenberger, D. L., Li, B., Herndon, J. G., Patel, M., Sharma, S., Chennareddi, L., Butera, S., McNicholl, J., McClure, H. M., Moss, B. & Robinson, H. L. (2005). Studies in macaques on cross-clade T cell responses elicited by a DNA/MVA AIDS vaccine, better conservation of CD8 than CD4 T cell responses. *AIDS Res Hum Retroviruses* **21**, 140-4.
Snijder, E. J., Bredenbeek, P. J., Dobbe, J. C., Thiel, V., Ziebuhr, J., Poon, L. L., Guan, Y., Rozanov, M., Spaan, W. J. & Gorbalenya, A. E. (2003). Unique and conserved features of genome and proteome of SARS-coronavirus, an early split-off from the coronavirus group 2 lineage. *J Mol Biol* **331**, 991-1004.
Song, K. S., Sargiacomo, M., Galbiati, F., Parenti, M. & Lisanti, M. P. (1997). Targeting of a G alpha subunit (Gi1 alpha) and c-Src tyrosine kinase to caveolae membranes: clarifying the role of N-myristoylation. *Cell Mol Biol (Noisy-le-grand)* **43**, 293-303.
Soo, Y. O., Cheng, Y., Wong, R., Hui, D. S., Lee, C. K., Tsang, K. K., Ng, M. H., Chan, P., Cheng, G. & Sung, J. J. (2004). Retrospective comparison of convalescent plasma with continuing high-dose methylprednisolone treatment in SARS patients. *Clin Microbiol Infect* **10**, 676-8.
Srivastava, I. K. & Liu, M. A. (2003). Gene vaccines. *Ann Intern Med* **138**, 550-9.
Staeheli, P., Grob, R., Meier, E., Sutcliffe, J. G. & Haller, O. (1988). Influenza virus-susceptible mice carry Mx genes with a large deletion or a nonsense mutation. *Mol Cell Biol* **8**, 4518-23.
Stark, G. R., Kerr, I. M., Williams, B. R., Silverman, R. H. & Schreiber, R. D. (1998). How cells respond to interferons. *Annu Rev Biochem* **67**, 227-64.
Stetson, D. B. & Medzhitov, R. (2006). Recognition of cytosolic DNA activates an IRF3-dependent innate immune response. *Immunity* **24**, 93-103.
Stojdl, D. F., Lichty, B. D., tenOever, B. R., Paterson, J. M., Power, A. T., Knowles, S., Marius, R., Reynard, J., Poliquin, L., Atkins, H., Brown, E. G., Durbin, R. K., Durbin, J. E., Hiscott, J. & Bell, J. C. (2003). VSV strains with defects in their ability to shutdown innate immunity are potent systemic anti-cancer agents. *Cancer Cell* **4**, 263-75.
Supekar, V. M., Bruckmann, C., Ingallinella, P., Bianchi, E., Pessi, A. & Carfi, A. (2004). Structure of a proteolytically resistant core from the severe acute respiratory syndrome coronavirus S2 fusion protein. *Proc Natl Acad Sci U S A* **101**, 17958-63.
Symons, J. A., Alcami, A. & Smith, G. L. (1995). Vaccinia virus encodes a soluble type I interferon receptor of novel structure and broad species specificity. *Cell* **81**, 551-60.

Talon, J., Horvath, C. M., Polley, R., Basler, C. F., Muster, T., Palese, P. & Garcia-Sastre, A. (2000). Activation of interferon regulatory factor 3 is inhibited by the influenza A virus NS1 protein. *J Virol* **74**, 7989-96.

Tan, S. L. & Katze, M. G. (1998). Biochemical and genetic evidence for complex formation between the influenza A virus NS1 protein and the interferon-induced PKR protein kinase. *J Interferon Cytokine Res* **18**, 757-66.

Usacheva, A., Tian, X., Sandoval, R., Salvi, D., Levy, D. & Colamonici, O. R. (2003). The WD motif-containing protein RACK-1 functions as a scaffold protein within the type I IFN receptor-signaling complex. *J Immunol* **171**, 2989-94.

Vennema, H., Heijnen, L., Rottier, P. J., Horzinek, M. C. & Spaan, W. J. (1993). A novel glycoprotein of feline infectious peritonitis coronavirus contains a KDEL-like endoplasmic reticulum retention signal. *Adv Exp Med Biol* **342**, 209-14.

Wang, R., Doolan, D. L., Le, T. P., Hedstrom, R. C., Coonan, K. M., Charoenvit, Y., Jones, T. R., Hobart, P., Margalith, M., Ng, J., Weiss, W. R., Sedegah, M., de Taisne, C., Norman, J. A. & Hoffman, S. L. (1998). Induction of antigen-specific cytotoxic T lymphocytes in humans by a malaria DNA vaccine. *Science* **282**, 476-80.

Wang, R., Richie, T. L., Baraceros, M. F., Rahardjo, N., Gay, T., Banania, J. G., Charoenvit, Y., Epstein, J. E., Luke, T., Freilich, D. A., Norman, J. & Hoffman, S. L. (2005). Boosting of DNA vaccine-elicited gamma interferon responses in humans by exposure to malaria parasites. *Infect Immun* **73**, 2863-72.

Wang, X., Li, M., Zheng, H., Muster, T., Palese, P., Beg, A. A. & Garcia-Sastre, A. (2000). Influenza A virus NS1 protein prevents activation of NF-kappaB and induction of alpha/beta interferon. *J Virol* **74**, 11566-73.

Watanabe, K., Handa, H., Mizumoto, K. & Nagata, K. (1996). Mechanism for inhibition of influenza virus RNA polymerase activity by matrix protein. *J Virol* **70**, 241-7.

Weber, F., Haller, O. & Kochs, G. (2000). MxA GTPase blocks reporter gene expression of reconstituted Thogoto virus ribonucleoprotein complexes. *J Virol* **74**, 560-3.

Weber, F., Kochs, G., Haller, O. & Staeheli, P. (2003). Viral evasion of the interferon system: old viruses, new tricks. *J Interferon Cytokine Res* **23**, 209-13.

Webster, R. G., Bean, W. J., Gorman, O. T., Chambers, T. M. & Kawaoka, Y. (1992). Evolution and ecology of influenza A viruses. *Microbiol Rev* **56**, 152-79.

Whittaker, G. R. & Helenius, A. (1998). Nuclear import and export of viruses and virus genomes. *Virology* **246**, 1-23.

Williams, B. R. (1999). PKR; a sentinel kinase for cellular stress. *Oncogene* **18**, 6112-20.

Wilson, B. S., Steinberg, S. L., Liederman, K., Pfeiffer, J. R., Surviladze, Z., Zhang, J., Samelson, L. E., Yang, L. H., Kotula, P. G. & Oliver, J. M. (2004). Markers for detergent-resistant lipid rafts occupy distinct and dynamic domains in native membranes. *Mol Biol Cell* **15**, 2580-92.

Wilson, C. C., McKinney, D., Anders, M., MaWhinney, S., Forster, J., Crimi, C., Southwood, S., Sette, A., Chesnut, R., Newman, M. J. & Livingston, B. D. (2003). Development of a DNA vaccine designed to induce cytotoxic T lymphocyte responses to multiple conserved epitopes in HIV-1. *J Immunol* **171**, 5611-23.

Xiao, X., Chakraborti, S., Dimitrov, A. S., Gramatikoff, K. & Dimitrov, D. S. (2003). The SARS-CoV S glycoprotein: expression and functional characterization. *Biochem Biophys Res Commun* **312**, 1159-64.

Yang, Z. Y., Kong, W. P., Huang, Y., Roberts, A., Murphy, B. R., Subbarao, K. & Nabel, G. J. (2004). A DNA vaccine induces SARS coronavirus neutralization and protective immunity in mice. *Nature* **428**, 561-4.

Yasuda, J., Nakada, S., Kato, A., Toyoda, T. & Ishihama, A. (1993). Molecular assembly of influenza virus: association of the NS2 protein with virion matrix. *Virology* **196**, 249-55.

Ye, Z. P., Baylor, N. W. & Wagner, R. R. (1989). Transcription-inhibition and RNA-binding domains of influenza A virus matrix protein mapped with anti-idiotypic antibodies and synthetic peptides. *J Virol* **63**, 3586-94.

Ying, W., Hao, Y., Zhang, Y., Peng, W., Qin, E., Cai, Y., Wei, K., Wang, J., Chang, G., Sun, W., Dai, S., Li, X., Zhu, Y., Li, J., Wu, S., Guo, L., Dai, J., Wan, P., Chen, T., Du, C., Li, D., Wan, J., Kuai, X., Li, W., Shi, R., Wei, H., Cao, C., Yu, M., Liu, H., Dong, F., Wang, D., Zhang, X., Qian, X., Zhu, Q. & He, F. (2004). Proteomic analysis on structural proteins of Severe Acute Respiratory Syndrome coronavirus. *Proteomics* **4**, 492-504.

Yokota, S., Saito, H., Kubota, T., Yokosawa, N., Amano, K. & Fujii, N. (2003). Measles virus suppresses interferon-alpha signaling pathway: suppression of Jak1 phosphorylation and association of viral accessory proteins, C and V, with interferon-alpha receptor complex. *Virology* **306**, 135-46.

Yoneyama, M., Kikuchi, M., Natsukawa, T., Shinobu, N., Imaizumi, T., Miyagishi, M., Taira, K., Akira, S. & Fujita, T. (2004). The RNA helicase RIG-I has an essential function in double-stranded RNA-induced innate antiviral responses. *Nat Immunol* **5**, 730-7.

Zhang, J. & Lamb, R. A. (1996). Characterization of the membrane association of the influenza virus matrix protein in living cells. *Virology* **225**, 255-66.

Zhang, Y., Li, T., Fu, L., Yu, C., Li, Y., Xu, X., Wang, Y., Ning, H., Zhang, S., Chen, W., Babiuk, L. A. & Chang, Z. (2004). Silencing SARS-CoV Spike protein expression in cultured cells by RNA interference. *FEBS Lett* **560**, 141-6.

Zhao, P., Cao, J., Zhao, L. J., Qin, Z. L., Ke, J. S., Pan, W., Ren, H., Yu, J. G. & Qi, Z. T. (2005). Immune responses against SARS-coronavirus nucleocapsid protein induced by DNA vaccine. *Virology* **331**, 128-35.

Ziebuhr, J. (2004). Molecular biology of severe acute respiratory syndrome coronavirus. *Curr Opin Microbiol* **7**, 412-9.

12 ACKNOWLEDGMENTS

I thank…

…Prof. Dr. Karin Mölling for the opportunity to realize my PhD thesis in her institute and for her ideas and support in scientific discussions. Her input was always very fruitful.

…Prof. Dr. Urs Greber for his support in progress report presentations and in reading my thesis.

…PD Dr. Jovan Pavlovic, my supervisor, for teaching me classical virology and advising me for experimental hurdles.

…Dr. Lina Elzaouk for helping me with the mice experiments.

…Dr. Stefan Deuber for interesting virology-discussions and helpful inputs when I was helpless with my experiments.

…Dr. Alexey Maskevich for reading my thesis, showing me how to write a scientific text and giving me general advices how to successfully proceed for my defense.

…my family and friends who supported me during three years and carried me through scientific success and frustration.